

Review

The Role of Functionalization in the Applications of Carbon Materials: An Overview

Giorgio Speranza ^{1,2,3} ¹ CMM-FBK, via Sommarive 18, 38123 Trento, Italy; speranza@fbk.eu² IFN-CNR, CSMFO Lab. & FBK CMM, via alla Cascata 56/C Povo, 38123 Trento, Italy³ Department of Material Engineering, University of Trento, via Mesiano 77, 38123 Trento, Italy

Received: 14 October 2019; Accepted: 5 December 2019; Published: 11 December 2019



Abstract: The carbon-based materials (CbMs) refer to a class of substances in which the carbon atoms can assume different hybridization states (sp^1 , sp^2 , sp^3) leading to different allotropic structures -. In these substances, the carbon atoms can form robust covalent bonds with other carbon atoms or with a vast class of metallic and non-metallic elements, giving rise to an enormous number of compounds from small molecules to long chains to solids. This is one of the reasons why the carbon chemistry is at the basis of the organic chemistry and the biochemistry from which life on earth was born. In this context, the surface chemistry assumes a substantial role dictating the physical and chemical properties of the carbon-based materials. Different functionalities are obtained by bonding carbon atoms with heteroatoms (mainly oxygen, nitrogen, sulfur) determining a certain reactivity of the compound which otherwise is rather weak. This holds for classic materials such as the diamond, the graphite, the carbon black and the porous carbon but functionalization is widely applied also to the carbon nanostructures which came at play mainly in the last two decades. As a matter of fact, nowadays, in addition to fabrication of nano and porous structures, the functionalization of CbMs is at the basis of a number of applications as catalysis, energy conversion, sensing, biomedicine, adsorption etc. This work is dedicated to the modification of the surface chemistry reviewing the different approaches also considering the different macro and nano allotropic forms of carbon.

Keywords: carbon-based materials; carbon nanostructures; functionalization

1. Introduction

Diamond and graphite are the most known forms of carbon since antiquity although it has long been recognized that carbon is present in nature also in different types of compounds such as the various types of amorphous carbon, in organic molecules and biomolecules. The multiform nature of carbon is due to the peculiar characteristic of its electronic structure forming different hybrids namely sp^1 , sp^2 , sp^3 . The different orientation of orbitals in these hybrids gives origin to different structures possessing markedly different properties [1–5]. As an example, diamond is formed by pure sp^3 hybrids where bonds are oriented along the principal axis of a tetrahedron. In this structure the four strong covalent bonds are indistinguishable and make diamond the hardest material in nature, highly transparent, electrically insulating but characterized by high thermal conductivity [5–8]. Differently, graphite is formed by pure sp^2 hybrids. In this case three bonds of carbon lie in a plane and form an angle of 120° with the three nearest neighbor atoms. The fourth bond is perpendicular to this plane. This peculiar electronic structure determines the layered structure of graphite. While the in-plane bonds are covalent and very strong, the out-of-plane is a weak π bond responsible for the graphite electrical conductivity, the high absorption coefficient over an extended spectral range, and the material softness [9–11]. In other materials the coexistence of these two kinds of hybrids leads to amorphous carbon structures where the bond orientation is undetermined.

With respect to CbMs, in the fifties were identified novel forms of carbon at the nanoscale, possessing unique properties thus opening new perspectives and potential technological applications [10,12–15]. The nanostructure firstly discovered was the nanodiamond (ND) obtained by detonation in 1950 [16]. Interest in nanodiamonds derives from the possibility to obtain at a relatively low cost a reasonable amount of material retaining the properties of bulk diamond. ND particulate is utilized as abrasive material and recently its color centers are exploited in more sophisticated applications such as fluorescent tags [17] for diverse applications as the biomedical one [18] and as single photon sources [19]. NDs are also employed as seeds for chemical vapor deposition (CVD) nano-diamond films growth [20]. Other forms of nanostructures such as fullerenes were discovered in 1985 [21]. Fullerenes are very interesting both for the fundamental studies and the applicative potentialities. Fullerenes represent a family of spherical structures formed by 20, 60, 70 and larger numbers of carbon atoms. With respect to other fullerenes, the C_{60} molecule is the more frequent, stable and widely studied system. In C_{60} , C atoms are organized in adjacent pentagons and hexagons providing the bond curvature allowing the formation of a spherical structure (truncated icosahedron). In C_{60} molecules, all carbon atoms are sp^2 hybrids. However, differently from the organization in a perfect hexagon structure as in graphite sheets, presence of pentagons causes bond resonance to be absent. This makes fullerenes be efficient charge acceptors, a property which is of paramount importance in reactions with radicals and in surface functionalization [22]. Different from fullerenes, perfect resonance is present in graphene where atoms are organized in a two dimensional hexagonal lattice forming a monoatomic layer. Graphene exhibits unique properties deriving from the electron quantum confinement in the single atomic sheet [23]. Among others, it possesses a high absorbance on the whole visible optical range, the electron motion is ballistic, leading to a remarkable electron mobility so that graphene can be considered as a zero gap semiconductor [23]. There is a broad list of different methods which can be applied to functionalize the graphene sheets depending on the desired application. Parallel to the development of techniques to obtain an effective production of well-defined sheets, methods for surface chemical modification were developed [24]. Among other, covalent functionalization consisting in attaching organic functionalities as free radicals and dienophiles exploiting the chemistry of oxygen groups. The covalent functionalization includes the attachment of hydrogen and halogens. To better preserve the electrical properties, noncovalent functionalization and interactions is preferred since they do not disrupt the extended π delocalization of the graphene electrons. The graphene surface can also be modified attaching nanoparticles to induce specific properties required for example in catalysis or in plasmonics. Carbon nanotubes (CNTs) can be considered as rolled graphene sheets but they possess different electronic properties due to the presence of curvature. CNTs were discovered soon after fullerenes [25,26] and have been extensively studied both from the fundamental and applicative point of view. CNTs are characterized by a chirality which describes how the hexagon bond directions are oriented with respect to the CNT axis. This orientation strongly influence the CNT electronic properties [25,27]. CNTs are widely applied in sensing applications [28] as well as reinforcing element in a wide class of materials [29–33]. A CNT competing material are the carbon fibers (CFs), widely utilized in industrial applications [34]. CFs are a less expensive material with respect to carbon nanotubes and are massively produced. As for CNTs, they essentially find application as a reinforcing element in a many different compounds including organic materials [35], biomaterials [36], inorganic materials [37], and metals [38]. The strong covalent C–C bond is exploited to improve the mechanical properties of the composite. Within the class of fibers, those based on carbon are characterized by the highest specific modulus and highest specific strength [39]. At room temperatures, CFs do not suffer from corrosion problems or stress induced failures as glassy and organic polymer fibers. In addition, at high temperatures, CFs display outstanding strength and modulus if compared to other materials [39]. Additional information can be found in the following review papers [2,33,40–45].

If industrial applications are concerned, other carbon forms widely utilized are glassy carbon, porous carbon [46] and carbon black [47]. Glassy carbon is composed by microcrystalline stacks of

narrow graphite-like interconnected layers. This leads to a closed pore rigid structure that is chemically inert, hard but brittle [48–50].

Due to the highly resistant, conductive, and inert network, glassy carbons are utilized in a series of rather different applications. They are utilized as electrodes in solid state batteries and in industrial harsh chemical processes where also high temperatures are involved such as crystallization of CaF₂, CdS and ZnS. Glassy carbon can be utilized to manufacture high temperature furnace elements. Due to the chemical inertness, glassy carbons are utilized also in fabrication of prostheses. Porous carbon and carbon black are much softer. Generally, in industrial applications important is the extension of the surface which is exposed to the external environment. The porous carbon is characterized by a high specific surface area enhancing the interaction with the external medium. Although it possesses a lower conductivity with respect to glassy carbon, the high porosity and the presence of active sites makes it a good material to fabricate electrodes for applications in electrochemistry [51–53] and bioelectrodes for sensing and stimulation [54,55].

The same holds for the carbon black mainly utilized as additive in rubbers and polymers to improve their mechanical properties, or as a pigment [56] although new potentialities have been recently envisaged [57].

Common to all the forms of carbon which are briefly summarized above, is the interaction with other substances occurring at the surface which strongly depends on the surface chemistry. This work will provide a broad overview on the diverse functionalization processes applied to carbon materials. We will focus on the surface chemistry and the role of various treatments that can be utilized for specific applications.

2. Functionalization of Carbon Materials and Applications

The surface functionalization indicates a processing carried out to modify the chemistry of the material surface to provide specific properties [58]. Different functionalization methods are applied to different carbon species [59]. One of the main results of this processing is the change of the surface energy. This change enables better coupling with other substances at the molecular level with bonding of specific active molecules such as drugs, genomic materials, luminescent agents, metallic nanostructures for catalysis or plasmonics, etc. In addition, attaching polar/non-polar groups on the surface it is possible to modulate the surface wettability [60–62] which, at the macroscopic level, leads to a better coupling with solvents or other materials as in composites.

The functionalization of the material surface also includes grafting well defined molecules to change the surface reactivity towards specific chemical species. This also encompasses the electrochemical properties which are tailored for specific applications as catalysis, batteries, supercapacitors, fuel cells electrochemical cells, and organic photovoltaics. The functionalization also imparts luminescent properties to carbon-based nanostructures or allows bonding molecular luminescent species to the material surface. The functionalization is, in the end, an unavoidable step at the basis of the preparation of carbon materials for the different applications as depicted in Figure 1.

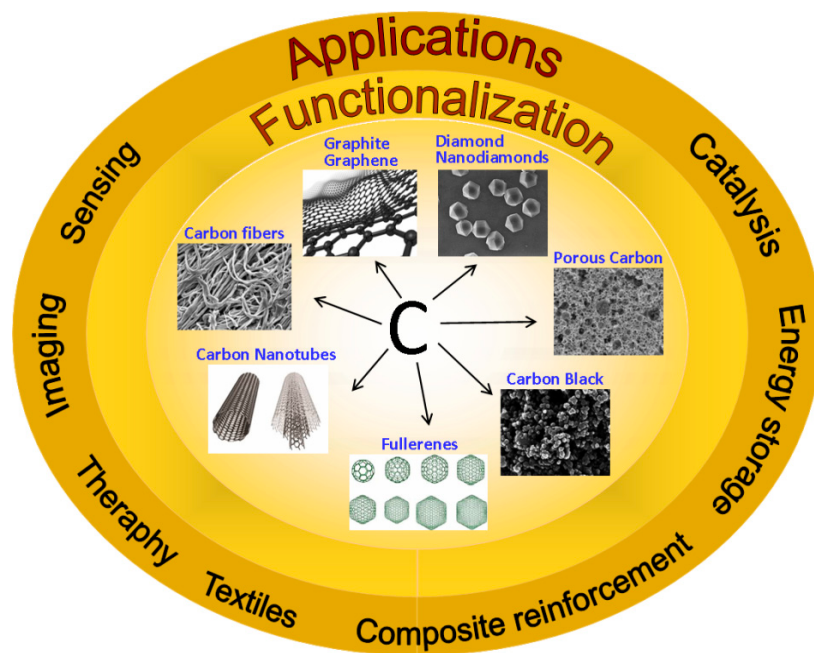


Figure 1. Different forms of carbon-based materials. Different possible applications are also indicated where carbon materials can be utilized thanks to the functionalization of their surface.

2.1. Solubilization of Carbon Materials and Bio-Applications

The common characteristic of pure carbon allotropes is their low solubility. The possibility of dispersing carbon nanostructures or coupling the surfaces of CbMs with liquids by tuning the surface energy is of paramount importance for a number of different technologies or for the development of new materials with improved properties. The solubilization is the precondition for using carbon-based nanostructures in biomedical applications such as in vitro and in vivo imaging, photoacoustic imaging, drug delivery, protein separation, biosensing, tissue engineering and photothermal therapy [28,63–65]. All these applications require the carbon particulate to be dispersed in solvents and particularly in water [66]. The hydrophobic character of carbon-based materials is generally attributed to the non-polarity of the bonds formed by sp^2 hybridized carbon atoms. However, recent studies enlightens that these surfaces are mildly hydrophilic and the hydrophobic character is caused by hydrogenated contaminations [67]. The common manner to solve this problem is to change the surface chemistry by functionalizing the carbon surfaces.

2.1.1. Graphite and Graphene

The process of graphite solubilization is described by several authors and generally ends up in the exfoliation with the production of graphene sheets [68–70]. In [68], the authors used a series of perfluorinated aromatic solvents and sonication to make a suspension of graphite powder. The solubilization is based on a charge transfer mechanism from electron-rich carbon layers to the electron-deficient aromatic molecules due to strong electron withdrawing fluorine atoms. Similar mechanisms are claimed to be at the basis of graphite intercalation processes [71,72]. The solubilization of graphite is generally desired to optimize the exfoliation with production of high fractions of graphene monolayers. Apart from ultrasound assisted exfoliation in which polar/non-polar, surfactant, and organic solvent are used, the graphite is chemically modified to facilitate the dispersion in aqueous solvents. Very popular is the Hummers process in which graphite is oxidized in a concentrated solution of potassium permanganate, sodium nitrate, and sulfuric acid at a temperature of 98 °C [73]. This process leads to graphite exfoliation and, at the same time, production of strongly oxidized graphene sheets characterized by a high water solubility. This method can be modified to obtain oleylamine-functionalized graphite via reduction in trioctylphosphine [74]. In [75] a simple and

eco-friendly procedure of graphite oxide esterification is reported. The functionalization is made using acetic anhydride and Et-acetate leading to ~4.5 mol % of acetyl groups. Air, oxygen, and nitrogen are used in a jet system to produce carboxylic, carbonyl, amine/amide functionalities on the graphite surface [76]. Grinding is also utilized to generate graphite particulate and, at the same time, graft hydroxyl, carbonyl, and carboxyl functional groups [77]. 4-aminobenzoic acid was electropolymerized on graphite electrodes for immobilizing biomolecules [78]. Graphite electrodes are also widely utilized for biosensing. A low-cost, sensitive and selective graphite electrode modified with nickel hydroxide was utilized for sensing glucose [79]. The sensor reached a detection limit of 0.3 μ M of glucose and its original response towards glucose remained almost unchanged after 28 days. Another glucose sensor was fabricated by coating a graphite electrode with the 6-(4,7-bis(2,3-dihydrothieno[3,4-b][1,4]dioxin-5-yl)-2H-benzo[d][1,2,3]triazol-2-yl)hexan-1-amine conducting polymer used as an immobilization matrix for enzymes such as the glucose oxidase [80]. To improve the efficiency of the biosensor, gold nanoparticles functionalized with mercaptopropionic acid were immobilized onto the polymer surface through a carbodiimide coupling to achieve the most effective surface design for sensing. Graphitic hollow spheres were produced using a suspension of magnetite/silica-encapsulated core-shell sphere and glucose. A hydrothermal and subsequent partial or complete removal of the silica core with HF were applied to produce hollow graphitic nanoparticles [81]. A second hydrothermal process was applied to a suspension of these nanoparticles in ammonia and triethylamine for adding amino functional groups. The nanoparticles displayed tunable photoluminescence dependent on the fraction of the sp^2 domains and N-doping. Biocompatibility of the graphitic hollow nanoparticles was evaluated in human HeLa cells, demonstrating their potential for applications as cellular tags for imaging, delivery of therapeutics, and biosensing. Graphite electrodes were also utilized as transducer for the detection of specific oligonucleotide sequences. The graphite surface was electropolymerized with 4-hydroxyphenylacetic acid to reveal a specific sequence of the mycobacterium tuberculosis genome [82].

Due to the important technological implications, there is a rich literature dedicated to the solubilization of graphene [83–85]. The lack of graphene surface polarities causes an easy aggregation and precipitation in a variety of matrices. Physical methods such as ultrasounds are generally utilized to re-disperse graphene sheets. However, due to the stability of the π - π stacking, the solubilization is very poor. Good dispersions are obtained by functionalizing graphene sheets. There is a wide variety of molecules utilized at this aim and some of them are represented in Figure 2. Additional functionalization methods include: small organic molecules such as isocyanate [86], 1-ethyl-3-(3-polyethylene-glycole molecules [87], thionyl chloride [88], and N,N0-Dicyclohexylcarbodiimide [89]. Another convenient method is based on the π - π interaction. The method is based on the conjugation of hexatomic rings of graphene with other organic molecules possessing the same structure. This interaction was successfully utilized to detect or bond aromatic molecules and single stranded DNA on the graphene surface [87,90,91]. Another interesting way to render graphene soluble is the use of graphene quantum dots (GQD) [92]. The latter are produced by chemical oxidation of graphene or other graphitic carbon materials. This generates oxygen functional groups on the GQD surface rendering them hydrophilic. The π - π interaction is then used to attach the GQD to the monolayers rendering graphene water dispersible and fluorescent. Hydrogen bonding is another possibility to functionalize graphene. Recently it has been demonstrated that the solubility of graphene oxide (GO) and the stability of the solutions strongly depend on the chemical interactions between graphene sheets and solvents [93]. In particular, the GO dispersion is allowed by the strong hydrogen bonding formed by solvent molecules and the GO functional groups. The hydrogen bond is also exploited to attach a large variety of molecules to the hydroxyl and carboxyl groups highly abundant on the GO surfaces. For example, hydrogen bonds was demonstrated to be essential in stabilizing single-stranded DNA (ssDNA) on GO [94]. The DNA molecule adsorption proceeds first by DNA-GO surface interaction by hydrogen bonding, and then the π - π stacking interactions between the aromatic rings of the nucleobases.

Hydrogen bonds were utilized to disperse graphene into a chitosan-lactic acid matrix [95] allowing the fabrication of conductive chitosan hydrogels while improving their mechanical properties. The gels show great promise to be used in scaffolds for electro-responsive cells in tissue engineering. Hydrogen bonding was successfully utilized to disperse graphene as a reinforcing element, in polyvinyl alcohol (PVA), a hydrophilic polymer [96]. Graphene is dispersed in elastomers where strong hydrogen bonds lead to an increase of the tensile strength and of the tear strength by 357% and 117%, respectively [97].

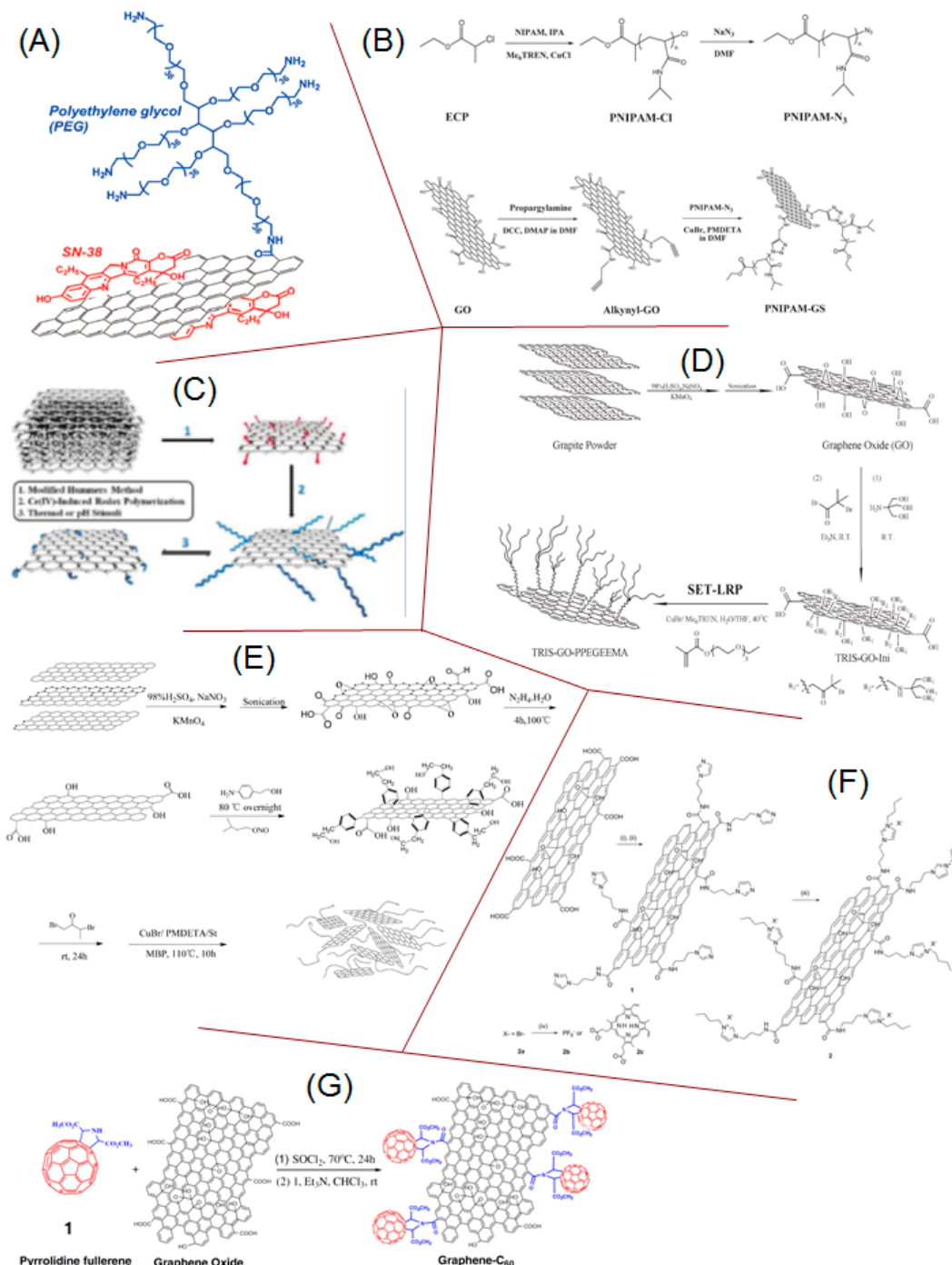


Figure 2. Different kinds of graphene surface functionalization. (A) Schematic draw of loaded nano-graphene oxide (GO) sheet polyethyleneglycol (PEG) functionalization. Reproduced with permission from [87]; (B) Synthesis of graphene sheet functionalized with PNIPAM-N₃. Reproduced with permission from [98]; (C) Schematic synthetic route of polymer-grafted GO. Reproduced with permission from [99]; (D) In situ growing of PPEGEEMA polymer chains via SET-LRP from the surface

of tris(hydroxymethyl) aminomethane modified graphene oxide sheets. Reproduced with permission from [100]; (E) Synthesis route of polystyrene-functionalized graphene nanosheets. Reproduced with permission from [101]; (F) Preparation of imidazolium-modified graphene-oxide hybrid materials and anion exchange reactions. (i) $(COCl)_2$, at 80 °C for 18 h, (ii) 1-(3-aminopropyl)imidazole, at 100 °C for 18 h, (iii) 1-bromobutane, at 90 °C for 18 h, (iv) H_2O , $NaPF_6$ or protoporphyrin IX disodium salt, at 25 °C, for 18 h. Reproduced with permission from [102]; (G) Synthesis procedure of the graphene-C₆₀ hybrid material. Reproduced with permission from [88].

2.1.2. Carbon Nanotubes

The carbon nanotubes (CNTs) are other high impact nanostructures broadly utilized in a high number of applications. There is a large literature describing methods to disperse CNTs in various solvents (see for example [103] and references there in). Solubilization of CNTs is performed by both physical and chemical processing [33]. In the first case, we can mention ultrasounds [104], gel electrophoresis [105], dielectrophoresis [106], chromatography [107], density gradient ultracentrifugation [108]. Other methods such as plasma treatments, and UV light [109] are utilized for modifying the surface chemistry grafting polar functional groups. In particular, UV radiation is able of inducing defects on the CNT surface thus leading to exfoliation and opening of the CNT ends. Plasma treatments are widely utilized for grafting desired chemical functions to non-reactive surfaces [110,111] with the advantage to be a very clean processing method. Different precursors may be utilized to graft different functional groups [112] enabling different functionalization mechanisms [110]. The selection of plasma parameters is crucial to optimize the grafting efficiency. Generally, pure oxygen, Ar/O mixtures, CO₂ and their mixture with H are utilized to generate oxygen based functional groups, while N, H, ammonia are utilized to amine the CNTs [110]. There are also wet chemical procedures to functionalize CNTs. In these cases, acids are commonly used inducing the formation of oxygen based functional groups and defects [113,114] thus making the CNTs soluble. Salts are also utilized to disperse CNTs in water [112]. As an example, aryl diazonium salts are frequently introduced as organic intermediates in radical addition of CNTs [115]. Results show that the functionalization promotes the accessibility to spun CNTs enabling a more extensive and uniform additional modifications. Surface modifications with primary and secondary amines and enzymes is also possible [116]. The authors of ref. [116] were able to bind various primary and secondary achiral and chiral amines to CNTs providing the chemistry to synthesize three-dimensional enzyme arrays with potential use in biosensing. Solubility of CNTs may also be improved by adding porphyrins [117]. The efficient dispersion of CNTs in water allowed the authors to align the nanotubes on PDMS and transfer them onto silicon or glass substrates for potential fabrication of devices. Pyrrolidine molecules can be utilized as an alternative method for functionalizing CNTs. In [118] pyridinium ylides reacted with single-walled carbon nanotubes through cycloaddition, a simple and convenient process for covalent modification of the CNT surfaces. The indolizine functionalized CNTs, when excited at 335 nm, emit blue light which can be used for imaging. In [119] a similar reaction was utilized to bind biological molecules.

2.1.3. Fullerenes

Another important carbon class of nanostructures is that of fullerenes. Their solubility has been widely studied in the past leading to several review papers [22,120,121] due to the vast range of applications of fullerenes. The main difference with graphitic sheets or CNTs which can be seen as graphite ribbons rolled around the main axis, derives from the presence of a curvature leading to the spherical shape. This structure cannot be generated by simply using a hexagon base unit. The spherical cages of carbon atoms can be obtained only alternating hexagons and pentagons. However, the presence of pentagons forbids the bond resonance, thereby making C₆₀ a superaromatic structure with poor electron delocalization.

C_{60} and other similar carbon spherical molecules show a rather poor solubility in aqueous solvents, which causes aggregation. The fullerene surface functionalization is a convenient route to solve the problem. The functionalization leads to fullerenes with excellent solubility both in aqueous and organic solvents [122,123]. The chemical modification of the fullerene surfaces may be performed following two different methods: (i) the complexation with solubilizing agents to partially hide the fullerene hydrophobic surface [124]; (ii) the covalent functionalization of the fullerene surface [125].

An example of the first chemical processing is the C_{60} complexation with cyclodextrins [126], which were utilized to disperse fullerene in water. The solution was then utilized for photodynamic therapy exploiting the capability of C_{60} of generating reactive oxygen species (ROS). The introduction of oxygen based functional groups, mainly hydroxyl groups, on the fullerene surface can be made using strong acids at high temperature [127]. Another route is the use of a basic solution where an excess NaOH in water is mixed to a suspension of C_{60} in benzene [128]. The reaction is carried out in the presence of a small amount of tetrabutylammonium hydroxide acting as a catalyst. Despite the lack of control on the addend density, these reactions are widely utilized to make fullerenes hydrophilic. The property of OH functionalized fullerenes (fullerenols) preventing the process of lipid peroxidation, and the scavenging activity towards superoxide, hydroxyl radical, and nitric oxide chemical species has been demonstrated [129].

Another common surface modification is the grafting of amine groups which can be carried out mixing C_{60} with different aliphatic primary amines (n-propylamine, t-butylamine, and dodecylamine) [130]. In other reactions, smaller primary-, secondary-amine chains (methylamine, diethylamine) are reacted with C_{60} , C_{70} fullerenes. The reaction mechanism for amination of C_{60} with addition at the [6,6] bond is represented in Figure 3.

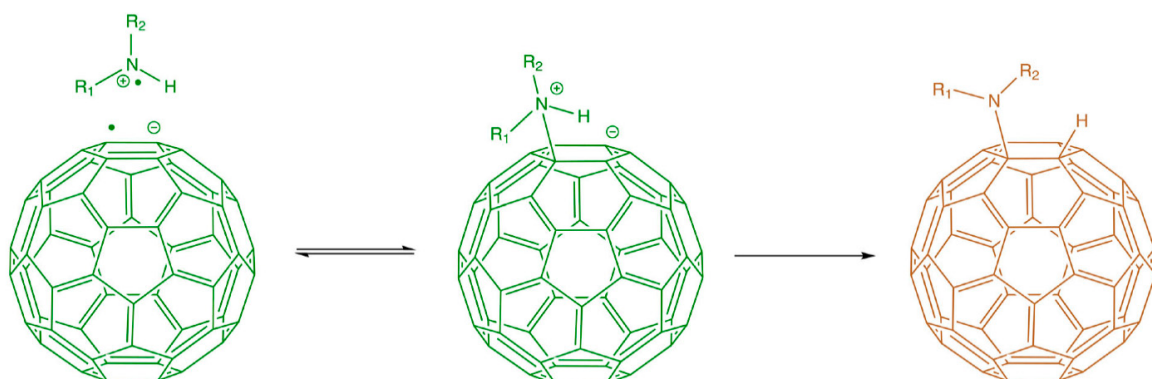


Figure 3. Amination mechanism of C_{60} . Initially a single-electron transfer (a fast process) produces a C_{60} anion radical. Radical recombination gives a zwitterion which can be stabilized by proton transfer to give the final product. Reproduced with permission from [22].

Another popular reaction is the 1,3-dipolar cycloaddition of an azomethine ylide to a C_{60} molecule producing a stable compound formed by a C_{60} with a pyrrolidine ring attached across the [6,6] bond [131]. The amin-functionalized fullerenes are utilized for gene transfection [132]. The authors demonstrated the ability of two-handed fullerenes of binding to duplex DNA in a reversible manner enabling the transfection to cells. In another work [133], the authors utilized fullerenes functionalized with multiple amines as an efficient transfer mean to deliver extra-cellular DNA to mammalian cells. An efficient gene delivery was also obtained in vitro with the positively charged octa-amino derivatized C_{60} and a dodeca-amino derivatized C_{60} [134].

An alternative process is the cyclopropanation where an α -halo ester/ketone is bonded to the fullerene under strongly basic conditions [135]. The reaction scheme is reported in Figure 4 where the strong basic environment causes deprotonation of the 2-diethyl bromomalonate or methyl 2-chloroacetoacetate and a nucleophilic attack at the [6,6] position of the fullerene. The popularity of

this reaction stems from the possibility of easily modifying the original reaction to produce a vast class of different complexes [136].

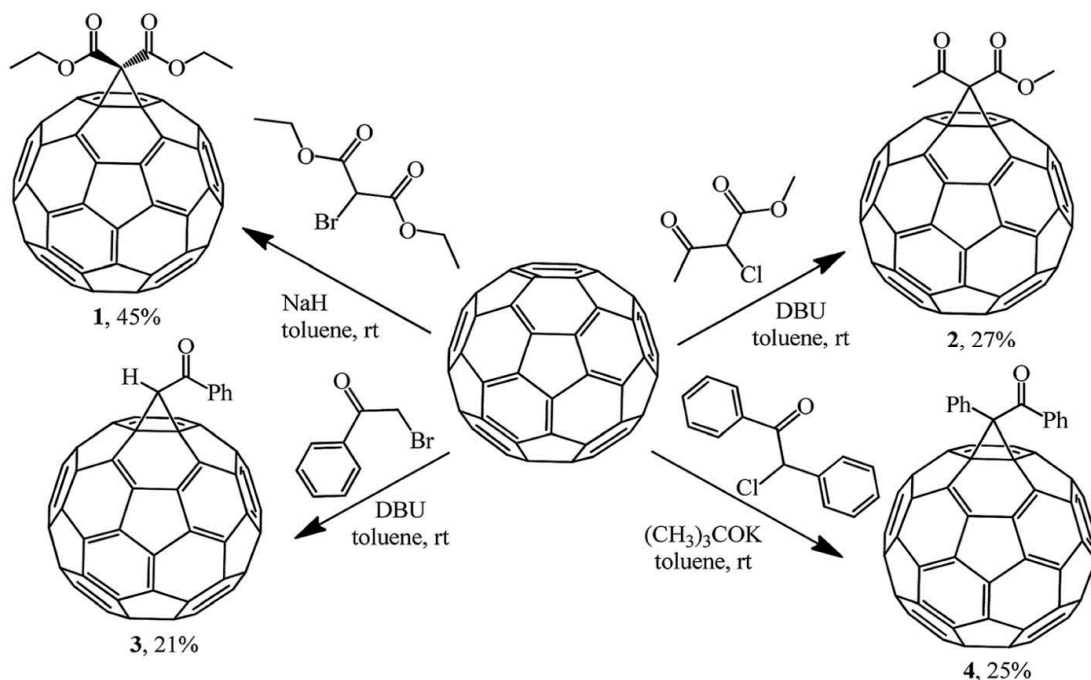


Figure 4. Cycloaddition reaction of C_{60} with 2-diethyl bromomalonate, methyl 2-chloro-acetoacetate. Reproduced with permission from [136].

Sugars in a variety of forms are rather common in biological processes. The sugar complexation leading to glycofullerenes opens interesting possibilities for biological applications. There are a number of possible routes of complexating fullerenes with sugars [137]. The most popular are: reaction via diazoniums, reactions with azides, the Prato reaction, the Diels-Alder reaction. The variety of chemical processes gives the possibility to attach different molecules producing simple complexes, branched complexes, and dendrimers [137]. During the reactions, the individual properties of fullerenes and sugars are generally retained though mutual influences have also been observed. In a study, glycofullerenes were utilized to recognize concavilin exploiting the binding affinity of this protein with glycofullerenes [138]. Affinity of glycofullerenes for specific molecules has been exploited for pathogen deactivation [139]. It has been shown that initial stages of viral infections proceed through the interaction of glycoconjugates on the surface of several pathogens with cellular receptors. In ref. [140], glycofullerenes were utilized to hinder this interaction, thus blocking the viral infections.

In particular, the mechanism is based on the capability of the glycofullerene to inhibit the C-type lectin DC-SIGN binding site on cell surfaces with the mannose-containing glycans [140], thus impeding the interaction with the Ebola virus as shown in Figure 5. Another interesting example is the use of glycol-functionalized C_{60} as a multimodal platform to bind lectins and carbohydrate-processing enzymes such as glycosidases which are essential in living organisms [141]. Carbohydrate-protein interactions are often at the basis of the adhesion of bacteria to living tissues leading to infections. To block the bacterial colonization, a possible strategy consists in inactivating the bacterial lectin's binding sites with high-affinity ligands. Fullerene sugar balls $C_{60}(8)_{12}$ and $C_{60}(18)_{12}$ showed an extraordinary affinity for the PA-IL (Pseudomonas aeruginosa lectin A) site and can be considered efficient anti-adhesive agents against Pseudomonas aeruginosa bacteria [142].

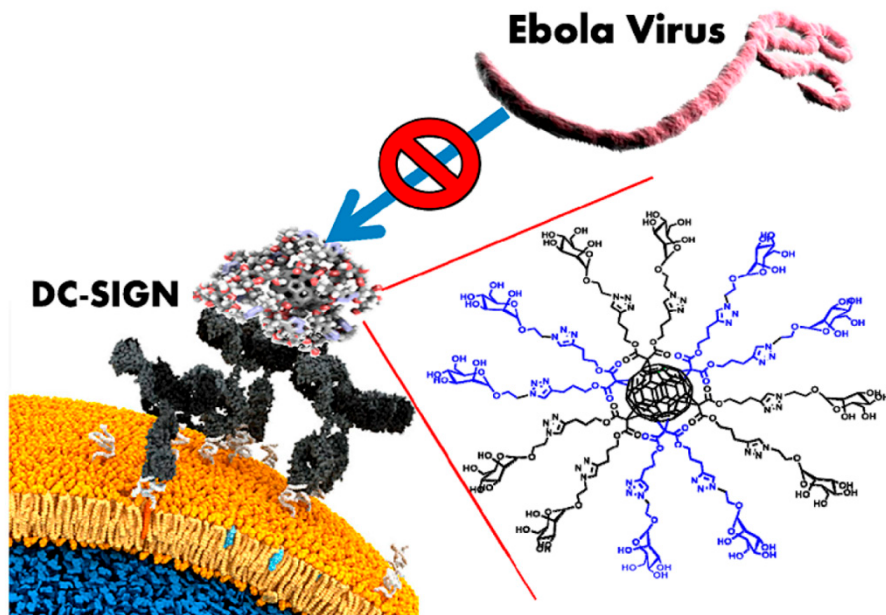


Figure 5. C_{60} glycofullerenes (sketched on the right) binds to the DC-SIGN cell site (in black) inactivating the interaction with the Ebola virus. Reprinted with permission from [140].

2.1.4. Diamond

Diamond is another interesting carbon structure widely utilized in biological research. In diamond, carbon atoms are sp^3 hybridized leading to a tetrahedral orientation of the strong covalent bonds. This symmetric arrangement of the four electron orbitals has a density higher than that of graphite, an unpaired resistance to compression, and hardness which, on both the Vickers and the Mohs scales, is the highest with respect to all other substances. To the high strength of the C–C bonds corresponds a high chemical inertness of the diamond surfaces. The possibility of depositing diamond films at reasonable cost by chemical vapor deposition (CVD) technology, was utilized in a variety of diamond-based technologies with outcomes in a number of commercial products.

Here we will confine our attention to the functionalization of nanodiamonds (NDs) since the same chemistry holds for the diamond films. NDs are produced by fragmentation of diamond powder, or are produced by CVD, laser ablation or detonation. In all the cases, NDs require a processing which consists in an accurate purification, deagglomeration, and fractionation. The quality of material manipulation during these steps strongly affects the properties of the final material.

The use of NDs in biology and medicine has begun when it was demonstrated that NDs do not influence the cell metabolic activity, the cell differentiation, growth, and proliferation [143]. In addition to the safety and high biocompatibility, NDs show a rich surface chemistry [144] which enables grafting a wide variety of molecules [145,146]. Depending on the synthesis method, the diamond surface is characterized by rather different chemistries. The identified chemical groups on the nanodiamond surfaces may include H, O, COOH, OH, CO, CNH, NH₂, CH₂, SH, alcohol functions, ether, anhydrides, and lactones [147]. The polarity of these moieties easily causes aggregation in most solutions unless a surface homogenization is performed [148]. This process is carried out under oxidative or reductive conditions leading to hydrogen terminated surfaces, hydroxylated surfaces or to a high density of acidic carboxyl groups. Reduction is generally performed using a plasma treatment while oxidation is obtained in strong acids. Finally, the surface hydroxylation is the result of a reduction treatment applied to the oxidized ND surfaces [148]. After surface homogenization, functionalization processes are generally applied to obtain colloidal dispersibility, solubility and stability in different media at different pH values, and specific chemical species needed for interaction with targeted biomolecules. In this regard, both covalent and non-covalent approaches may be utilized. Non-covalent interactions are utilized to immobilize drugs on the ND surface through hydrophobic

interactions [149,150]. The advantage of this conjugation is the possibility to suspend various water insoluble therapeutics preserving their functionality as demonstrated in [151]. Also, the electrostatic interaction developed by polar groups on the ND surface is exploited to attach the desired molecules. Carboxylated NDs were utilized to immobilize proteins through non-covalent interactions which can be useful for protein separation and proteomics [152]. The non-covalent interactions were also exploited to adsorb poly-L-lysineas that is the first step for further surface engineering of the NDs [153]. Another example is the electrostatic immobilization of lysozymes on the ND surface [154]. The authors demonstrated that the molecules are not denatured and after their adsorption much of the enzymatic activity is preserved.

The covalent bonding of specific molecular species to the ND surface is widely utilized in delivery of therapeutics. Using a photochemical reaction it was possible to covalently attach an amine layer on the NDs to further conjugate DNA strands [155]. Another example is the reaction of hydroxylated NDs with functional silanes [156]. The silanes can be used for subsequent grafting of active biomolecules as well as for the immobilization of other structures (monomers for polymerization, initiators, etc.). The covalent reactions occur on fluorinated or chlorinated diamonds obtained, for example, with direct reaction with fluorine gas at 400–500 °C [157]. Hydrogen terminated diamond surfaces can be chlorinated via thermal reaction [158] or with an electron beam irradiation [159]. Fluorinated and chlorinated diamonds may then be utilized for binding alkyl- and amino-groups, and aminoacids [160].

Finally, the ND surfaces may be functionalized utilizing polymeric molecules. Polyethyleneglycol (PEG) and polyglycerol PG are widely utilized to functionalize the diamond surfaces [59]. These polymers provide oxygen-based functionalities which improve the ND dispersivity and, at the same time, mimetic properties towards the immune system. Hydroxyl-terminated nanodiamond particles were functionalized using dopamine derivatives, bearing terminal azide groups or poly-N-isopropylacrylamide [161]. Other authors functionalized a carboxylated NDs with silane molecules rendering their surface hydrophobic [162]. In [163], the authors utilized two routes, namely hexamethylene diisocyanate and acyl chloride processing, to graft poly(ϵ -caprolactone) to NDs. The results demonstrate that the functionalization with the biodegradable polymer led to stable dispersions in various solvents. The NDs are also widely utilized for bioimaging. The diamond luminescence properties are based on the presence of color centers in the diamond matrix [164,165]. These defects are generated during the diamond synthesis or intentionally produced for example by an ion or electron bombardment. It has been demonstrated that the emission properties of the NDs are sensitive to surface chemistry [166]. The authors compared hydrogen, hydroxyl, carboxyl, ethylenediamine, and octadecylamine-terminated NDs samples. The results show that octadecylamine-functionalized particles possess the brightest fluorescence with respect to the other terminated diamond surfaces. In other works, authors demonstrate the use of NDs both for imaging and drug delivery applied to cancer therapy [167]. The rich surface chemistry, the small dimensions, the high biocompatibility are very attractive properties for using NDs as drug delivery fluorescent systems enabling theranostics. Thanks to the different kinds of surface termination obtained by different processing, it is possible to adsorb a variety of therapeutic molecules on the ND surface, such as doxorubicin, epirubicin, daunorubicin as well as mitoxantrone [167], that are potent DNA intercalating agents. In [168], the authors were able to efficiently deliver doxorubicin in living cells. In another work NDs were utilized to deliver doxorubicin in adenocarcinoma cells with pH activated drug release [169]. ND-Mitoxantrone complexes were utilized to kill the drug-resistant variant of breast MDA-MB-231 cancer cells [170].

2.2. Electrochemistry, Energy Conversion, Storage and Sensing

Electrochemical technology is becoming increasingly important in modern societies, due to the existing and the potential applications in crucial areas such as catalysis, energy conversion and storage, electro-synthesis, electrochemical/biochemical sensing, and recovery of environmental pollution. Key components in electrochemical processes are the electrodes. In this respect, CbMs occupy a special place for their properties which, among other, encompass high chemical stability, a good electrical

conductivity, and suitable porosity. Importance of these parameters is clearly shown in Figure 6 displaying a typical electrochemical cell such those in batteries and supercapacitors.

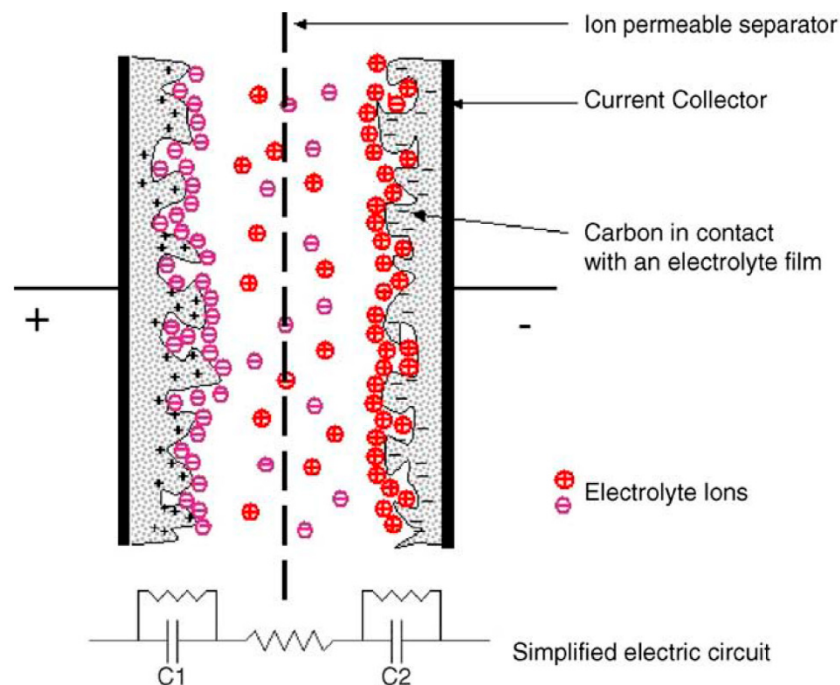


Figure 6. Representation of an electrochemical cell. The density of ions on the electrodes depends on electrode/electrolyte coupling, i.e., the surface wettability, the surface corrugation/porosity, the electrode resistivity. Reprinted with permission from [171].

However, alongside good material properties, a common problem with the CbMs is the low surface wettability. This generates important difficulties when these materials get in contact with an electrolyte. Change of the surface chemistry by functionalization is a common route to optimize the interaction of the carbon surface with the external environment [172]. As described above, the modification of the surface chemistry of CbMs strongly improves their solubility in both aqueous and organic environments rendering easier the development of new technologies.

An important consideration concerns the density of electronic states (DOS) of carbon-based electrodes, which changes greatly for different forms of carbon. For an electrode possessing a high density of states (DOS) the likelihood of electron transfer to a redox system is high. Presence of defects, disorder or changes in the surface chemistry which may affect the DOS, have remarkable effects on the charge transfer during redox reactions thus influencing the efficiency of an electrode. As an example, bonds with oxygen are very frequent and relevant in interfacial phenomena. Functionalization with oxygen groups results in a negative surface charge, which can lead to significant electrochemical effects on adsorption and electron transfer rates [173]. $\text{Ru}(\text{NH}_3)_6^{3+/2+}$ and $\text{Fe}(\text{CN})_6^{3-/4-}$ redox systems are useful benchmarks for comparing the electron transfer reactivity of various carbon electrodes. Both these redox systems are insensitive to presence of oxygen on carbon electrodes. A significantly slower kinetics of $\text{Fe}(\text{CN})_6^{3-/4-}$ is found when the electrode surface is modified with a monolayer of covalently bonded nitrophenyl groups [173]. Differently from the previous redox systems, $\text{Fe}(\text{H}_2\text{O})_6^{3+/2+}$ strongly depends on the presence of surface oxides and in particular carbonyl functional groups [174,175]. It was observed that presence of oxygen significantly accelerates the electron transfer between the $\text{Fe}^{3+/2+}$ and the carbon surfaces. Then, the different kind of functionalization and the methods utilized to achieve specific surface chemical composition assume a crucial role to improve the efficiency of electrochemical processes. Charge mobility, which is at the base of the chemical reactions, is also important in electronics. Different functionalization are applied to obtain the desired surface properties allowing optimization of CbMs in electronics are reviewed in [176].

2.2.1. Graphite, Graphitic Carbons, and Graphene

Recently, electrodes made of graphite and graphitic nanostructure pastes are utilized because they exhibit a large potential windows and low background currents, and a rapid surface regeneration. A clear correlation with the particle dimensions and the electrochemical activity was observed with an improvement of the heterogeneous electron transfer kinetics at smaller sizes. The accepted interpretation of this effect explains the heterogeneous electron transfer as primarily due to the reactivity of plane edge sites/defects while the basal planes are considered more or less inert [177,178]. This is due to a higher amount of oxygenated species at the edges of smaller particulate [179]. Considering the crystalline graphite as the highly-oriented pyrolytic graphite (HOPG), the defects density is rather low and found in regions as large as a few micrometers [173,180]. Thus, the main part of the surface is non-useful for electrochemistry and defects are mainly at step edges and grain boundaries. Defects created during exfoliation readily react with the atmosphere or water and bonds with oxygen are formed. The negative charge deriving from oxygen functional groups, and in particular the carboxylates, have significant effects on the electrochemical processes with enhanced adsorption of ionic analytes and increased electron transfer rates. Surface oxidation treatments are then performed to improve the electrochemical properties of graphitic carbons [181–183]. In graphitic carbons as disordered amorphous carbon, and glassy carbon, higher density of defect is present leading to much better electrochemical performances despite presence of residual C–H bonds limiting the electron mobility [173]. The use of plasma to graft oxygen-based functional groups dates back to the seventies [184], where a radiofrequency plasma was proposed as a more controlled alternative method to oxidation in air at high temperature able to introduce oxygen functionalities both at edges and in the basal planes. More recently, air, argon, nitrogen and oxygen discharge plasmas were utilized to enrich the surface of graphite electrodes with defects and electroactive sites [185]. The plasma-treated cathodes showed enhanced electro-Fenton oxidation of Acid Orange 7. In another work, the authors utilized ammonia and hydrogen plasmas to tune the electrical properties of graphite oxide [186]. Ammonia plasma led to tunable semiconducting properties of reduced graphite oxide useful for Field Effect Transistor (FET) devices. Using argon:hydrogen mixture, the authors were able to increase the graphite oxide conductivity to 630 S cm^{-1} .

Maleimide-thiophene copolymer functionalized with graphite oxide sheets was developed for polymer solar cell applications. The performances of the polymer solar cell were improved thanks to a better charge transfer/transport through the active polymer [187]. Water solutions of triethylmethylammonium methylsulfate and acetonitrile were utilized to produce oxygen based functional groups on exfoliated sheets of graphite. The nanographite platelets were then utilized to fabricate electrodes for supercapacitors reaching a specific capacitance value of 140 F g^{-1} at 0.25 A g^{-1} [188]. In another work [189], to optimize the supercapacitor performances, the graphite oxygen functionalities were adjusted in alkali electrochemical baths such as KOH, NaOH or LiOH. The electrochemical reduction of the graphite oxide led to a relatively high cation adsorption capacitance of 140 F/g .

The considerations drawn for the graphite electrochemistry hold for graphene-based electrodes. Graphene is obtained from graphite by exfoliation as described in Section 2.1, leading to strongly oxidized graphene sheets. Graphene oxide (GO) consists of a single graphite-like monolayer with randomly distributed oxidized aliphatic regions (sp^3 carbon atoms) containing hydroxyl, epoxy, carbonyl, and carboxyl functional groups. The epoxy and hydroxyl groups lie above and below each graphene layer while the carboxylic groups are usually located at the edges of the graphene patches. The presence of oxygen groups on the GO provides a remarkable hydrophilic character and an analogous reactivity. GO and reduced GO (rGO) are utilized to fabricate electrodes for electrical double-layer capacitors. Important when dealing with 2D graphene sheets, is avoiding the restacking induced by van der Waals and π - π interaction. To this aim, crumpled structures may be generated as in [190], which facilitate the charge transport especially at high current densities. In addition, the heterogeneous electron transfer depends also on the extension of the graphene flakes [191], thus affecting their electrochemical properties. In graphene, the density of defects is mainly linked to the

flake dimensions and, as seen for graphite, the chemistry associated with the defects plays a critical role in electrochemistry. A careful control over the degree of oxidation was performed on graphene sheets to optimize the charge transfer properties [192] of the graphene flakes. A possible chemical functionalization of graphene sheets is performed using diazonium salts [193]. This process results in a remarkable decrease of the conductivity due to the change of C-atom hybridization from sp^2 to sp^3 with disruption of the hexagon aromaticity. An alternative free radical addition to graphene is the reaction of benzoyl peroxide [194]. Graphene sheets deposited on a silicon substrate were immersed in a benzoyl peroxide/toluene and the photochemical reaction was initiated using an Ar-ion laser beam. The appearance of a strong D band at 1343 cm^{-1} proves the attachment of the phenyl groups to the graphene sheets.

Graphene can be functionalized with amine groups using the Leuckart reaction, which not only reduces the graphene oxide but leads to a 3.2% amination degree [195]. Other common methods utilized to aminate graphene include nitrogen plasma treatments, chemical vapor deposition, and the reduction of graphene oxide in nitrogen gas or ammonia [196,197]. Plasma treatments led to doping of the graphene oxide, and in general, to modification and improvement of its electrical properties. Considering energy conversion, attention is dedicated to dye-sensitized solar cells (DSSCs) for the low cost, easy fabrication and reasonable solar energy conversion [198]. Nitrogen-doped porous graphene foams (NPGFs) were produced hydrothermally treating a mixed solution of GO and ammonia leading to an overall power conversion efficiency (PCE) of 4.5% for the iodide-based electrolyte [199]. Nitrogen-doped graphene (NrG) was obtained by annealing a mixture of GO and cyanamide at $900\text{ }^\circ\text{C}$ in N_2 atmosphere, which was then utilized as an alternative to the Pt electrocatalyst for DSSCs obtaining a PCE of 5.4% [200]. In another work, 3D N-doped graphene structures obtained by freeze-drying graphene oxide foams and subsequent annealing in ammonia resulting in a PCE as high as 7.07% [201]. Besides amines, other kinds of graphene doping are performed using HNO_3 , HCl , H_2O_2 , SOCl_2 [202]. Comparing the best sheet resistance of the functionalized graphene sheets, the lowest sheet resistance was obtained in the case of SOCl_2 .

Finally, graphene patches in the nanometer size can be produced by liquid exfoliation of graphitic carbons. The edges of the nanoparticulate are functionalized by oxygen-based groups. The nanosized dimensions of graphene patches and the presence of functional groups lead to luminescent properties and for this reason they are called graphene quantum dots (GQD). GQD emission is in the blue-green range, they display high stability and absence of photobleaching. GQD can also be doped modifying the emission properties (see for example [203]). GQD have wide applications in different technological areas [204] such as photodetector [205], light emitting diodes [206], photocatalysis [207], biology [208]. More information may be found in [204,208]. Graphene optical properties can be exploited to fabricate graphene based optical biosensors. They are based on the efficient light absorption from UV to NIR. Graphene is generally functionalized to bind fluorescent molecules. The light emitted by these dyes is quenched by graphene when the two systems are coupled while dye emission becomes visible when the coupling is broken. This scheme was utilized to detect DNA folding or interactions with specific complexes [209], or to detect particular substances which can interact directly with the dye molecules [210].

2.2.2. Porous Carbon and Carbon Fibers and Felt

Differently from the crystalline forms of graphite and graphene, there are other systems in which carbon atoms are arranged in partially disordered structures characterized by different densities and degrees of crystalline perfection, or others with highly disordered structures as in glassy carbons. Similarly to graphite, glassy carbons have a bulk density greater than 1 g cm^{-3} , corresponding to pore volume/fractions <0.5 . Glassy carbon is produced by pyrolysis at high temperatures ($\sim 1000\text{ }^\circ\text{C}$) of resins, such as phenol formaldehyde. Lower temperatures lead to activated carbons, that are disordered networks characterized by higher number of defects and typically lower conductivity. Glassy carbons possess a highly cross-linked structure explaining the high Young modulus ranges from

20 to 40 GPa [49,211]. Glassy carbons display a closed porosity due to the presence of fullerene-like structures [212,213] which render the material impermeable to liquids. To improve the coupling with electrolytes, the surface of glassy carbon is functionalized by mechanical polishing, washing, plasma treatment, thermal and laser activation, ultrasonication, or by electrochemical treatments [49,214–216]. These pretreatments induce a grafting of radicals like NH⁴⁺ or of electroactive species such as hydroquinone that are specific for the desired application. The modification of the glassy carbon surface involves also the decoration with nanoparticles [217], nanotubes [218], other carbon nanostructures [219] to improve the electrode performances.

Activated porous carbons are a different form of carbonaceous materials which are obtained from coal, wood, petroleum pitch at high temperatures ranging from 600 to 900 °C in inert or oxidizing atmosphere, or using strong oxidizing acids or bases. Activated carbons are highly porous materials exhibiting a high surface area but much poorer mechanical properties. Electrochemical processes that produce interesting models of these two different disordered structures may be found in [220].

3-D electrodes made of porous carbon, carbon fibers, carbon felt and carbon in other structured forms have obtained great attention because they generally possess a high surface area. Typical values measured by Brunauer-Emmett-Teller BET method are: 500–3100 m²/g for porous carbon produced from different biomass precursors [221], 700–3100 m²/g for carbon fibers [222] and 1800–1970 m²/g for virgin and KOH treated carbon felt respectively [223]. Generally, these systems need a pretreatment to improve the coupling with the electrolyte and reduce the charge transfer resistance. They include plasma [224], irradiation treatments [225], thermal [226,227] and chemical processing [228–232]. It is demonstrated that these treatments induce oxygen or nitrogen functional groups on the carbon surface which affects the wettability of the electrodes and the redox reactions of the active species, the point of zero charge, the electrical contact resistance, the adsorption of ions (capacitance), and the self-discharge characteristics [225,231,233–235]. Generally, the carbon materials are derived from organic precursors by carbonization, a heat treatment in inert atmospheres. The ultimate properties of the carbonized materials are dependent on a number of critical factors such as the carbon precursor and its phase state during carbonization (i.e., gas, liquid or solid), the thermal processing conditions, and the structural and textural features of the ultimate products [236]. Carbonization is used to remove the volatile compounds and the heteroatoms leading to a pure graphitic-like carbon residual. The emission of these compounds leads to a porous structure. However, to increase the specific area, which is a key parameter to improve the charge transfer to the electrolyte, a thermal or chemical activation processes are generally performed [237,238]. The thermal activation is carried out at 700 and 1100 °C in the presence of suitable oxidizing gases. Wet chemical activation is performed at lower temperatures from 400 to 700 °C, exploiting the dehydrating action of phosphoric acid, zinc chloride and potassium hydroxide. As a result of the activation, a fraction of the carbon powder is principally functionalized with oxygen atoms, and, to a lesser extent, to hydrogen, nitrogen and sulphur depending on the original precursor utilized to produce the carbon powder [237]. The oxygen functionalities are preferentially generated at the edges or defects of the graphite like microcrystallites. Activated carbons easily react with oxygen (physisorption, chemisorption) also at room temperature and this is another reason making the carbon-oxygen complexes the more frequent functionalities [173]. Plasma treatments was applied to graphite nanofibers used as a supports for Pt-Ru catalysts [239]. The concentration of the functional groups on the electrode surface was tuned by controlling the plasma intensity, the N₂/O₂ proportion of the feeding precursors, and the treatment duration. The changes of the surface chemistry of the graphite nanofibers allowed a better control size and density of the Pt, Ru catalysts, enhancing the efficiency of the electroactivity of the nanofiber electrodes. In another work, activated carbons obtained from carbonization of coconuts, were treated in a dielectric barrier discharge plasma using H₂O vapors as activating gas [240]. The plasma treatment induced oxygen based functional groups grafting, and in particular carbonyl groups, leading to a better surface wettability and improved charge transfer to the electrolyte.

Generally, the functional groups increase the porous carbon wettability as well as that of carbon fibers and felt, thus improving the carbon/electrolyte coupling. In addition, carbons possessing a high concentration of oxygen-based acidic functionalities are prone to exhibit high rates of self-discharge in supercapacitors. This suggests that the oxygen functional groups act as active sites catalyzing the electrochemical oxidation or reduction of this class of carbon materials, or the electrolyte decomposition [241]. Also, nitrogen functional groups deeply modify the electrode electrical properties. As an example, N doping was obtained by chemically treating mesoporous carbon having a specific surface of $\sim 1900 \text{ m}^2 \text{ g}^{-1}$ [242]. Doping was induced in the graphene-like layered graphitic sheets with a HNO_3 treatment that preserved the material conductivity. In a 0.5 M H_2SO_4 electrolyte, the electrode displayed a specific capacitance as high as 790 F g^{-1} at 1 A g^{-1} . Nitrogen-Doped Carbon Nanocuboids arrays grown on carbon fibers were synthesized by pyrolyzing cobalt-containing zeolite imidazole frameworks [243] sketched in Figure 7. The active materials were used as supercapacitors were the doped carbon and cobalt provided the electron transport. The electrodes achieved an areal capacitance of 1200 mF cm^{-2} at 1 mA cm^{-2} , and highly stable performances with more than 90% capacitance maintained after 20,000 charge-discharge cycles.

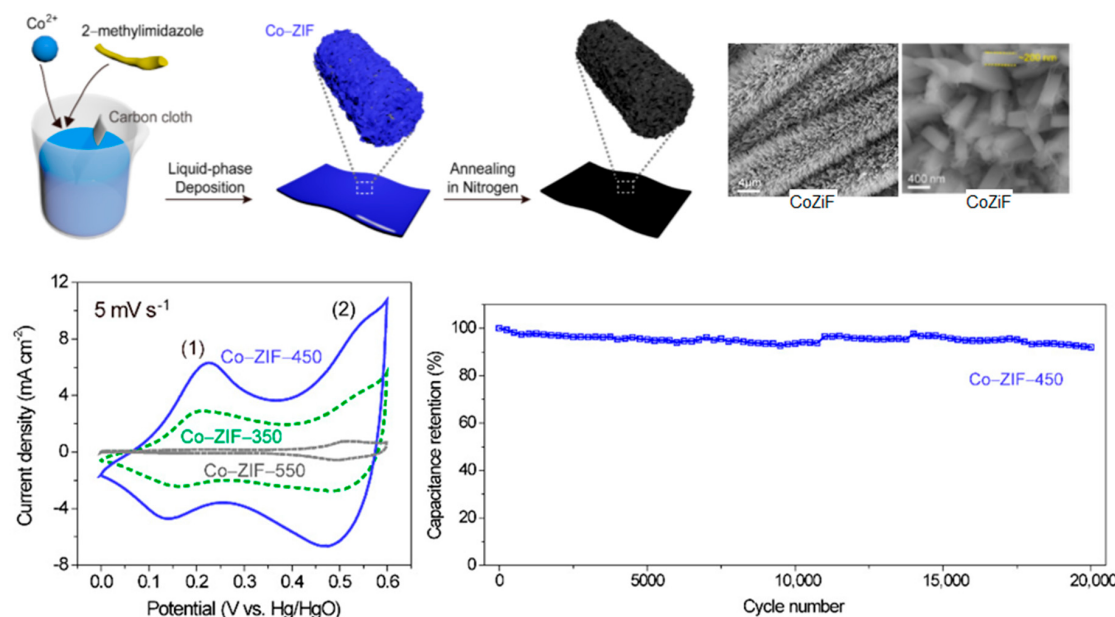


Figure 7. Top left, the synthesis scheme of cobalt-containing zeolite imidazole framework (Co-ZIF) and top-right the SEM image of the resulting material; bottom left the Cyclic voltammetry curves of Co-ZIF composites for obtained for Co-ZIF annealed at 350, 450 and 550 °C; bottom right, the cycling stability of Co-ZIF-450 after 20,000 consecutive charge-discharge cycles. Adapted with permission from [243].

However, the presence of surface oxygen also increases the resistivity of the carbon powders [244,245]. Bonds with oxygen increase the barrier for electrons to transfer from one microcrystalline unit to the next [246]. Then a careful balance between degree of wettability and oxygen-induced loss of conductivity is required. In [247], porous carbon activated by KOH was utilized as an electrode for supercapacitors and the effect of the surface porosity and of the chemistry was studied. In particular, the authors investigated the hydrogen chemisorption capability of the electrodes. The results show that the increase of oxygen species on the electrode surface enhances the wettability, thus favoring the H chemisorption. However, if the KOH carbon treatment generates pores with too small sizes, the active sites cannot be reached by the electrolyte preventing H chemisorption.

Amines can be electrochemically grafted on carbon surfaces using a large number precursors such as the primary amines (methylamine, n-butylamine, ethylenediamine, triethylenetetramine, nitrobenzylamine, aminomethylthiazole, . . .), the secondary amines (dimethylamine, diphenylamine, di-n-butyl, di-isobutyl, . . .), and tertiary alkylamines [248]. XPS shows that the grafting efficiency

is higher for the primary amines, it is about half with the secondary amines and hardly detectable for tertiary amines. Amines can react spontaneously with carbon fibers tough high concentrations, temperatures and long reaction times (15 h) are required [249].

The high specific surface area is also important in electrochemical sensing. Recently, a new type of glucose sensor based on porous carbon has been developed [250]. The sensor is based on porous, high surface area, fluorine-doped carbon obtained by pyrolysis of fluorinated polymer nanofibers. The fibers are then functionalized with a boronic acid receptor with a sensitivity from 50 μM to 5 mM of glucose, excellent specificity for fructose, ascorbic acid, and uric acid.

2.2.3. Carbon Nanotubes

Carbon nanotube electrochemical properties are also at the basis of the sensing functions. There are a few key parameters, which are fundamental in sensing applications: (i) a large surface area allowing great adsorptive capacity; (ii) a significant modulation of the electrical properties upon coupling with the analytes; (iii) the possibility to tune the electrical properties of the sensing element by changing composition and size; (iv) the possibility to fabricate the sensing element with desired geometries. In this respect, carbon systems and nanostructures are materials of choice also for the development of miniaturized chemical sensors. However, carbons have drawbacks like lack of specificity to different analytes and the low sensitivity towards analytes that have low affinity to them. The surface functionalization reduces these limitations and is unavoidable processing step. The electrochemical properties of carbon materials are utilized since years in biomedicine to sense the blood glucose. The sensing is based on a redox mediation between the carbon surface and NADH [251,252]. In some sensors, the electron transfer is mediated by electroactive species covalently bonded to the carbon surface [253]. Specific surface area is generally increased using carbon nanostructures and in particular CNT and graphene. However, Van der Waals attraction and π - π stacking lead to agglomeration of CNTs and graphene which strongly reduces the adsorption capacity of electrodes with loss of sensitivity. Functionalization renders these nanostructures more soluble in both polar and non-polar solvents protecting from aggregation. Surface functionalization is accomplished via covalent and non-covalent bonding.

Oxidation is the more common covalent functionalization of CNTs [59,172]. As already observed, oxygen functional groups are obtained on the carbon nanostructures using strong acid treatments [254,255]. Oxygen based groups lead to a reduction of the Van der Waals forces and allow a further surface engineering by attaching other molecules or nanoparticles as polymeric molecules, dendrimers, DNA strands, enzymes [256].

In a sensor, the sensitivity is related to the extent of electron transfer for a given redox reaction. The rate of electron transfer is proportional to the density of oxygen based functionalities on the electrode surface [257]. As a consequence, these functionalities accelerate the reaction kinetic and the sensitivity towards the analytes [258]. Other highly reactive species are utilized to functionalize CNTs, graphene and fullerenes like halogens, radicals, carbenes, or nitrenes [22,259]. Other popular reaction utilized to functionalize the carbon nanostructures are the cycloaddition and the amination processes [22,255,260]. Non-covalent functionalization relies on the electrostatic interactions, the van der Waals force, the hydrophobic or hydrophilic interactions, the π - π stacking to immobilize of biomolecules onto carbon nanostructures. In Figure 8, some of the chemical processes for CNT functionalization are schematized.

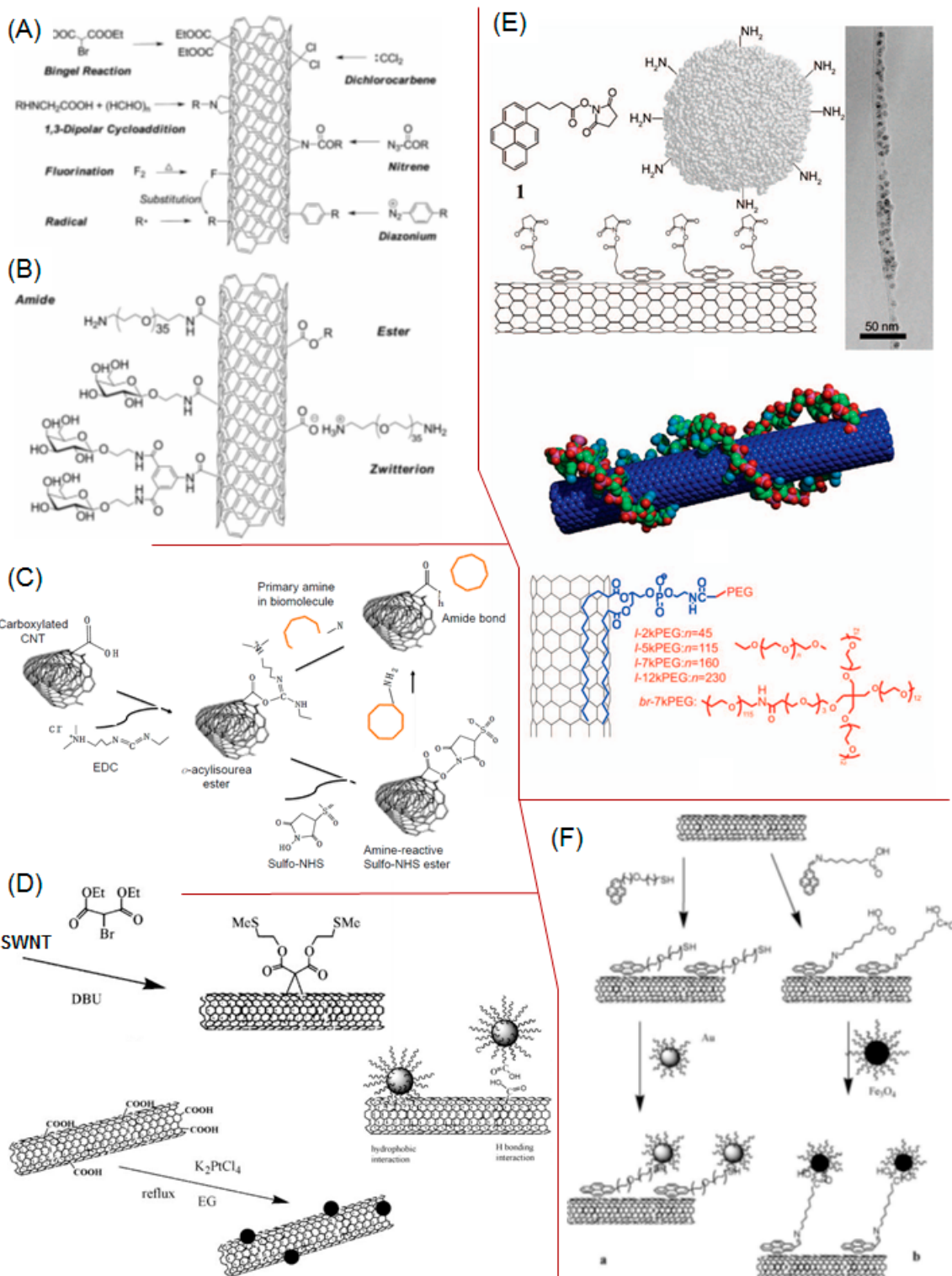


Figure 8. (A) Covalent addition reactions on the sidewall of carbon nanotubes. (B) Reactions targeting carboxylic acids (derived from nanotube surface defects). Reprinted with permission from [261]; (C) Reaction scheme for N-ethyl-N'-(3 dimethyl aminopropyl) carbodiimide methiodide (EDC) and EDC-N-hydroxysuccinimide (NHS) based covalent crosslinking of biomolecule with carbon nanotube.

Reprinted with permission from [262]; (D) Some decoration schemes involving chemical reactions and hydrophobic or hydrogen bonding. Reprinted with permission from [263]; (E) Schemes of non-covalent functionalization of carbon nanotubes. From top to bottom: proteins are anchored on the single walled carbon nanotubes (SWNT) surface via pyrene π - π stacked on a nanotube surface. Right: A transmission electron microscope (TEM) image of an SWNT conjugated with proteins; a SWNT coated by a single-stranded DNA via π - π stacking; a SWNT functionalized with PEGylated phospholipids. Both linear PEG (l-PEG) or branched PEG (br-PEG) can be used in this method. Reprinted with permission from [264]; (F) Noncovalent attachment of gold or magnetic NPs onto SWNTs using pyrene derivatives as interlinkers. Reprinted with permission [263].

The enzymatic biosensors couple the high specificity of the enzyme with the electrochemical sensitivity of the electrodes providing interesting perspectives in the early diagnosis [265]. CNT-based biosensors with this configuration have also been used to monitor biological reactions. This kind of sensor was utilized to follow the enzymatic degradation of starch [266]. Non-covalent adsorption of enzymes preserves the structural integrity; however, enzymes may progressively be lost during the use. In [267], the enzyme was adsorbed into a CNT/graphene polymer to solve the problem. High sensitivity was obtained functionalizing a forest of CNT coated with gold and then modified with GO_x [268] obtaining a detection limit of 0.01 mM glucose. DNA can be adsorbed on CNT although covalent attachment via COOH-groups increases the conjugation stability. In [269], the fast charge transfer between CNTs and daunomycin, selected as the redox intercalator, led to a detection sensitivity of $1.0 \times 9 \times 10^{-10}$ mol L⁻¹ in differential pulse voltammetry measurements. In another work the Mn(II) complexes were selected as intercalators for charge transfer from DNA to CNTs leading to a detection limit of $1.4 \times 9 \times 10^{-10}$ mol L⁻¹ [270]. Other authors utilized single wall CNTs to fabricate an impedance DNA sensor [271] conjugated with DNA single strands. A change of impedance was measured upon DNA hybridization. CNT are also utilized in FET sensors as sketched in Figure 9. Semiconducting SWNT is utilized as a gate electrode and can change the electrical FET characteristics when a molecule binds on its surface [272–274]. Recently, graphene and graphene-CNT based FETs were developed for sensing applications. FET biosensors based on graphene based were constructed to detect DNA hybridization [275–277]. Ultra-sensitive FET were fabricated integrating graphene and CNT in the gate electrode [278]. The high selectivity of the biorecognition element immobilized on the CNTs and the high sensitivity of the FET allowed detection of mRNA at attomolar concentration levels. FET sensors are utilized also for detection at molecular level. When uncharged molecules are targeted, no electrostatic gating is present, thus inhibiting the FET sensing. To circumvent this problem, the gate elements (CNT, graphene or Graphene-CNT) are functionalized with specific biorecognition molecules (e.g., antibodies) which strongly amplify the amount of analyte bound on the gate electrode thus inducing appreciable and detectable electrical changes in the sensor [279–281].

The CNTs may be utilized as optical biosensors. Upon excitation, semiconducting single walled CNTs (SWCNTs) can emit a photons in the NIR range [282]. Since the SWCNTs bandgap is sensitive to the chemical environment, the DNA polymorphism on SWCNT conjugations were optically detected [283]. Polyethyleneglycol (PEG)-modified SWCNTs functionalized with specific antibodies can selectively recognize cells with the appropriate surface receptor. This idea was utilized to recognize HER2/neu-positive breast cancer cells [284].

Finally, CNT are utilized also in dye sensitized solar cells (DSSC) for efficient energy conversion. In [285], multi walled CNTs (MWCNTs) were successfully integrated in poly(3,4-ethylenedioxothiophene) (PEDOT), polyaniline (PANI) and polythiophene (PTh) using RF-rotating plasma grafting method. The composites were used as counter electrodes in DSSCs showing short-circuit photocurrent densities of 11.19, 10.70 and 8.54 mA/cm² for PANI/MWCNTs, PTh/MWCNT and PEDOT/CNTs, respectively. In [286] a 3D structure made of graphene/CNTs with a transmittance of 56.6% was synthesized. The DSSC showed a maximum PCE of 10.69% which was attributed to the three-dimensional system structure characterized by a large specific surface area. Interestingly, ink-jet printers are recently utilized in the area of flexible electronics [176]. In [287], the

authors utilized dodecyl-benzene sulfonate as a surfactant to suspend SWCNT in water. Then they utilized the suspension as an ink to screen print electronic circuits on cellulose.

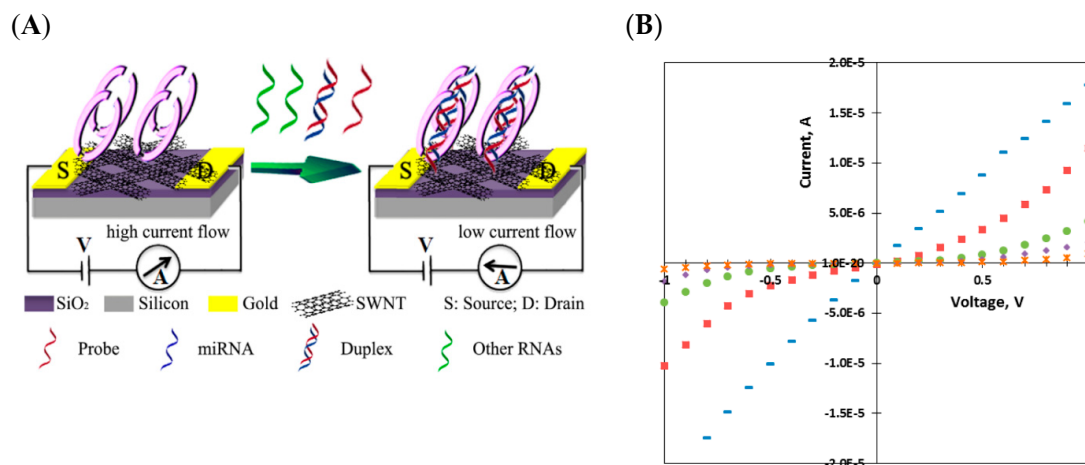


Figure 9. (A) schematic of miRNA detection principle by the p-19 functionalized carbon nanotubes-field effect transistor (CNTs-FET) nanobiosensor; (B) I–V characteristics of the biosensor at various stages of miRNA detection. (blue –) Bare CNTs; (pink ■) CNTs functionalized with 1-pyrenebutanoic acid succinimidyl ester (PBASE); (green circle) after p19 immobilization; (purple ♦) after blocking unoccupied sites with Tween 20; (orange x) 10 μL of 10 fM miRNA-122a target + 1 μM miRNA-122a probe after 1 h incubation at 37 $^{\circ}\text{C}$. Reprinted with permission from [278].

2.2.4. Fullerenes

Coupling carbon nanostructures to materials for electrocatalysis has been recently explored as an effective route to improve their electrochemical properties [288]. In this respect, graphene and CNTs are widely utilized to enhance the electrical conductivity and electrochemical activity of composite electrodes [289–291] which are also characterized by expanded surface area. These 2D carbon systems are also coupled to inorganic materials like metals, hydroxides, metal oxides, and metal chalcogenides to improve their functionalities. For this reason, fullerenes can be utilized as electrodes in different areas such as fuel cells, photovoltaics, screen printed systems, and sensing. Despite the promising electrical properties and the high electrical conductivity, fullerenes has been much less used to fabricate high performance electrodes compared to graphene and CNTs. In redox processes, fullerenes display a high electrochemical activity [292]. This derives from the strong electron-withdrawing ability of the fullerenes [293] leading to a prominent modification of the electronic structure of the chemical species during hybridization. An example is the coupling of the fullerenes with the positively charged Ni-Fe-layered double hydroxide (LDH) with a significant change of the electronic structure of the 2D LDH thin layers. This has beneficial effects on the electrical properties of the composite electrodes thus improving the performances of batteries, and supercapacitors [294].

The carbon particulate is commonly used as catalyst supports because of the high specific surface area and good electric conductivity. In this respect, the special features of fullerenes including electrochemical stability, small size, specific morphology, and good thermal conductivity enable their application in energy conversion systems [295]. As an example, fullerenes are integrated in electrodes of a direct methanol fuel cells (DMFCs) [296]. In DMFCs C_{60} is coupled to Pt to improve the catalytic oxidation of methanol [297] thanks to its strong electron accepting ability [298]. Fullerenes also find applications in organic photovoltaics where an electron-deficient compound (acceptor) and an electron-rich conjugated polymer (donor) are coupled together to generate charge separation under light irradiation. Recently, fullerenes are introduced in polymer solar cells (PSC) as acceptor substances due to their inherent high electron affinity and conductivity [299]. Different combinations of polymer/fullerenes have been tested to fabricate the active layer of the PSCs [300]. The best results were obtained coupling a [6,6]-phenyl-C₆₁-butyric acid methyl ester/C₆₀ derivative, used as electron acceptor

with poly(3-hexylthiophene) which is an electron donor, reaching a PCE of up to 5.5% for single layer devices [301]. Other works show that functionalizing the fullerene cage with donor molecules like triphenylamines or indenes has positive effects on the overall performances of the PSC [302]. One problem that affects PSCs is the exciton diffusion range which is 10 times shorter than the optical absorption, leading to frequent charge recombination. Fullerenes are introduced in the heterojunctions based on poly(3,4-ethylenedioxothiophene) polystyrene sulfonate (PEDOT:PSS) to enhance the charge separation. In [303], the authors combined C₆₀ with graphene oxide/poly(3-hexylthiophene) (GO-P3HT) hybrid as illustrated in Figure 10. The GO-P3HT/C₆₀ photovoltaic device displayed a 200% increase in the PCE respect to the pure P3HT/C₆₀ analogous system. The increase in the device efficiency is attributed to an extended electron delocalization induced by GO in comparison to pure P3HT.

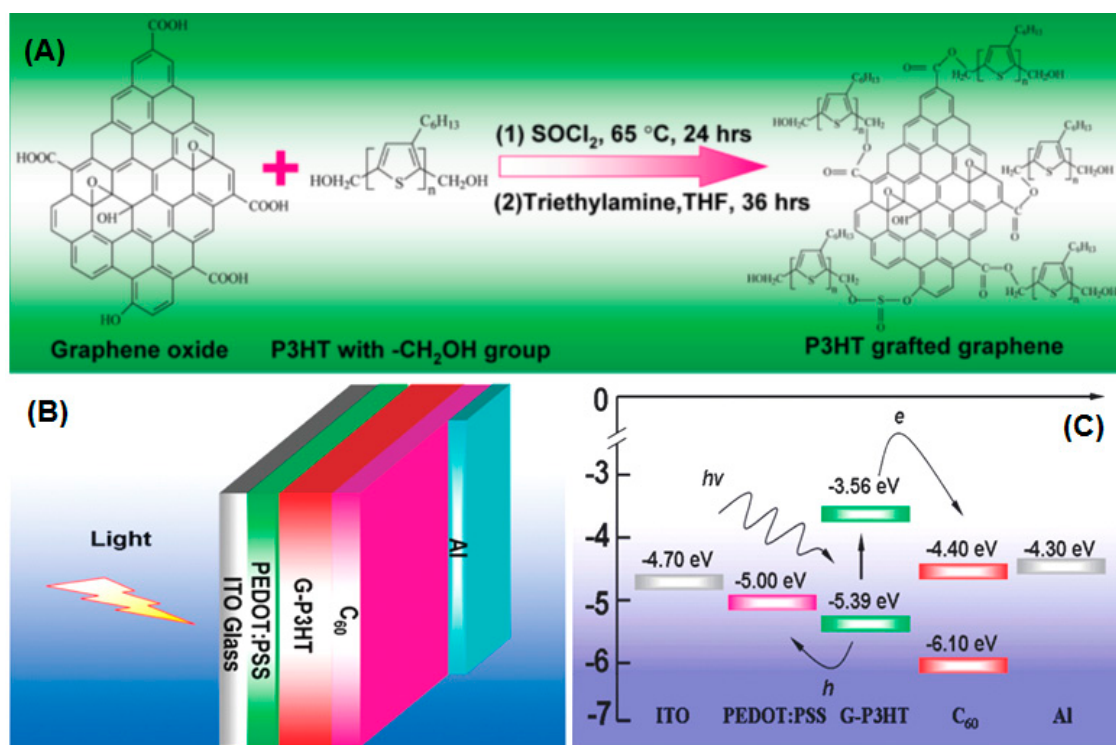


Figure 10. (A) Synthesis procedure for chemical grafting of CH₂OH-terminated P3HT chains onto graphene, which involves the SOCl₂ treatment of GO (step 1) and the esterification reaction between acyl-chloride functionalized GO and MeOH-terminated P3HT (step2). (B) Schematic and (C) energy level diagram of an ITO/PEDOT: PSS/G-P3HT/C₆₀/Al photovoltaic device. Reprinted with permission from [303].

Finally, fullerenes are extensively used in sensing due to the possibility to functionalize the surface through different reactions. We briefly mention the Bingel reaction consisting of a cyclopropanation, the Diels-Alder [4 + 2] cycloaddition reaction, the Prato [3 + 2] cycloaddition reaction, the [2 + 2] cycloaddition, and others [22]. These reactions are sketched in Figure 11.

The Bingel reaction is frequently utilized to add a deprotonated halo ester or ketone to one of the double bonds in C₆₀. The cyclopropanation is utilized to prepare fullerene derivatives for biomedical applications [304]. In [305], the authors were able to immobilize DNA onto a screen printed electrode impregnated with fullerenes for detecting DNA strands of *Escherichia coli*.

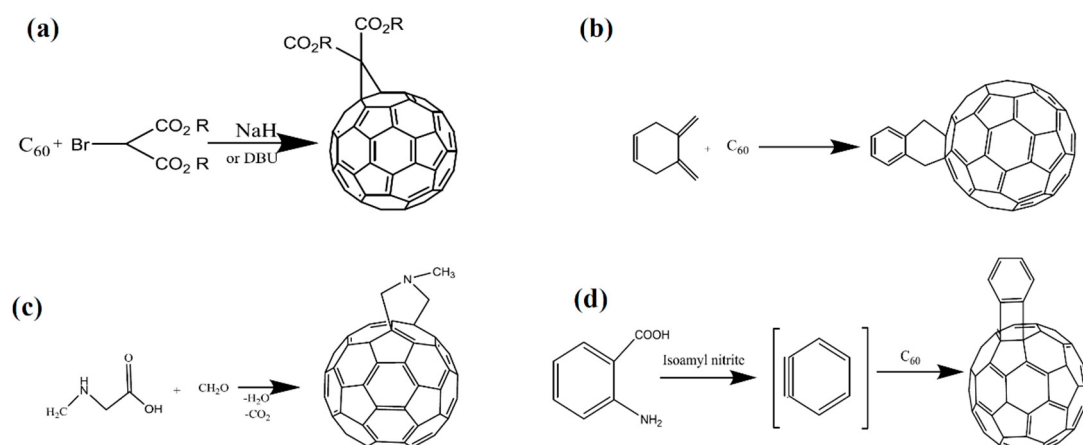


Figure 11. (a) The Bingel reaction; (b) the Diels-Alder reaction; (c) the Prato reaction; and (d) the Cycloaddition reaction. Reprinted with permission from [306].

The Bingel reaction has been frequently used to prepare C_{60} derivatives in which a halo ester or ketone is first deprotonated by a base and subsequently added to one of the double bonds in C_{60} resulting in an anionic intermediate that reacts further into a cyclopropanated C_{60} derivative. Amines also react with C_{60} [307] showing different reaction patterns, forming hydrogenation products or aminoketal-fullerenes upon the amine precursor utilized [308,309].

An aptasensor [310] was developed by mimicking a bi-enzyme cascade catalysis leading to formation of O_2 and consequent detection of the thrombin aptamer via electrochemiluminescence [311]. Most of the limitations of conventional immunosensors such as complexity and the need signal amplification, can be solved using nanostructures like C_{60} . In fact, fullerenes, as electrophilic molecules, can be attacked by amines, antibodies, and enzymes which are electron-donating molecules. This principle is exploited to fabricate fullerene-antibody immune sensor [312] composed by a C_{60} , ferrocene (Fc) and thiolated chitosan (CHI-SH) composite utilized to bind avidin coated Au nanoparticles. The avidin was then utilized to capture antibodies of *Escherichia coli* exploiting the biotin and avidin covalent reaction. Fullerenes were also utilized to detect glucose oxidase GOD important for the diagnosis of diabetes. GOD is an enzyme catalyzing the oxidation of glucose with the production of gluconic acid and hydrogen peroxide. Fullerene C_{60} is expected to efficiently immobilize the electron donating GOD molecules. In [313], the authors fabricated a GOD/fullerene platform to catalyze the glucose oxidation producing gluconic acid that was detected by a piezoelectric system.

2.2.5. D Hybrid Structures

As discussed previously, the specific surface area of electrodes is a key parameter governing the electrochemical processes. Use of carbon nanostructures as graphene, CNTs, carbon fibers, fullerenes and their mixture is used to generate high specific surface materials. 3D porous systems were fabricated either using graphene nanofibers [314], combination of carbon nanostructures [315] or nanoporous carbon sheets [316]. Thanks to the hierarchical nanoporous structures, these materials display good ion transport and electrolyte permeability. Another strategy to optimize the specific surface is the coupling of different carbon nanostructure ensuring accessible ion transport channels while increasing the electrode energy density. As an example, porous coupling CNT to graphene fibers allowed optimizing the ion accessibility to the electrode surface. The electrodes showed excellent mechanical flexibility and structural stability with negligible capacitance differences upon bending and twisting [317].

CNTs and graphene are also utilized in gas sensors. Sensing is based on the change of the electronic properties of these materials upon adsorption of the gas molecules on their surface. Essentially, gases like NH_3 and H_2 are electron donor so that a charge transfer occurs when these molecules adsorb on the CNTs and graphene thus modifying their conductance increasing their resistivity. In contrast, electron acceptor gas molecules such as NO_2 and O_2 induce a resistance decrease [318–320]. Measuring

the change of the resistivity, a qualitative and quantitative information about the gas is obtained. Unfortunately, these kinds of sensors suffer from low specificity and sensitivity. These problems can be solved by an appropriate decoration of CNT and graphene surfaces with metal nanoparticles. Functionalization of these carbon nanostructures is utilized to attach metal nanoparticles like Pt, Ag, Au, Al, Cu, Sn, Pd which enable selective sensing of gases like H₂, NH₃, NO₂, CH₄, H₂S, and CO [321–324] and their oxides [325–329]. More information about CNTs, graphene gas sensors may be found in [318,320,330]. Mixed fullerenes CNTs hybrids were utilized to fabricate a gas diffusion electrode for the production of H₂O₂ with a production rate of 4834.57 mg·L⁻¹ h⁻¹ [331]. Fullerenes CNT hybrids are utilized to fabricate highly performing electrocatalysts for the oxidation of catechols utilized to detect presence of tumor necroses [332]. Sequences of single stranded DNA were physisorbed on C₆₀/CNTs complexes that were utilized to modify a glassy carbon electrode to sense dopamine [333]. C₆₀/graphene hybrids were utilized to fabricate superior electrodes for supercapacitors [334]. Modified electrodes led to a specific capacitance of 135.36 F g⁻¹ at the current density of 1 A g⁻¹ that outperforms that of pure graphene of 101.88 F g⁻¹.

2.3. Composite Materials

Carbon nanomaterials are widely utilized in combination with a large class of materials to improve their properties. Composite materials are then utilized in a number of different applications as packaging, automotive, aerospace, energy, healthcare with an annual global market expected to reach \$5 billions in 2020 [335]. The carbon nanostructures utilized in composites materials are graphene nanoplatelets (GNPs), carbon nanotubes (CNTs), carbon nanofibers (CNFs), and carbon black (CB). Generally, they are incorporated in the materials to improve their mechanical properties (tensile strength, stiffness, fracture toughness, etc.) as sketched in Figure 12, enhance the electrical conductivity and the thermal stability, decrease gas permeability and improve the flame-retardant properties. CNFs are a good example. They find application where strength, stiffness, outstanding resistance to fatigue and low weight are key requirements. They are also utilized where chemical inertness, high temperatures, electrical conductivity and high damping are critical criteria [336]. When the interaction between nanostructure and matrix is strong, composites display much better mechanical properties deriving from the large interfacial area [337]. Conversely, when CNFs are used without surface treatment, they produce composites with low interlaminar shear strength due to the weak adhesion and poor bonding between the fiber and matrix [338]. The CNFs surface is chemically inert, it leads to an insufficient adhesion with the hosting matrix.

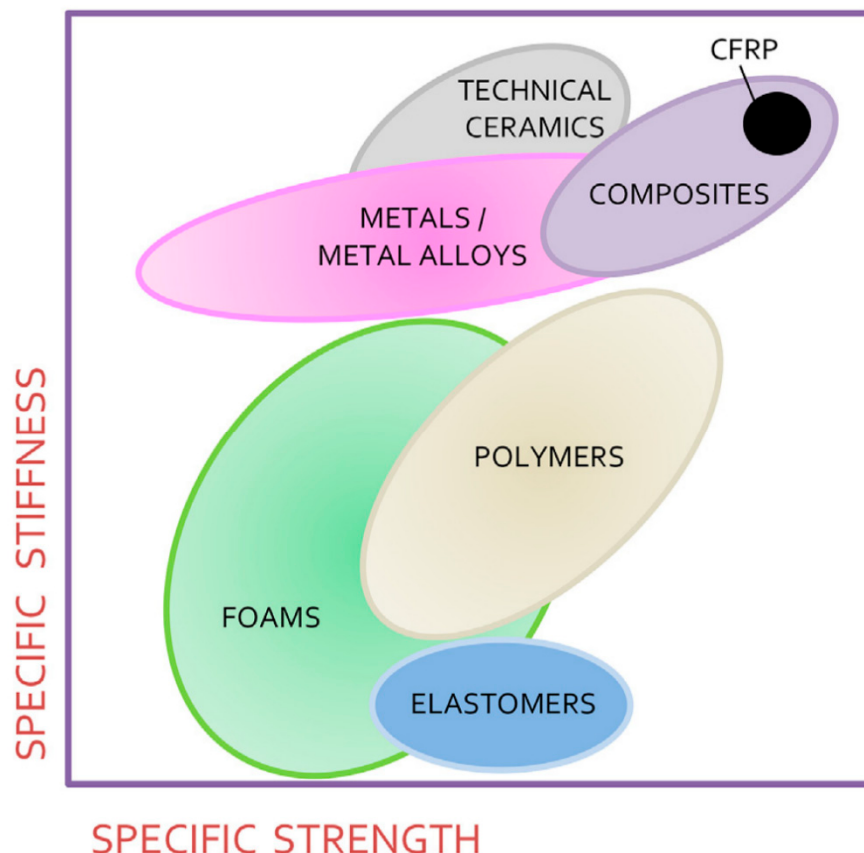


Figure 12. Simplified log-log Ashby diagram showing the specific stiffness against specific strength for different engineering materials. Reprinted with permission from [339].

2.3.1. Carbon Nanofibers and Carbon Nanotubes

Surface functionalization is an essential step of the synthesis of composite materials. Adhesion can be improved by increasing the CNFs surface roughness. Physical methods enhance the density of contact points, micro-pores and pits in an already porous surface. Chemical methods involve grafting of functional groups leading to a stronger interaction with the surrounding matrix. Extensive description of the surface functionalization of the carbon nanostructures is reported in the previous sections. Chemical modifications of CNFs often involve both changes simultaneously. Oxidation of CNFs is induced by acid (nitric, hydrochloric, etc.), ozone, air at high temperature or plasma treatments [340]. O-C-, -C=O, -O-C=O functional groups were obtained on CNFs surface with a HNO₃ acid treatment [341]. Oxygen groups increased the surface wettability and the adhesion of with polyimide (PI) matrix. Same treatment was applied to oxidize CNFs surface increasing the number of sites active for hydrogen and Van der Waals forces improving the adhesion with PI [342]. Other kinds of CNT functionalization utilized for composite production are fluorination and derivative reactions, hydrogenation, cyclopropanation and cycloaddition, radical attachment, amidation esterification thiolation silanization [343].

The authors of [344] describe a plasma treatment by air dielectric barrier discharge (DBD) at atmospheric pressure to treat the surface of CNFs to induce COOH, -C-OH and =C=O groups leading to a higher reactivity between fiber surface and matrix and a higher surface roughness. Atmospheric CO₂ and O₂ plasma treatments were used to activate graphite nanoplatelets as well as highly graphitic fibers used as reinforcing elements in composites [345]. The plasma treatments induced an increase of the oxygen functionalities on the treated surfaces. The inclusion of the functionalized graphitic nanoplatelets and fibers in epoxy resins led to an increase of the tensile strength up to 50% and 79% respectively.

Considering high performance materials, CNTs exhibit a tensile strength 10 times higher than that of CNFs and a Young's modulus six times higher than that of steel [346]. It is then expected that CNT based composites will display much better properties as compared to CNFs. As a matter of fact, experiments show that CNTs-based polymer nanocomposites possess an interfacial average shear stress of ~500 MPa which is much larger than of conventional fiber composites [347]. 1 wt % of multi walled CNTs embedded in polystyrene elastic modulus and break stress increase 36–42% and ~25%, respectively [348]. An improvement of 3.5 times of the material hardness was obtained adding ~ 2 wt % of SWCNTs to an epoxy matrix [349]. At the same time, samples loaded with 1 wt % unpurified SWNT material showed an increase of 125% in the thermal conductivity at room temperature and the enhancement was three time higher with respect to vapor grown carbon fibers. Nanocomposites based on epoxy resins and MWCNTs organized in 1D and 2D structures improving the material resistance with an increase of 138% in fracture strength in comparison to the neat epoxy matrix [350]. CNT/polymer nanocomposites were prepared by free radical polymerization of an imidazolium ion-based ionic liquid containing a methacrylate group [351]. With an inclusion of 7 wt % of SWCNT, the authors reported a 120-fold enhancement of the Young's modulus with respect to the parent unmodified methacrylate. In addition, such a high amount of SWCNT led to a remarkable improvement of the electrical conductivity of the material.

2.3.2. Graphene Oxide

Similar improvements are obtained using graphene as filler [352], which remarkably improves also the electrical conductivity [353] and the gas barrier properties [354]. Graphene oxide obtained by chemical exfoliation generates oxygen-containing polar functionalities such as carbonyl, hydroxyl, epoxides, and carboxyl groups [355]. Oxygen groups are utilized to form amide groups by reacting the amine group in N-ethyl-N'-(3 dimethyl aminopropyl) carbodiimide methiodide (EDC) with the carboxyl group in GO [355]. Poly (2-(dimethylamino)ethyl methylacrylate) was grafted to GO via atom transfer radical polymerization [356]. GO can be coupled to hydrophilic polymers as and poly(ethylene oxide) (PEO) [357] and poly(vinyl alcohol) (PVA) [358], to form nanocomposites. Organic isocyanates can react with carboxyl and hydroxyl group of the GO which, in turn, are known to form composites with polystyrene, acrylonitrile-butadiene-styrene (ABS), and styrene-butadiene rubbers [359]. Other examples are addition of GO to polystyrene [360], polymethylmethacrylate [361], polyurethane [362,363], polyvinyl acetate [364,365], polyaniline [366] and polyesters [367]. In all cases it was observed an improvement of the polymer mechanical properties. Graphene based nanocomposites were successfully implemented in electrochemical applications [368,369], supercapacitors [370,371], lithium ion batteries [372,373], solar cell [374,375], sensors [376,377], drug delivery and tissue engineering [378–380], water purification [381,382].

2.3.3. Nanodiamonds

Among the carbon-based materials utilized in composites are also nanodiamonds (NDs). As for the other carbon nanostructures, also in the case of NDs the surface chemistry strongly influence the properties of the nanodiamond based composite [383]. There are two main routes to perform the functionalization of the ND surfaces: wet chemical processes at low temperatures or gas treatment at high temperatures [384,385] which are illustrated in Figure 13.

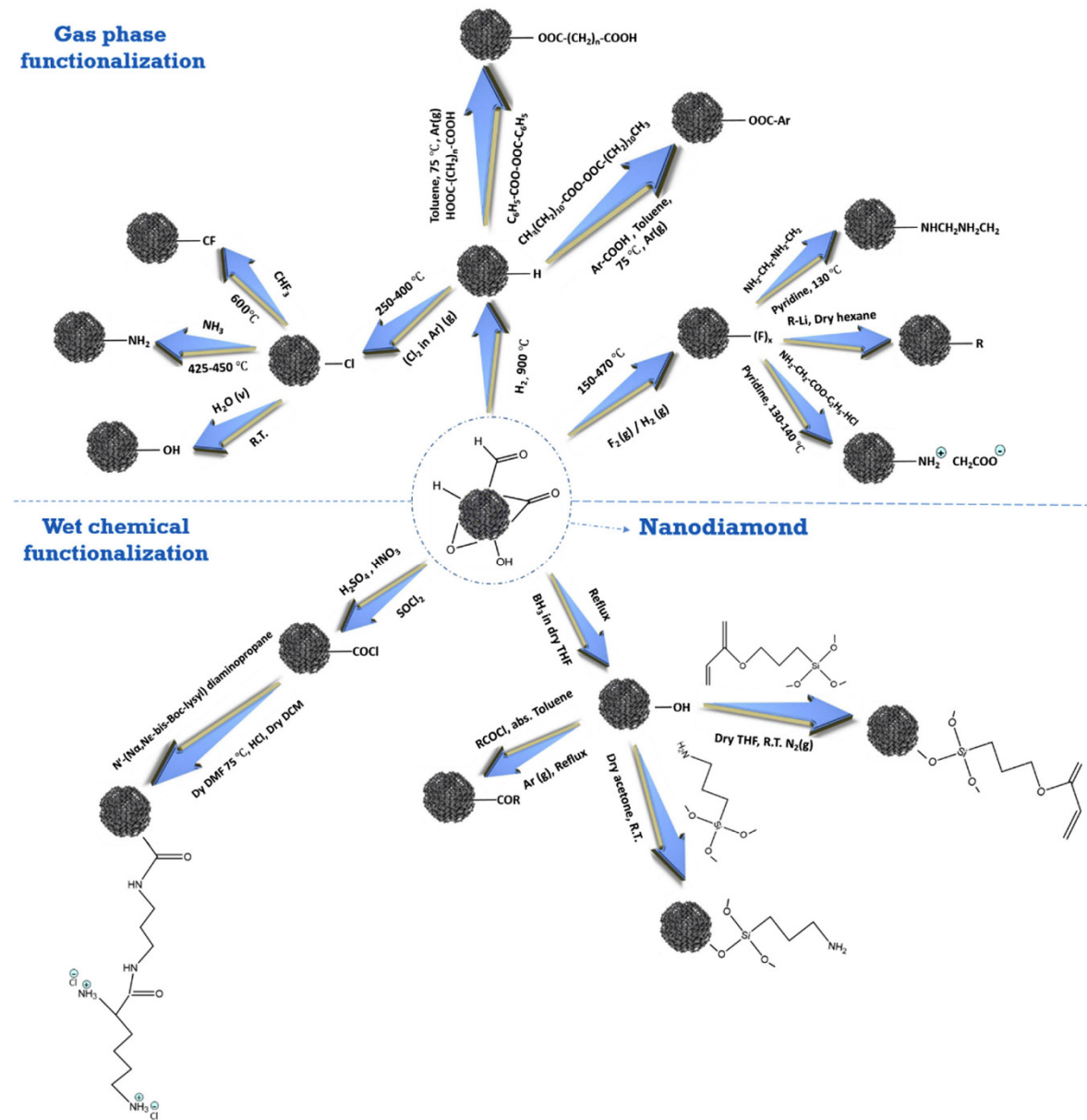


Figure 13. Representation of different approaches for surface functionalization of NDs. Reprinted with permission from [386].

In the case of wet chemistry, strong acids (H_2SO_4 , HNO_3 , HCl) are generally utilized to graft oxygen based and chlorine functionalities [387–389]. These polar functionalities render the NDs dispersible in polymeric matrixes [390–395] and are utilized to improve the composite mechanical properties. Amination is another widely utilized functionality to couple NDs with other organic molecules as in [396] where functionalization of NDs led to covalent bonding with the epoxy matrix. This led to three times higher hardness, 50% higher Young's modulus, and two times lower creep compared to the composites in which the NDs were not chemically linked to the matrix.

In another work, inclusion of NDs 0.5 wt % in cellulose acetate membranes induced maximum improvement in hydrophilicity and higher critical flux and anti-fouling properties were obtained with inclusion of PEG functionalized NDs [397]. A good degree of oxidation can be obtained also with reactive gasses alogenated [398]. Surface fluorination was utilized to prepare a series of functionalized nanodiamonds by subsequent reactions with alkyl-lithium reagents, diamines, and amino acids to obtain fluoro-nanodiamond and the corresponding alkyl-, amino-, and aminoacid-nanodiamond derivatives [160,399]. Finally, non-covalent functionalization based on electrostatic interaction has

been also utilized to modify the ND surface. In [400], the authors utilized oleylamine as surfactant which interacted with carboxyl groups of the NDs through a charge transfer. Other examples are the use of the electrostatic interaction to couple NDs in epoxy based composites [401] or in polyacrylic matrices [383].

3. Conclusions

Carbon-based materials are utilized in a broad variety of applications ranging from the electronics, electrochemistry and sensing, energy, biomedicine, composites, airplane and automotive, and environment. A key element is the interaction of the carbons with the external environment. In this respect, the functionalization processes play a critical role defining the surface properties which are at play in regulating the material solubility in various solvents, its electrical properties, the chemical reactivity, or determining the coupling with other materials as in composites or the interaction with therapeutic substances and with living matter. As a consequence, different functionalization techniques were developed for specific applications. There is a variety of covalent and noncovalent modification of the carbon surface involving different chemical or physical treatments. This review provides an overview of the recent research works on carbon systems with new insights into the processing and consequent material properties. Interaction with other substances or with the external environment needs great attention in choosing the correct treatment to avoid undesired outcomes. In this regard, great effort has been devoted to implement the efficient surface modification strategies providing the desired surface chemistry. In conclusion, carbon-based materials either in bulk or nanosized particulate, offer great challenges in making the research exciting. The extraordinary long list of applications makes carbon an “ever green” material still rich in opportunities for future new developments.

Funding: This research received no external funding.

Conflicts of Interest: The author declares no conflict of interest.

References

1. Prasanth, R.; Ammini, S.K.; Ge, L.; Thakur, M.K.; Thakur, V.K. Carbon Allotropes and Fascinated Nanostructures: The High-Impact Engineering Materials of the Millennium. In *Chemical Functionalization of Carbon Nanomaterials: Chemistry and Applications*; Taylor & Francis Group, LLC: Boca Raton, FL, USA, 2016; pp. 3–28.
2. Thakur, V.K.; Thakur, M.K. *Chemical Functionalization of Carbon Nanomaterials: Chemistry and Applications*, 1st ed.; CRC Press Taylor & Francis Group: Boca Raton, FL, USA, 2016.
3. Dos Santos, M.C.; Maynard, M.C.; Aveiro, L.R.; da Paz, E.; dos Santos Pinheiro, V. Carbon-Based Materials: Recent Advances, Challenges, and Perspectives. In *Reference Module in Materials Science and Materials Engineering*; Elsevier: Amsterdam, The Netherlands, 2017. [[CrossRef](#)]
4. Toktam, N.; Tan, A.; Seifalian, A.M. Different Functionalization Methods of Carbon-Based Nanomaterials. In *Chemical Functionalization of Carbon Nanomaterials: Chemistry and Applications*; Taylor & Francis Group, LLC: Boca Raton, FL, USA, 2016; pp. 29–58.
5. Field, J.E. *The Properties of Natural and Synthetic Diamond*; Academic: New York, NY, USA, 1992.
6. Kalish, R. Diamond as a unique high-tech electronic material: Difficulties and prospects. *J. Phys. D* **2007**, *40*, 6467–6478. [[CrossRef](#)]
7. Nebel, C.E.; Shin, D.; Rezek, B.; Tokuda, N.; Uetsuka, H.; Watanabe, H. Diamond and biology. *J. R. Soc. Interface* **2007**, *4*, 439–461. [[CrossRef](#)] [[PubMed](#)]
8. Nebel, C.E.; Kato, H.; Rezek, B.; Shin, D.; Takeuchi, D.; Watanabe, H.; Yamamoto, T. Electrochemical properties of undoped hydrogen terminated CVD diamond. *Diam. Relat. Mater.* **2006**, *15*, 264–268. [[CrossRef](#)]
9. Chung, D.D.L. Review Graphite. *J. Mater. Sci.* **2002**, *37*, 1475–1489. [[CrossRef](#)]
10. Burchell, T.D. Graphite: Properties and Characteristics. In *Comprehensive Nuclear Materials*; Elsevier Ltd.: Amsterdam, The Netherlands, 2012; Volume 2, pp. 285–306.
11. Kelly, B.T. *Physics of Graphite*; Applied Science: London, UK, 1981.

12. Elham, A.; Masoumeh, G.; Saeed, S. Electrochemical sensing based on carbon nanoparticles: A review. *Sens. Actuators B* **2019**, *293*, 183–209.
13. Zhai, Y.; Zhu, Z.; Dong, S. Carbon-Based Nanostructures for Advanced Catalysis. *ChemCatChem* **2015**, *7*, 2806–2815. [CrossRef]
14. Marchesan, S.; Melchionna, M.; Prato, M. Carbon nanostructures for nanomedicine: Opportunities and challenges. *Fuller. Nanotub. Carbon Nanostruct.* **2014**, *22*, 190–195. [CrossRef]
15. Yang, Z.; Ren, J.; Zhang, Z.; Chen, X.; Guan, G.; Qui, L. Recent Advancement of Nanostructured Carbon for Energy Applications. *Chem. Rev.* **2015**, *115*, 5159–5223. [CrossRef]
16. Shenderova, O.A.; Zhirnov, V.V.; Brenner, D.V. Carbon Nanostructures. *Crit. Rev. Solid State Mater. Sci.* **2002**, *27*, 227–356. [CrossRef]
17. Chang, Y.R.; Lee, H.Y.; Chen, K.; Chang, C.C.; Tsai, D.S.; Fu, C.C.; Lim, T.S.; Tzeng, Y.K.; Fang, C.Y.; Han, C.C.; et al. Mass production and dynamic imaging of fluorescent nanodiamonds. *Nat. NanoTechnol.* **2008**, *3*, 284–288. [CrossRef]
18. Turcheniuk, K.; Mochalin, V.N. Biomedical applications of nanodiamond. *Nanotechnology* **2017**, *26*, 252001/1–252001/27. [CrossRef] [PubMed]
19. Rabeau, J.R.; Stacey, A.; Rabeau, A.; Prawer, S.; Jelezko, F.; Mirza, I.; Wrachtrup, J. Single Nitrogen Vacancy Centers in Chemical Vapor Deposited Diamond Nanocrystals. *Nano Lett.* **2007**, *7*, 3433–3437. [CrossRef] [PubMed]
20. Williams, O.A.; Douheret, O.; Daenen, M.; Haenen, K.; Osawa, E.; Takahashi, M. Enhanced diamond nucleation on monodispersed nanocrystalline diamond. *Chem. Phys. Lett.* **2007**, *445*, 255–258. [CrossRef]
21. Kroto, H.W.; Heath, J.R.; O’Brien, S.C.; Curl, R.F.; Smalley, R.E. C60: Buckminsterfullerene. *Nature* **1985**, *318*, 162–163. [CrossRef]
22. Rašović, I. Water-soluble fullerenes for medical applications. *Mater. Sci. Technol.* **2017**, *33*, 777–794. [CrossRef]
23. Geim, A.K.; Novoselov, K.S. The rise of graphene. *Nat. Mater.* **2007**, *6*, 183–191. [CrossRef] [PubMed]
24. Georgakilas, V.; Otyepka, M.; Bourlinos, A.B.; Chandra, V.; Kim, N.; Kemp, K.C.; Hobza, P.; Zboril, R.; Kim, K.S. Functionalization of Graphene: Covalent and Non-Covalent Approaches, Derivatives and Applications. *Chem. Rev.* **2012**, *112*, 6156–6214. [CrossRef]
25. Iijima, S. Helical microtubules of graphitic carbon. *Nature* **1991**, *354*, 56–58. [CrossRef]
26. Iijima, S.; Ichihashi, T. Single-shell carbon nanotubes of 1-nm diameter. *Nature* **1993**, *363*, 603–605. [CrossRef]
27. Liu, J.; Lu, J.; Lin, X.; Tang, Y.; Liu, Y.; Wang, T.; Zhu, H. The electronic properties of chiral carbon nanotubes. *Comput. Mater. Sci.* **2017**, *129*, 209–294. [CrossRef]
28. Qureshi, A.; Kang, W.K.; Davidson, J.L.; Gurbuz, Y. Review on carbon-derived, solid-state, micro and nano sensors for electrochemical sensing applications. *Diam. Relat. Mater.* **2009**, *18*, 1401–1420. [CrossRef]
29. Bethune, D.S.; Klang, C.H.; de Vries, M.S.; Gorman, G.; Savoy, R.; Vasquez, J.; Beyers, R. Cobalt-catalysed growth of carbon nanotubes with single-atomic-layer walls. *Nature* **1993**, *363*, 605–607. [CrossRef]
30. Pint, C.L.; Islam, A.E.; Weatherup, R.S.; Hofmann, S.; Meshot, E.R.; Wu, F.; Zhou, C.; Dee, N.; Amama, P.B.; Carpena-Nuñez, J.; et al. Carbon Nanotubes and Related Nanomaterials: Critical Advances and Challenges for Synthesis toward Mainstream Commercial Applications. *ACS Nano* **2018**, *12*, 11756–11784.
31. Camilli, L.; Passacantando, M. Advances on sensors based on carbon nanotubes. *Chemosensors* **2018**, *6*, 62. [CrossRef]
32. Loos, M. *Carbon Nanotube Reinforced Composites*, 1st ed.; Plastic Design Library (PDL) handbook series; William Andrew Applied Science Publishers: Oxford, UK, 2015; ISBN 978-1-4557-3195-4.
33. Nayak, L.; Rahaman, M.; Giri, R. Surface Modification_Functionalizationof Carbon Materials by DifferentTechniques: An Overview. In *Carbon-Containing Polymer Composites*; Springer Series on Polymer and Composite Materials; Springer Nature: Singapore, 2019; pp. 65–98. ISBN 978-981-13-2687-5.
34. Pusch, J.; Wohlmann, B. Carbon Fibers. In *Inorganic and Composite Fibers: Production, Properties, and Applications*; The Textile Institute Book Series; Woodhead Publishing: Oxford, UK, 2018; pp. 31–51. ISBN 978-0-08-102228-3.
35. Yao, S.-S.; Jin, F.-L.; Rhee, K.Y.; Hui, D.; Park, S.-J. Recent advances in carbon-fiber-reinforced thermoplastic composites: A review. *Composites B* **2018**, *142*, 241–250. [CrossRef]
36. Saito, N.; Aoki, K.; Shimizu, M.; Hara, K.; Narita, N.; Ogihara, N.; Nakamura, K.; Ishigaki, N.; Kato, H.; Haniu, H.; et al. Application of carbon fibers to biomaterials: A new era of nano-level control of carbon fibers after 30-years of development. *Chem. Soc. Rev.* **2011**, *40*, 3824–3834. [CrossRef]

37. Du, J.; Zhang, H.; Geng, Y.; Ming, W.; He, W.; Ma, J.; Cao, Y.; Li, X.; Liu, K. A review on machining of carbon fiber reinforced ceramic matrix composites. *Ceram. Int.* **2019**, *45*, 18155–18166. [[CrossRef](#)]
38. Galyshev, S.; Gomzin, A.; Musin, F. Aluminum Matrix Composite Reinforced by Carbon Fibers. *Mater. Today Proc.* **2019**, *11*, 281–285. [[CrossRef](#)]
39. Hiremath, N.; Mays, J.; Bhata, G. Recent Developments in Carbon Fibers and Carbon Nanotube-Based Fibers: A Review. *Polym. Rev.* **2017**, *57*, 339–368. [[CrossRef](#)]
40. Rehman, M.; Park, S.J. Current Progress on the Surface Chemical Modification of Carbonaceous Materials. *Coatings* **2019**, *9*, 103. [[CrossRef](#)]
41. Burg, P.; Cagniant, D. Characterization of carbon surface chemistry. In *Chemistry and Physics of Carbon*; CRC Press Taylor & Francis Group: Boca Raton, FL, USA, 2008; Volume 30.
42. Brender, P.; Gadiou, R.; Rietsch, J.C.; Fioux, P.; Dentzer, J.; Ponche, A.; Vix-Guterl, C. Characterization of Carbon Surface Chemistry by Combined Temperature Programmed Desorption with in Situ X-ray Photoelectron Spectrometry and Temperature Programmed Desorption with Mass Spectrometry Analysis. *Anal. Chem.* **2012**, *84*, 2147–2153. [[CrossRef](#)] [[PubMed](#)]
43. Inagaki, M. *Materials Science and Engineering of Carbon: Characterization*, 1st ed.; Butterworth-Heinemann: Oxford, UK, 2016.
44. Titirici, M.M.; White, R.J.; Brun, N.; Budarin, V.L.; Su, D.S.; del Monte, F.; Clark, J.H. Sustainable carbon materials. *Chem. Soc. Rev.* **2015**, *44*, 250–290. [[CrossRef](#)] [[PubMed](#)]
45. Zhang, M.; Naik, R.R.; Dai, L. *Carbon Nanomaterials for Biomedical Applications*; Springer Series in Biomaterials Science and Engineering; Springer International Publishing: Cham, Switzerland, 2016; Volume 5.
46. Meenakshi, G. Nonenvironmental industrial applications of activated carbon adsorption. In *From Novel Carbon Adsorbents*; Elsevier: Oxford, UK, 2012; pp. 605–638.
47. Wang, M.-J.; Gray, C.A.; Reznek, S.R.; Mahmud, K.; Kutsovsky, Y. Carbon black. In *Encyclopedia of Polymer Science and Technology*; John Wiley & Sons Inc.: Hoboken, NJ, USA, 2014; Volume 2, pp. 426–466.
48. Kamau, G.N. Surface preparation of glassy carbon electrodes. *Anal. Chim. Acta* **1988**, *207*, 1–16. [[CrossRef](#)]
49. Sharma, S. Glassy Carbon: A Promising Material for Micro- and Nanomanufacturing. *Materials* **2018**, *11*, 1857. [[CrossRef](#)] [[PubMed](#)]
50. Pesin, L.A. Review Structure and properties of glass-like carbon. *J. Mater. Sci.* **2002**, *37*, 1–28. [[CrossRef](#)]
51. Matos, I.; Bernardo, M.; Fonseca, I. Porous carbon: A versatile material for catalysis. *Catal. Today* **2017**, *285*, 194–203. [[CrossRef](#)]
52. Wang, L.; Hu, X. Recent advances in porous carbon materials for electrochemical energy storage. *Chem.-Asian J.* **2018**, *13*, 1518–1529. [[CrossRef](#)]
53. Li, W.; Fang, R.; Xia, Y.; Zhang, W.; Wang, X.; Xia, X.; Tu, J. Multiscale Porous Carbon Nanomaterials for Applications in Advanced Rechargeable Batteries. *Batter. Supercaps* **2019**, *2*, 9–36. [[CrossRef](#)]
54. VanDersarl, J.J.; Mercanzini, A.; Renaud, P. Integration of 2D and 3D Thin Film Glassy Carbon Electrode Arrays for Electrochemical Dopamine Sensing in Flexible Neuroelectronic Implants. *Adv. Funct. Mater.* **2014**, *25*, 78–84. [[CrossRef](#)]
55. Vomero, M.; Castagnola, E.; Ciarpella, F.; Maggiolini, E.; Goshi, N.; Zucchini, E.; Carli, S.; Fadiga, L.; Kassegne, S.; Ricci, D. Stable Glassy Carbon Interfaces for Long-Term Neural Stimulation and Low-Noise Recording of Brain Activity. *Sci. Rep.* **2017**, *7*, 40332/1–40332/14.
56. Kurihara, M. Characteristics and applications of carbon black. *J. Technol. Assoc. Refract. Jpn.* **2011**, *31*, 152–155.
57. Kausar, A. Contemporary applications of carbon black-filled polymer composites: An overview of essential aspects. *J. Plast. Film. Sheeting* **2018**, *34*, 256–299. [[CrossRef](#)]
58. Radovic, L.R. *Chemistry and Physics of Carbon*, 1st ed.; CRC Press Taylor & Francis Group: Boca Raton, FL, USA, 2012; Volume 31.
59. Zhao, L.; Komatsu, N. Surface Functionalization of Nanodiamond for Biomedical Applications Polyglycerol Grafting and Further Derivatization. In *Chemical Functionalization of Carbon Nanomaterials: Chemistry and Applications*; Taylor & Francis Group, LLC: Boca Raton, FL, USA, 2016; pp. 651–664.
60. Muzammil, I.; Duy, K.D.; Qasim, A.; Muhammad, I.; Harse, S.; Aqrab, U.A. Controlled Surface Wettability by Plasma Polymer Surface Modification. *Surfaces* **2019**, *2*, 349–371.
61. Tsubokawa, N. Functionalization of Carbon Material by Surface Grafting of Polymers. *Bull. Chem. Soc. Jpn.* **2002**, *75*, 2115–2136. [[CrossRef](#)]

62. Ulman, A. Wetting studies of molecularly engineered surfaces. *Thin Solid Film.* **1996**, *273*, 48–53. [[CrossRef](#)]
63. Lin, Z.; Wu, G.; Zhao, L.; Lai, K.W.C. Carbon nanomaterial-based biosensors A review of design and applications. *IEEE Nanotechnol. Mag.* **2009**, *18*, 1401–1420. [[CrossRef](#)]
64. Nagappa, L.T.; Raz, J. Carbon Nanomaterials in Biological Studies and Biomedicine. *Adv. Healthc. Mater.* **2017**, *6*, 1700574/1–1700574/36.
65. Patel, K.D.; Singh, R.K.; Kim, H.-W. Carbon-based nanomaterials as an emerging platform for theranostics. *Mater. Horiz.* **2019**, *6*, 434–469. [[CrossRef](#)]
66. Eswaran, S.V. Water soluble nanocarbon materials: A panacea for all? *Curr. Sci.* **2018**, *114*, 1846–1850. [[CrossRef](#)]
67. Kozbial, A.; Zhou, F.; Li, Z.; Liu, H.; Li, L. Are Graphitic Surfaces Hydrophobic? *Acc. Chem. Res.* **2016**, *49*, 2765–2773. [[CrossRef](#)]
68. Bourlinos, A.B.; Georgakilas, V.; Zboril, R.; Steriotis, T.A.; Stubos, A.K. Liquid-Phase Exfoliation of Graphite Towards Solubilized Graphenes. *Small* **2009**, *5*, 1841–1845. [[CrossRef](#)] [[PubMed](#)]
69. Kelly, K.F.; Billups, W.E. Synthesis of Soluble Graphite and Graphene. *Acc. Chem. Res.* **2013**, *46*, 4–13. [[CrossRef](#)] [[PubMed](#)]
70. Lotya, M.; Hernandez, Y.; King, P.J.; Smith, R.J.; Nicolosi, V.; Karlsson, L.S.; Blighe, F.M.; De, S.; Wang, Z.; McGovern, I.T.; et al. Graphene by Exfoliation of Graphite in Surfactant/Water Solutions. *J. Am. Chem. Soc.* **2009**, *131*, 3611–3620. [[CrossRef](#)] [[PubMed](#)]
71. Inagaki, M. *New Carbons—Control of Structure and Functions*, 1st ed.; Elsevier Science: Oxford, UK, 2000; ISBN 978-0-08-043713-2.
72. Hao, R.; Qian, W.; Zhang, L.; Hou, Y. Aqueous dispersions of TCNQ-anion-stabilized graphene sheets. *Chem. Commun.* **2008**, *48*, 6576–6578. [[CrossRef](#)] [[PubMed](#)]
73. Hummers, W.S.; Offeman, R.E. Preparation of Graphitic Oxide. *J. Am. Chem. Soc.* **1958**, *80*, 1339. [[CrossRef](#)]
74. Liu, J.; Jeong, H.; Liu, J.; Lee, K.; Park, J.Y.; Ahn, Y.H.; Lee, S. Reduction of functionalized graphite oxides by trioctylphosphine in non-polar organic solvents. *Carbon* **2010**, *48*, 2282–2289. [[CrossRef](#)]
75. Acocella, M.R.; D’Urso, L.; Maggio, M.; Avolio, R.; Errico, M.E.; Guerra, G. Green and Facile Esterification Procedure Leading to Crystalline-Functionalized Graphite Oxide. *Langmuir* **2017**, *33*, 6819–6825. [[CrossRef](#)]
76. Ardhaoui, M.; Zheng, M.; Pulpytel, J.; Dowling, D.; Jolivalt, C.; Khonsari, F.A. Plasma functionalized carbon electrode for laccase-catalyzed oxygen reduction by direct electron transfer. *Bioelectrochemistry* **2013**, *91*, 52–61. [[CrossRef](#)]
77. Ji, H.B.; He, Z.W.; Song, S.S.; Zhao, Z.D. Scalable preparation of functionalized graphite nanoplatelets via magnetic grinding as lubricity-enhanced additive. *J. Cent. South Univ.* **2016**, *23*, 2800–2808. [[CrossRef](#)]
78. Ferreira, L.F.; Santos, C.C.; da Cruz, F.S.; Correa, R.A.M.S.; Verly, R.M.; Da Silva, L.M. Preparation, characterization, and application in biosensors of functionalized platforms with poly (4-aminobenzoic acid). *J. Mater. Sci.* **2015**, *50*, 1103–1116. [[CrossRef](#)]
79. Chelaghmia, M.L.; Nacef, M.; Affoune, A.M.; Pontie, M.; Derabla, T. Graphite Electrode and its Application for Highly Sensitive Non-enzymatic Glucose Sensor. *Electroanalysis* **2018**, *30*, 1117–1124. [[CrossRef](#)]
80. Kesik, M.; Kanik, F.E.; Hizalan, G.; Kozanoglu, D.; Esenturk, E.N.; Timur, S.; Toppore, L. A functional immobilization matrix based on a conducting polymer and functionalized gold nanoparticles: Synthesis and its application as an amperometric glucose biosensor. *Polymer* **2013**, *54*, 4463–4471. [[CrossRef](#)]
81. Park, J.; Grayfer, E.D.; Jung, Y.; Kim, K.; Wang, K.K.; Kim, Y.R.; Yoon, D.; Cheong, H.; Chung, H.E.; Choi, S.J.; et al. Photoluminescent nanographitic/nitrogen-doped graphitic hollow shells as a potential candidate for biological applications. *J. Mater. Chem. B* **2013**, *1*, 1229–1234. [[CrossRef](#)]
82. Correa, R.A.M.S.; da Cruz, F.S.; Santos, C.C.; Pimenta, T.C.; Franco, D.L.; Ferreira, L.F. Optimization and application of electrochemical transducer for detection of specific oligonucleotide sequence for Mycobacterium tuberculosis. *Biosensors* **2018**, *8*, 84. [[CrossRef](#)] [[PubMed](#)]
83. Azani, M.R.; Hassanpour, A.; Carcelén, V.; Gibaja, C. Highly concentrated and stable few-layers graphene suspensions in pure and volatile organic solvents. *Appl. Mater. Today* **2016**, *2*, 17–23. [[CrossRef](#)]
84. Liang, A.; Jiang, X.; Hong, X.; Jiang, Y.; Shao, Z.; Zhu, D. Recent Developments Concerning the Dispersion Methods and Mechanisms of Graphene. *Coatings* **2018**, *8*, 33. [[CrossRef](#)]
85. Ghosh, A.; Rao, K.V.; Voggu, R.; George, S.J. Non-covalent functionalization, solubilization of graphene and single-walled carbon nanotubes with aromatic donor and acceptor molecules. *Chem. Phys. Lett.* **2010**, *488*, 198–201. [[CrossRef](#)]

86. Stankovich, S.; Piner, R.D.; Nguyen, S.T.; Ruoff, R.S. Synthesis and exfoliation of isocyanate-treated graphene oxide nanoplatelets. *Carbon* **2006**, *44*, 3342–3347. [CrossRef]
87. Liu, Z.; Robinson, J.T.; Sun, X.; Dai, H. PEGylated nanographene oxide for delivery of water-insoluble cancer drugs. *J. Am. Chem. Soc.* **2008**, *130*, 10876–10877. [CrossRef] [PubMed]
88. Zhang, X.; Huang, Y.; Wang, Y.; Ma, Y.; Liu, Z.; Chen, Y. Synthesis and characterization of a graphene–C₆₀ hybrid material. *Carbon* **2009**, *47*, 334–337. [CrossRef]
89. Veca, L.M.; Lu, F.; Meziani, M.J.; Cao, L.; Zhang, P.; Qi, G.; Qu, L.; Shrestha, M.; Sun, Y.-P. Polymer functionalization and solubilization of carbon nanosheets. *Chem. Commun.* **2009**, *18*, 2565–2567. [CrossRef] [PubMed]
90. Sun, X.; Liu, Z.; Welsher, K.; Robinson, J.T.; Goodwin, A.; Zaric, S.; Dai, H. Nano-Graphene Oxide for Cellular Imaging and Drug Delivery. *Nano Res.* **2008**, *1*, 203–212. [CrossRef] [PubMed]
91. Tang, Z.; Wu, H.; Cort, J.R.; Buchko, G.W.; Zhang, Y.; Shao, Y.; Aksay, A.; Liu, J.; Lin, Y. Constraint of DNA on Functionalized Graphene Improves its Biostability and Specificity. *Small* **2010**, *6*, 1205–1209. [CrossRef] [PubMed]
92. He, P.; Sun, J.; Tian, S.; Yang, S.; Ding, S.; Ding, G.; Xie, X.; Jang, M. Processable aqueous dispersions of graphene stabilized by graphene quantum dots. *Chem. Mater.* **2015**, *27*, 218–226. [CrossRef]
93. Neklyudov, V.V.; Khafizov, N.R.; Sedov, I.A.; Dimiev, A.M. New insights into the solubility of graphene oxide in water and alcohols. *Phys. Chem. Chem. Phys.* **2017**, *19*, 17000–17008. [CrossRef]
94. Xu, Z.; Lei, X.; Song, B.; Fang, H.; Tu, Y.; Tan, Z.-J. Dynamic Cooperation of Hydrogen Binding and π Stacking in ssDNA Adsorption on Graphene Oxide. *Chemistry* **2017**, *23*, 13100–13104. [CrossRef]
95. Sayyar, S.; Murray, E.; Thompson, B.C.; Chung, J.; Officer, D.L.; Gambhir, S.; Spinks, G.M.; Wallace, G.G. Processable conducting graphene/chitosan hydrogels for tissue engineering. *J. Mater. Chem. B* **2015**, *3*, 481–490. [CrossRef]
96. Liang, J.; Huang, Y.; Zhang, L.; Wang, Y.; Ma, Y.; Guo, T.; Chen, Y. Molecular-Level Dispersion of Graphene into Poly(vinyl alcohol) and Effective Reinforcement of their Nanocomposites. *Adv. Funct. Mater.* **2009**, *19*, 2297–2302. [CrossRef]
97. Kang, H.; Zuo, K.; Wang, Z.; Zhang, L.; Liu, L.; Guo, B. Using a green method to develop graphene oxide/elastomers nanocomposites with combination of high barrier and mechanical performance. *Compos. Sci. Technol.* **2014**, *92*, 1–8. [CrossRef]
98. Pan, Y.; Bao, H.; Sahoo, N.G.; Wu, T.; Li, L. Water-Soluble Poly (N-isopropylacrylamide)–Graphene Sheets Synthesized via Click Chemistry for Drug Delivery. *Adv. Funct. Mater.* **2011**, *21*, 2754–2763. [CrossRef]
99. Wang, B.; Yang, D.; Zhang, J.; Xi, C.; Hu, J. Stimuli-Responsive Polymer Covalent Functionalization of Graphene Oxide by Ce(IV)-Induced Redox Polymerization. *J. Phys. Chem. C* **2011**, *115*, 24636–24641. [CrossRef]
100. Deng, Y.; Li, Y.; Dai, J.; Lang, M.; Huang, X. Functionalization of Graphene Oxide Towards Thermo-Sensitive Nanocomposites via Moderate In Situ SET-LRP. *J. Polym. Sci. A* **2011**, *49*, 4747–4755. [CrossRef]
101. Fang, M.; Wang, K.; Lu, H.; Yang, Y.; Nutt, S. Covalent polymer functionalization of graphene nanosheets and mechanical properties of composites. *J. Mater. Chem.* **2009**, *19*, 7098–7105. [CrossRef]
102. Karousis, N.; Economopoulos, S.P.; Sarantopoulou, E.; Tagmatarchis, N. Porphyrin counter anion in imidazolium-modified graphene-oxide. *Carbon* **2010**, *48*, 854–860. [CrossRef]
103. Vasilieva, K.O.; Ildusovich, K.B. *Solubilization and Dispersion of Carbon Nanotubes*, 1st ed.; Springer International Publishing: Cham, Switzerland, 2017; ISBN 978-3-319-62949-0.
104. Caneba, G.T.; Dutta, C.; Agrawal, V.; Rao, M. Novel Ultrasonic Dispersion of Carbon Nanotubes. *J. Miner. Mater. Charact. Eng.* **2010**, *9*, 165–181. [CrossRef]
105. Vetcher, A.A.; Fan, J.H.; Vetcher, I.A.; Lin, T.; Abramov, S.M.; Draper, R.; Kozlov, M.E.; Baughman, R.H.; Levene, S.D. Electrophoretic fractionation of carbon nanotube dispersion on agarose gels. *Int. J. NanoSci.* **2007**, *6*, 1–7. [CrossRef]
106. Burg, B.R.; Schneider, J.; Muoth, M.; Durrer, L.; Helbling, T.; Schirmer, N.C.; Schwamb, T.; Hierold, C.; Poulikakos, D. Aqueous dispersion and dielectrophoretic assembly of individual surface synthesized single-walled carbon nanotubes. *Langmuir* **2009**, *25*, 7778–7782. [CrossRef]
107. Zheng, M.; Jagota, A.; Semke, E.D.; Diner, B.A.; McLean, R.S.; Lustig, S.R.; Richardson, R.E.; Tassi, N.G. DNA-assisted dispersion and separation of carbon nanotubes. *Nat. Mater.* **2003**, *2*, 338–342. [CrossRef]

108. Zhao, P.; Einarsson, E.; Xiang, R.; Murakami, Y.; Maruyama, S. Controllable expansion of single-walled carbon nanotube dispersions using density gradient ultracentrifugation. *J. Phys. Chem. C* **2010**, *114*, 4831–4834. [[CrossRef](#)]
109. Czech, B.; Oleszczuk, P.; Wiącek, A. Advanced oxidation (H_2O_2 and/or UV) of functionalized carbon nanotubes (CNT-OH and CNT-COOH) and its influence on the stabilization of CNTs in water and tannic acid solution. *Environ. Pollut.* **2015**, *200*, 161–167. [[CrossRef](#)]
110. Saka, C. Overview on the Surface Functionalization Mechanism and Determination of Surface Functional Groups of Plasma Treated Carbon Nanotubes. *Crit. Rev. Anal. Chem.* **2018**, *48*, 1–14. [[CrossRef](#)] [[PubMed](#)]
111. Ruelle, B.; Bittencourt, C.; Dubois, C. Surface treatment of carbon nanotubes via plasma technology. Chap. 2. In *Polymer–Carbon Nanotube Composites Preparation, Properties and Applications*; Woodhead Publishing Series in Composites Science and Engineering: Oxford, UK, 2011; pp. 25–54.
112. Kharissova, O.V.; Kharisov, B.I.; de Casas Ortiz, E.G. Dispersion of carbon nanotubes in water and non-aqueous solvents. *RSC Adv.* **2013**, *3*, 24812–24852. [[CrossRef](#)]
113. Sezer, N.; Koç, M. Oxidative acid treatment of carbon nanotubes. *Surf. Interface* **2019**, *14*, 1–8. [[CrossRef](#)]
114. Dong, C.; Campbell, A.S.; Eldawud, R.; Perhinschi, G.; Rojanasakul, Y.; Dinu, C.Z. Effects of acid treatment on structure, properties and biocompatibility of carbon nanotubes. *Appl. Surf. Sci.* **2013**, *264*, 261–268. [[CrossRef](#)]
115. Cai, J.Y.; Min, J.; McDonnell, J.; Church, J.S.; Easton, C.D.; Humphries, W.; Lucas, S. An improved method for functionalisation of carbon nanotube spun yarns with aryl diazonium compounds. *Carbon* **2012**, *50*, 4655–4662. [[CrossRef](#)]
116. Wang, Y.; Iqbal, Z.; Malhotra, S.V. Functionalization of carbon nanotubes with amines and enzymes. *Chem. Phys. Lett.* **2005**, *402*, 96–101. [[CrossRef](#)]
117. Chen, J.; Collier, C.P. Noncovalent Functionalization of Single-Walled Carbon Nanotubes with Water-Soluble Porphyrins. *J. Phys. Chem. B* **2005**, *109*, 7605–7609. [[CrossRef](#)]
118. Bayazit, M.K.; Coleman, K.S. Fluorescent Single-Walled Carbon Nanotubes Following the 1,3-Dipolar Cycloaddition of Pyridinium Ylides. *J. Am. Chem. Soc.* **2009**, *131*, 10670–10676. [[CrossRef](#)]
119. Fabbro, C.; Chaloin, O.; Moyon, C.M.; Smulski, C.R.; Da Ros, T.; Kostarelos, K.; Prato, M.; Bianco, A. Antibody covalent immobilization on carbon nanotubes and assessment of antigen binding. *Small* **2011**, *7*, 2179–2187.
120. Ruoff, R.S.; Tse, D.S.; Malhotra, R.; Lorents, D.C. Solubility of fullerene C60 in a variety of solvents. *J. Phys. Chem.* **1993**, *97*, 3379–3383. [[CrossRef](#)]
121. Al-Hamadani, Y.A.J.; Chu, K.H.; Son, A.; Heo, J.; Her, N.; Jang, M.; Park, C.M.; Yoon, Y. Stabilization and dispersion of carbon nanomaterials in aqueous solutions: A review. *Sep. Purif. Technol.* **2015**, *156*, 861–874. [[CrossRef](#)]
122. Jensen, A.W.; Wilson, S.R.; Schuster, D.I. Biological applications of fullerenes. *Bioorg. Med. Chem.* **1996**, *4*, 767–779. [[CrossRef](#)]
123. Da Ros, T.; Prato, M. Medicinal chemistry with fullerenes and fullerene derivatives. *Chem. Commun.* **1999**, *8*, 663–669. [[CrossRef](#)]
124. Diederich, F.; Gomez-Lopez, M. Supramolecular fullerene chemistry. *Chem. Soc. Rev.* **1999**, *28*, 263–277. [[CrossRef](#)]
125. Diederich, F.; Thilgen, C. Covalent Fullerene Chemistry. *Science* **1996**, *271*, 317–323. [[CrossRef](#)]
126. Ikeda, A.; Iizuka, T.; Maekubo, N.; Aono, R.; Kikuchi, J.; Akiyama, M.; Konishi, T.; Ogawa, T.; Ishida-Kitagawa, N.; Tatebe, H.; et al. Cyclodextrin Complexed [60] Fullerene Derivatives with High Levels of Photodynamic Activity by Long Wavelength Excitation. *ACS Med. Chem. Lett.* **2013**, *4*, 752–756. [[CrossRef](#)]
127. Chiang, L.Y.; Swirczewski, J.W.; Hsu, C.S.; Chowdhury, S.K.; Cameron, S.; Creegan, K. Multi-hydroxy additions onto C60 fullerene molecules. *J. Chem. Soc. Chem. Commun.* **1992**, *24*, 1791–1793. [[CrossRef](#)]
128. Li, J.; Takeuchi, A.; Ozawa, M.; Li, X.; Saigo, K.; Kitazawa, K. C60 fullerol formation catalysed by quaternary ammonium hydroxides. *J. Chem. Soc. Chem. Commun.* **1993**, *23*, 1784–1785. [[CrossRef](#)]
129. Djordjevic, A.; Srdjenovic, B.; Seke, M.; Petrovic, D.; Injac, R.; Mrdjanovic, J. Review of Synthesis and Antioxidant Potential of Fullerenol Nanoparticles. *J. Nanomater.* **2015**, *2015*, 567073. [[CrossRef](#)]
130. Qiao, J.; Gong, Q.J.; Qiao, J.G.; Li, M.D.; Wei, J.J. Spectroscopic study on the photoinduced reaction of fullerene C60 with aliphatic amines and its dynamics—strong short wavelength fluorescence from the adducts. *Spectrochim. Acta Part A* **2001**, *57*, 17–25. [[CrossRef](#)]

131. Maggini, M.; Scorrano, G.; Prato, M. Addition of azomethine ylides to C₆₀: Synthesis, characterization, and functionalization of fullerene pyrrolidines. *J. Am. Chem. Soc.* **1993**, *115*, 9798–9799. [[CrossRef](#)]
132. Nakamura, E.; Isobe, H.; Tomita, N.; Sawamura, M.; Jinno, S.; Okayama, H. Functionalized fullerene as an artificial vector for transfection. *Angew. Chem. Int. Ed.* **2000**, *39*, 4254–4257. [[CrossRef](#)]
133. Isobe, H.; Tomita, N.; Jinno, S.; Okayama, N.; Nakamura, E. Nonviral gene delivery by tetraamino fullerene. *Mol. Pharm.* **2006**, *3*, 124–134. [[CrossRef](#)]
134. Sitharaman, B.; Zakharian, T.Y.; Saraf, A.; Misra, P.; Ashcroft, J.; Pan, S.; Pham, Q.P.; Mikos, A.G.; Wilson, L.J.; Engler, D.A. Water-soluble fullerene (C₆₀) derivatives as nonviral gene-delivery vectors. *Mol. Pharm.* **2008**, *5*, 567–578. [[CrossRef](#)] [[PubMed](#)]
135. Bingel, C. Cyclopropanierung von fullerenen. *Chem. Ber.* **1993**, *126*, 1957–1959. [[CrossRef](#)]
136. Biglova, N.; Mustafin, A.G. Nucleophilic cyclopropanation of [60] fullerene by the addition–elimination mechanism. *RSC Adv.* **2019**, *9*, 22428–22498. [[CrossRef](#)]
137. Zhou, S.; Trochimczyk, P.; Sun, L.; Hou, S.; Li, H. Sugar-Functionalized Fullerenes. *Curr. Org. Chem.* **2016**, *20*, 1490–1501. [[CrossRef](#)]
138. Sánchez-Navarro, M.; Muñoz, A.; Illescas, B.I.; Rojo, J.; Martín, N. [60] Fullerene as Multivalent Scaffold: Efficient Molecular Recognition of Globular Glycofullerenes by Concanavalin A. *Chem. Eur. J.* **2011**, *17*, 766–769. [[CrossRef](#)]
139. Nierengarten, I.; Nierengarten, J.F. Fullerene Sugar Balls: A New Class of Biologically Active FullereneDerivatives. *Chem. Asian J.* **2014**, *9*, 1436–1444. [[CrossRef](#)]
140. Luczkowiak, J.; Muñoz, A.; Sánchez-Navarro, M.; Ribeiro-Viana, R.; Ginieis, A.; Illescas, B.M.; Martín, N.; Delgado, R.; Rojo, J. Glycofullerenes Inhibit Viral Infection. *Biomacromolecules* **2013**, *14*, 431–437. [[CrossRef](#)]
141. Rísquez-Cuadro, R.; García Fernández, J.; Nierengarten, J.F.; Ortiz Mellet, C. Fullerene-sp₂-Iminosugar Balls as Multimodal Ligands for Lectins and Glycosidases: A Mechanistic Hypothesis for the Inhibitory Multivalent Effect. *Chem. Eur. J.* **2013**, *19*, 16791–16803. [[CrossRef](#)] [[PubMed](#)]
142. Cecioni, S.; Oerthel, V.; Iehl, J.; Holler, M.; Goyard, D.; Praly, J.P.; Imbeerty, A.; Nierengarten, J.F.; Vidal, S. Synthesis of Dodecavalent Fullerene-Based Glyoclusters and Evaluation of Their Binding Properties towards a Bacterial Lectin. *Chem. Eur. J.* **2011**, *17*, 3252–3261. [[CrossRef](#)] [[PubMed](#)]
143. Lin, Y.C.; Wu, K.T.; Perevedentseva, E.; Karmenyan, A.; Lin, M.D.; Cheng, C.L. Nanodiamond for biolabelling and toxicity evaluation in the zebrafish embryo in vivo. *J. Biophotonics* **2016**, *9*, 827–836. [[CrossRef](#)] [[PubMed](#)]
144. Shergold, H.L.; Hartley, C.J. The surface chemistry of diamond. *Int. J. Miner. Process.* **1982**, *9*, 219–233. [[CrossRef](#)]
145. Szunerits, S.; Nebel, C.E.; Hamers, R.J. Surface functionalization and biological applications of CVD diamond. *MRS Bull.* **2014**, *39*, 517–524. [[CrossRef](#)]
146. Stavis, C.; Lasseter Clare, T.; Butler, J.E.; Radadia, A.D.; Carr, R.; Zeng, H.; King, W.P.; Carlisle, J.A.; Aksimentiev, A.; Bashir, R.; et al. Surface functionalization of thin-film diamond for highly stable and selective biological interfaces. *Proc. Natl. Acad. Sci. USA* **2011**, *18*, 983–988. [[CrossRef](#)]
147. Ho, D. *Nanodiamonds Applications in Biology and Nanoscale Medicine*; Springer: New York, NY, USA, 2010; ISBN 978-1-4419-0531-4.
148. Krueger, A. The structure and reactivity of nanoscale diamond. *J. Mater. Chem.* **2008**, *18*, 1485–1492. [[CrossRef](#)]
149. Wang, P.; Su, W.; Ding, X. Control of nanodiamond-doxorubicin drug loading and elution through optimized compositions and release environments. *Diam. Relat. Mater.* **2018**, *88*, 43–50. [[CrossRef](#)]
150. Tinwala, H.; Waikar, S. Production, surface modification and biomedical applications of nanodiamonds: A sparkling tool for theranostics. *Mater. Sci. Eng. C* **2019**, *97*, 913–931. [[CrossRef](#)]
151. Chen, M.; Pierstorff, E.D.; Lam, R.; Li, S.-Y.; Huang, H.; Osawa, E.; Ho, D. Nanodiamond-Mediated Delivery of Water-Insoluble Therapeutics. *ACS Nano* **2009**, *3*, 2016–2022. [[CrossRef](#)]
152. Kong, X.L.; Huang, L.C.L.; Hsu, C.M.; Chen, W.H.; Han, C.C.; Chang, H.C. High-Affinity Capture of Proteins by Diamond Nanoparticles for Mass Spectrometric Analysis. *Anal. Chem.* **2005**, *77*, 259–265. [[CrossRef](#)] [[PubMed](#)]
153. Huang, L.C.L.; Chang, H.C. Adsorption and Immobilization of Cytochrome c on Nanodiamonds. *Langmuir* **2004**, *20*, 5879–5884. [[CrossRef](#)] [[PubMed](#)]
154. Nguyen, T.T.B.; Chang, H.C.; Wu, V.W.K. Adsorption and hydrolytic activity of lysozyme on diamond nanocrystallites. *Diam. Relat. Mater.* **2007**, *16*, 872–876. [[CrossRef](#)]

155. Yang, W.S.; Auciello, O.; Butler, J.E.; Cai, W.; Carlisle, J.A.; Gerbi, J.; Gruen, D.M.; Knickerbocker, T.; Lasseter, T.L.; Russell, J.N.; et al. DNA-modified nanocrystalline diamond thin-films as stable, biologically active substrates. *Nat. Mater.* **2002**, *1*, 253–257. [[CrossRef](#)]
156. Krueger, A.; Liang, Y.; Jarre, G.; Stegk, J. Surface functionalisation of detonation diamond suitable for biological applications. *J. Mater. Chem.* **2006**, *16*, 2322–2328. [[CrossRef](#)]
157. Ando, T.; Yamamoto, K.; Matsuzawa, M.; Takamatsu, Y.; Kawasaki, S.; Okino, F.; Touhara, H.; Kamo, M.; Sato, Y. Direct interaction of elemental fluorine with diamond surfaces. *Diam. Relat. Mater.* **1996**, *5*, 1021–1025. [[CrossRef](#)]
158. Ando, T.; Yamamoto, K.; Suehara, S.; Kamo, M.; Sato, Y.; Shimosaki, S.; Gamo, M.N. Interaction of Chlorine with Hydrogenated Diamond Surface. *J. Chin. Chem. Soc.* **1995**, *42*, 285–292. [[CrossRef](#)]
159. Zhou, J.; Laube, C.; Knolle, W.; Naumov, S.; Prager, A.; Kopinke, F.D.; Abel, B. Efficient chlorine atom functionalization at nanodiamond surfaces by electron beam irradiation. *Diam. Relat. Mater.* **2018**, *82*, 150–159. [[CrossRef](#)]
160. Liu, Y.; Gu, Z.; Margrave, J.L.; Khabashesku, V.N. Functionalization of Nanoscale Diamond Powder: Fluoro-, Alkyl-, Amino-, and Amino Acid-Nanodiamond Derivatives. *Chem. Mater.* **2004**, *16*, 3924–3930. [[CrossRef](#)]
161. Barras, A.; Lyskawa, J.; Szunerits, S.; Woisel, P.; Boukherroub, R. Direct Functionalization of Nanodiamond Particles Using Dopamine Derivatives. *Langmuir* **2011**, *27*, 12451–12457. [[CrossRef](#)]
162. Hajiali, F.; Shojaei, A. Silane functionalization of nanodiamond for polymer nanocomposites—effect of degree of silanization. *Colloids Surf. A* **2016**, *506*, 254–263. [[CrossRef](#)]
163. Ma, W.; Yu, X.; Qu, X.; Zhang, Q. Functionalization of agglomerating nanodiamonds with biodegradable poly(ϵ -caprolactone) through surface-initiated polymerization. *Diam. Relat. Mater.* **2016**, *62*, 14–21. [[CrossRef](#)]
164. Chatzimitakos, T.; Stalikas, C. Recent advances in carbon dots. *C-J. Carbon Res.* **2019**, *5*, 41. [[CrossRef](#)]
165. Hui, Y.Y.; Cheng, C.-L.; Chang, H.-C. Nanodiamonds for optical bioimaging. *J. Phys. D* **2010**, *43*, 374021/1–374021/11. [[CrossRef](#)]
166. Reineck, P.; Lau, D.W.M.; Wilson, E.R.; Fox, K.; Filed, M.R.; Deleepojananan, C.; Mochaklin, V.N.; Gibson, B.C. Effect of Surface Chemistry on the Fluorescence of Detonation Nanodiamonds. *ACS Nano* **2017**, *11*, 10924–10934. [[CrossRef](#)] [[PubMed](#)]
167. Lai, H.; Stenzel, M.H.; Xiao, P. Surface engineering and applications of nanodiamonds in cancer treatment and imaging. *Int. Mater. Rev.* **2019**, *1*–37, Published online. [[CrossRef](#)]
168. Huang, H.; Pierstorff, E.; Osawa, E.; Dean, H. Active nanodiamond hydrogels for chemotherapeutic delivery. *Nano Lett.* **2007**, *7*, 3305–3314. [[CrossRef](#)]
169. Yan, J.; Guo, Y.; Altawashi, A.; Moosa, B.; Lecommandoux, S.; Khashab, N.M. Experimental and theoretical evaluation of nanodiamonds as pH triggered drug carriers. *New J. Chem.* **2012**, *36*, 1479–1484. [[CrossRef](#)]
170. Toh, T.B.; Lee, D.K.; Hou, W.; Adullah, L.N.; Nguyen, J.; Ho, D.; Chow, E.K.H. Nanodiamond–mitoxantrone complexes enhance drug retention in chemoresistant breast cancer cells. *Mol. Pharm.* **2014**, *11*, 2683–2691. [[CrossRef](#)]
171. Pandolfo, A.G.; Hollenkamp, A.F. Review Carbon properties and their role in supercapacitors. *J. Power Sources* **2006**, *157*, 11–27. [[CrossRef](#)]
172. Babu, S.N.; Gopiraman, M.; Karvembu, R.; Kim, I.S. Carbon Material Supported Nanostructures in Catalysis. In *Chemical Functionalization of Carbon Nanomaterials: Chemistry and Applications*; Taylor & Francis Group, LLC: Boca Raton, FL, USA, 2016; pp. 147–172.
173. McCreery, R.L. Advanced Carbon Electrode Materials for Molecular Electrochemistry. *Chem. Rev.* **2008**, *108*, 2646–2687. [[CrossRef](#)] [[PubMed](#)]
174. McDermott, C.A.; Kneten, K.; McCreery, R.L. Electron Transfer Kinetics of Aquated Fe +3/+2, Eu +3/+2, and V +3/+2 at Carbon Electrodes. Inner Sphere Catalysis by Surface Oxides. *J. ElectroChem. Soc.* **1993**, *140*, 2593–2599. [[CrossRef](#)]
175. Chen, P.; Fryling, M.; McCreery, R.L. Electron Transfer Kinetics at Modified Carbon Electrode Surfaces: The Role of Specific Surface Sites. *Anal. Chem.* **1995**, *67*, 3115–3122. [[CrossRef](#)]
176. Kamran, U.; Heo, Y.J.; Lee, J.W.; Park, S.J. Functionalized Carbon Materials for Electronic Devices: A Review. *Micromachines* **2019**, *10*, 234. [[CrossRef](#)] [[PubMed](#)]

177. Rowley-Neale, S.J.; Brownson, D.A.C.; Banks, C.E. Defining the origins of electron transfer at screen-printed graphene-like and graphite electrodes: MoO₂ nanowire fabrication on edge plane sites reveals electrochemical insights. *Nanoscale* **2016**, *8*, 15241–15251. [CrossRef] [PubMed]
178. Banks, C.E.; Davies, T.J.; Wildgoose, G.G.; Compton, R.G. Electrocatalysis at graphite and carbon nanotube modified electrodes: Edge-plane sites and tube ends are the reactive sites. *Chem. Commun.* **2005**, *7*, 829–841. [CrossRef] [PubMed]
179. Clegg, A.D.; Rees, N.V.; Klymenko, O.V.; Coles, B.A.; Compton, R.G. Marcus Theory of Outer-Sphere Heterogeneous Electron Transfer Reactions: Dependence of the Standard Electrochemical Rate Constant on the Hydrodynamic Radius from High Precision Measurements of the Oxidation of Anthracene and Its Derivatives in Nonaqueous Solvents Using the High-Speed Channel Electrode. *J. Am. Chem. Soc.* **2004**, *126*, 6185–6192.
180. Chang, H.; Bard, A.J. Observation and characterization by scanning tunneling microscopy of structures generated by cleaving highly oriented pyrolytic graphite. *Langmuir* **1991**, *7*, 1143–1153. [CrossRef]
181. Peng, W.; Han, G.; Huang, Y.; Cao, Y.; Son, S. Insight the effect of crystallinity of natural graphite on the electrochemical performance of reduced graphene oxide. *Res. Phys.* **2018**, *11*, 131–137. [CrossRef]
182. Lu, Y.; Xu, H.; Kong, X.; Wang, J. Reversible redox reaction on the oxygen-containing functional groups of an electrochemically modified graphite electrode for the pseudo-capacitance. *J. Mater. Chem.* **2011**, *21*, 18753–18760.
183. Chiang, H.L.; Huang, C.P.; Chiang, P.C. The surface characteristics of activated carbon as affected by ozone and alkaline treatment. *Chemosphere* **2002**, *47*, 257–265. [CrossRef]
184. Evans, J.F.; Kuwana, T. Radiofrequency oxygen plasma treatment of pyrolytic graphite electrode surfaces. *Anal. Chem.* **1977**, *49*, 1632–1635. [CrossRef]
185. Khataee, A.; Sajjadi, S.; Pouran, S.R.; Hasanzadeh, A. Efficient electrochemical generation of hydrogen peroxide by means of plasma-treated graphite electrode and activation in electro-Fenton. *J. Ind. Eng. Chem.* **2017**, *56*, 312–320. [CrossRef]
186. Zhu, H.; Ji, D.; Jiang, L.; Dongand, H.; Hu, W. Tuning electrical properties of graphite oxide by plasma. *Philos. Trans. R. Soc. A* **2013**, *371*, 20120308/1–20120308/8. [CrossRef]
187. Lee, R.H.; Huang, J.L.; Chi, C.H. Conjugated polymer-functionalized graphite oxide sheets thin films for enhanced photovoltaic properties of polymer solar cells. *J. Polym. Sci. Part B* **2013**, *51*, 137–148. [CrossRef]
188. Sathyamoorthi, S.; Suryanarayanan, V.; Velayutham, D. Electrochemical exfoliation and in situ carboxylic functionalization of graphite in non-fluoro ionic liquid for supercapacitor application. *J. Solid State Electrochem.* **2014**, *18*, 2789–2796. [CrossRef]
189. Jeong, K.H.; Jeong, S.M. Enhanced capacitance of unexfoliated graphite oxide by coupled electro-deoxidation/functionalization in an alkali solution. *Electrochim. Acta* **2013**, *108*, 801–807. [CrossRef]
190. Luo, J.; Jang, H.D.; Huang, J. Effect of sheet morphology on the scalability of graphene-based ultracapacitors. *ACS Nano* **2013**, *7*, 1464–1471. [CrossRef]
191. Slate, A.J.; Brownson, D.A.C.; Abo Dena, A.S.; Smith, G.C.; Whitehead, K.A.; Banks, C.E. Exploring the electrochemical performance of graphite and graphene paste electrodes composed of varying lateral flake sizes. *Phys. Chem. Chem. Phys.* **2018**, *20*, 20010–20022. [CrossRef]
192. Ambrosi, A.; Pumera, M. Precise Tuning of Surface Composition and Electron-Transfer Properties of Graphene Oxide Films through Electroreduction. *Chemistry* **2013**, *19*, 4748–4753. [CrossRef]
193. Sinitskii, A.; Dimiev, A.; Corley, D.A.; Fursina, A.A.; Kosynkin, D.V. Kinetics of Diazonium Functionalization of Chemically Converted Graphene Nanoribbons. *ACS Nano* **2010**, *4*, 1949–1954. [CrossRef] [PubMed]
194. Liu, H.; Ryu, S.; Chen, Z.; Steigerwald, M.L.; Nuckolls, C.; Brus, L.E. Photochemical Reactivity of Graphene. *J. Am. Chem. Soc.* **2009**, *131*, 17099–17101. [CrossRef] [PubMed]
195. Aguilar-Bolados, H.; Vargas-Astudillo, D.; Yazdani-Pedram, M.; Acosta-Villavicencio, G.; Fuentealba, P.; Contreras-Cid, A.; Verdejo, R.; López-Manchado, M.A. Facile and Scalable One-Step Method for Amination of Graphene Using Leuckart Reaction. *Chem. Mater.* **2017**, *29*, 6698–6705. [CrossRef]
196. Neustroev, E.P. Plasma Treatment of Graphene Oxide chap. 2. In *Graphene Oxide—Applications and Opportunities*; IntechOpen: London, UK, 2018.
197. Imamura, G.; Saiki, K. Synthesis of Nitrogen-Doped Graphene on Pt (111) by Chemical Vapor Deposition. *J. Phys. Chem. C* **2011**, *115*, 10000–10005. [CrossRef]

198. Fakharuddin, A.; Jose, R.; Brown, T.M.; Santiago, F.F.; Bisquert, J. A perspective on the production of dye-sensitized solar modules. *Energy Environ. Sci.* **2014**, *7*, 3952–3981. [[CrossRef](#)]
199. Song, L.; Luo, Q.; Zhao, F.; Li, Y.; Lin, H.; Qu, L.; Zhang, Z. Dually functional, N-doped porous graphene foams as counter electrodes for dye-sensitized solar cells. *Phys. Chem. Chem. Phys.* **2014**, *16*, 21820–21826. [[CrossRef](#)]
200. Hou, S.; Cai, X.; Wu, H.; Yu, X.; Peng, M.; Yan, K.; Zou, D. Nitrogen-doped graphene for dye-sensitized solar cells and the role of nitrogen states in triiodide reduction. *Energy Environ. Sci.* **2013**, *6*, 3356–3362. [[CrossRef](#)]
201. Xue, Y.; Liu, J.; Chen, H.; Wang, R.; Li, D.; Qu, J.; Dai, L. Nitrogen-doped graphene foams as metal-free counter electrodes in high-performance dye-sensitized solar cells. *Angew. Chem. Int. Ed.* **2012**, *51*, 12124–12127. [[CrossRef](#)]
202. Cui, T.; Lv, R.; Huang, Z.H.; Chen, S.; Zhang, Z.; Gan, X.; Jia, Y.; Li, X.; Wang, K.; Wu, D. Enhanced efficiency of graphene/silicon heterojunction solar cells by molecular doping. *J. Mater. Chem. A* **2013**, *1*, 5736–5740. [[CrossRef](#)]
203. Hai, X.; Mao, Q.X.; Wang, W.J.; Wang, X.F.; Chen, X.W.; Wang, J.H. An acid free microwave approach to prepare highly luminescent boron-doped graphene quantum dots for cell imaging. *J. Mater. Chem. B* **2015**, *3*, 9109–9114. [[CrossRef](#)]
204. Tian, P.; Tang, L.; Teng, K.S.; Lau, S.P. Graphene quantum dots from chemistry to applications. *Mater. Today Chem.* **2018**, *10*, 221–258. [[CrossRef](#)]
205. Dhar, S.; Majumder, T.; Chakraborty, P.; Mondal, S.P. DMSO modified PEDOT: PSS polymer/ZnO nanorods Schottky junction ultraviolet photodetector: Photoresponse, external quantum efficiency, detectivity, and responsivity augmentation using N doped graphene quantum dots. *Org. Electron.* **2018**, *53*, 101–110. [[CrossRef](#)]
206. Kim, D.H.; Kim, T.W. Highly-efficient organic light-emitting devices based on poly (N,N'-bis-4-butylphenyl-N,N'-bisphenyl) benzidine: Octadecylamine graphene quantum dots. *Org. Electron.* **2018**, *57*, 305–310. [[CrossRef](#)]
207. Li, H.; Sun, C.; Ali, M.; Zhou, F.; Zhang, X.; McFarlane, D.R. Sulfated carbon quantum dots as efficient visible-light switchable acid catalysts for room temperature ring-opening reactions. *Angew. Chem. Int. Ed.* **2015**, *54*, 8420–8424. [[CrossRef](#)] [[PubMed](#)]
208. Lu, H.; Li, W.; Dong, H.; Wei, M. Graphene Quantum Dots for Optical Bioimaging. *Small* **2019**, *15*, 1902136/1–1902136/19. [[CrossRef](#)]
209. Zhang, M.; Yin, B.C.; Tan, W.; Ye, B.C. A versatile graphene based fluorescence “on/off” switch for multiplex detection of various targets. *Biosens. Bioelectron.* **2011**, *26*, 3260–3265. [[CrossRef](#)]
210. Lim, S.K.; Chen, P.; Lee, F.L.; Moochhala, S.; Liedberg, B. Peptide-assembled graphene oxide as a fluorescent turn-on sensor for lipopolysaccharide (endotoxin) detection. *Anal. Chem.* **2015**, *87*, 9408–9412. [[CrossRef](#)]
211. Garion, C. Mechanical Properties for Reliability Analysis of Structures in Glassy Carbon. *World J. Mech.* **2014**, *4*, 79–89. [[CrossRef](#)]
212. Harris, P.J.F. Fullerene-related structure of commercial glassy carbons. *Philos. Mag.* **2004**, *84*, 3159–3167. [[CrossRef](#)]
213. Shi, F.; Zhang, J.; Kenny-Benson, C.; Park, C.; Wang, Y.; Shen, G. Nanoarchitected materials composed of fullerene-like spheroids and disordered graphene layers with tunable mechanical properties. *Nat. Commun.* **2015**, *6*, 6212/1–6212/10.
214. Jouikov, V.; Simonet, J. Electrochemical conversion of glassy carbon into a poly-nucleophilic reactive material. Applications for carbon chemical functionalization. A mini-review. *ElectroChem. Commun.* **2014**, *45*, 32–36. [[CrossRef](#)]
215. Evans, J.F.; Kuwana, T. Introduction of functional groups onto carbon electrodes via treatment with radio-frequency plasmas. *Anal. Chem.* **1979**, *51*, 358–365. [[CrossRef](#)]
216. Kinoshita, K. *Carbon: Electrochemical and Physicochemical Properties*; Wiley: New York, NY, USA, 1988.
217. Chang, G.; Shu, H.; Ji, K.; Oyama, M.; Liu, X.; He, Y. Gold nanoparticles directly modified glassy carbon electrode for non-enzymatic detection of glucose. *Appl. Surf. Sci.* **2014**, *288*, 524–529. [[CrossRef](#)]
218. Dogan-Topal, B.; Bozal-Palabiyik, B.; Uslu, B.; Ozkan, S.A. Multi-walled carbon nanotube modified glassy carbon electrode as a voltammetric nanosensor for the sensitive determination of anti-viral drug valganciclovir in pharmaceuticals. *Sens. Actuators B* **2013**, *177*, 841–847. [[CrossRef](#)]

219. De Clements, R.; Swain, G.M.; Dallas, T.; Holtz, M.W.; Herick, R.D.; Stickney, J.L. Electrochemical and Surface Structural Characterization of Hydrogen Plasma Treated Glassy Carbon Electrodes. *Langmuir* **1996**, *12*, 6578–6586. [[CrossRef](#)]
220. Harris, P.J.F. Fullerene-like models for microporous carbon. *J. Mater. Sci.* **2013**, *48*, 565–577. [[CrossRef](#)]
221. Xu, M.; Li, D.; Yan, Y.; Guo, T.; Pang, H.; Xue, H. Porous high specific surface area-activated carbon with co-doping N, S and P for high-performance supercapacitors. *RSC Adv.* **2017**, *7*, 43780–43788. [[CrossRef](#)]
222. Lin, J.; Zhao, G. Preparation and Characterization of High Surface Area Activated Carbon Fibers from Lignin. *Polymers* **2016**, *8*, 369. [[CrossRef](#)]
223. Lee, J.H.; Ahn, H.J.; Cho, D.; Young, J.I.; Kim, Y.J.; Oh, H.J. Effect of surface modification of carbon felts on capacitive deionization for desalination. *Carbon Lett.* **2015**, *16*, 93–100. [[CrossRef](#)]
224. Kim, K.J.; Lee, S.W.; Kim, J.G.; Choi, J.W.; Kim, J.H.; Park, M.S. A new strategy for integrating abundant oxygen functional groups into carbon felt electrode for vanadium redox flow batteries. *Sci. Rep.* **2014**, *4*, 6906/1–6906/6. [[CrossRef](#)]
225. Kim, K.J.; Kim, Y.J.; Kim, J.H.; Park, M.S. The effects of modification on carbon felt electrodes for use in vanadium redox flow batteries. *Mater. Chem. Phys.* **2011**, *131*, 547–553. [[CrossRef](#)]
226. Fryszt, C.A.; Chung, D.D.L. Improving the electrochemical behavior of carbon black and carbon filaments by oxidation. *Carbon* **1997**, *35*, 1111–1127. [[CrossRef](#)]
227. Sun, B.; Skyllas-Kazacos, M. Modification of graphite electrode materials for vanadium redox flow battery application—Part I. Thermal treatment. *Electrochim. Acta* **1192**, *35*, 1253–1260.
228. Flox, C.; Rubio-Garcia, J.; Skoumal, M.; Andreu, T.; Morante, J.R. Thermo-chemical treatments based on NH₃/O₂ for improved graphite-based fiber electrodes in vanadium redox flow batteries. *Carbon* **2013**, *60*, 280–288. [[CrossRef](#)]
229. Moreno-Castilla, C.; Ferro-García, M.A.; Joly, J.P.; Bautista-Toledo, I.; Carrasco-Marín, F.; Rivera-Utrilla, J. Activated carbon surface modifications by nitric acid, hydrogen peroxide, and ammonium peroxydisulfate treatments. *Langmuir* **1995**, *11*, 4386–4392. [[CrossRef](#)]
230. Quian, H.; Diao, H.; Shirshova, N.; Greenhalgh, E.S.; Steinke, J.G.H.; Shaffer, M.S.P.; Bismarck, A. Activation of structural carbon fibres for potential applications in multifunctional structural supercapacitors. *J. Colloid Interface Sci.* **2013**, *395*, 241–248. [[CrossRef](#)] [[PubMed](#)]
231. Sun, B.; Skyllas-Kazacos, M. Chemical modification of graphite electrode materials for vanadium redox flow battery application.—Part II. Acid treatments. *Electrochim. Acta* **1992**, *37*, 2459–2465. [[CrossRef](#)]
232. Wu, T.; Huang, K.; Liu, S.; Zhuang, S.; Fang, D.; Li, S.; Dan, L.; Su, A. Hydrothermal ammoniated treatment of PAN-graphite felt for vanadium redox flow battery. *J. Solid State Electron.* **2012**, *16*, 579–585. [[CrossRef](#)]
233. Shao, Y.; Wang, X.; Engelhard, M.; Wang, C.; Dai, S.; Liu, J.; Yang, Z.; Lin, Y. Nitrogen-doped mesoporous carbon for energy storage in vanadium redox flow batteries. *J. Pow Sources* **2010**, *195*, 4375–4379. [[CrossRef](#)]
234. Kinoshita, K.; Chu, X. *Electrochemical Supercapacitors—Scientific Fundamentals and Technological Applications*; Kluwer: New York, NY, USA, 1999.
235. Delnick, F.M.; Tomkiewicz, M. *Proceedings of the Symposium on Electrochemical Capacitors*; Electrochemical Society Publisher: Pennington, NJ, USA, 1995; Volume 95-25.
236. Inagaki, M.; Radovic, L.R. Nanocarbons. *Carbon* **2002**, *40*, 2279–2282. [[CrossRef](#)]
237. Bansal, R.C.; Donnet, J.B.; Stoeckli, F. *Active Carbon—Chapter 2*; Marcel Dekker: New York, NY, USA, 1998.
238. Pierson, H.O. *Handbook of Carbon, Graphite, Diamond and Fullerenes*; Noyes Publications: Park Ridge, NJ, USA, 1993.
239. Lee, H.; Jung, Y.; Kim, S. Effect of plasma treatments to graphite nanofibers supports on electrochemical behaviors of metal catalyst electrodes. *J. NanoSci. Nanotechnol.* **2012**, *12*, 1513–1516. [[CrossRef](#)] [[PubMed](#)]
240. Zhou, X.; Chen, W.; Chen, M.; Liu, C. Enhancement of the electrochemical properties of commercial coconut shell-based activated carbon by H₂O dielectric barrier discharge plasma. *R. Soc. Open Sci.* **2019**, *6*, 180872/1–180872/11.
241. Hsieh, C.T.; Teng, H. Influence of oxygen treatment on electric double-layer capacitance of activated carbon fabrics. *Carbon* **2002**, *40*, 667–674. [[CrossRef](#)]
242. Lin, T.; Chen, I.W.; Liu, F.; Yang, C.; Bi, H.; Xu, F.; Huang, F. Nitrogen-doped mesoporous carbon of extraordinary capacitance for electrochemical energy storage. *Science* **2015**, *350*, 1508–1513. [[CrossRef](#)]

243. Song, Y.; Zhang, M.; Liu, T.; Li, T.; Guo, D.; Liu, X.X. Cobalt-Containing Nanoporous Nitrogen-Doped Carbon Nanocuboids from Zeolite Imidazole Frameworks for Supercapacitors. *Nanomaterials* **2019**, *9*, 1110. [[CrossRef](#)]
244. Biniak, S.; Swiatkowski, A.; Pakula, M.; Radovic, L.R. *Chemistry and Physics of Carbon*; Marcel Dekker: New York, NY, USA, 2001; Volume 27.
245. Hess, W.M.; Herd, C.R.; Donet, J.B.; Bansal, R.C.; Wang, M.J. *Carbon Black*, 2nd ed.; Marcel Dekker: New York, NY, USA, 1993.
246. Radeke, K.H.; Backhaus, K.O.; Swiatkowski, A. Microporosity of a Graphitized Rayon Fabric Oxidized in Air. *Carbon* **1991**, *29*, 122–123. [[CrossRef](#)]
247. Abouelamaiem, D.I.; Mostazo-López, M.J.; He, G.; Patel, D.; Neville, T.P.; Parkin, I.P.; Lozano-Castelló, D. New insights into the electrochemical behaviour of porous carbon electrodes for supercapacitors. *J. Energy Storage* **2018**, *19*, 337–347. [[CrossRef](#)]
248. Deinhammer, R.S.; Ho, M.; Anderegg, J.W.; Porter, M.D. Electrochemical oxidation of amine-containing compounds: A route to the surface modification of glassy carbon electrodes. *Langmuir* **1994**, *10*, 1306–1313. [[CrossRef](#)]
249. Buttry, D.A.; Peng, J.C.; Donnet, J.B.; Rebouillat, S. Immobilization of amines at carbon fiber surfaces. *Carbon* **1999**, *37*, 1929–1940. [[CrossRef](#)]
250. Ogata, A.F.; Song, S.W.; Cho, S.H.; Koo, W.T.; Jang, J.S.; Jeong, Y.J.; Kim, M.H.; Cheong, J.Y. An Impedance-Transduced Chemiresistor with a porous carbon channel for rapid, nonenzymatic, glucose sensing. *Anal. Chem.* **2018**, *90*, 9338–9346. [[CrossRef](#)]
251. Huang, T.; Warsinke, A.; Koroljova-Skorobogatko, O.V.; Makower, A.; Kuwana, T.; Scheller, F.W. A Bienzyme Carbon Paste Electrode for the Sensitive Detection of NADPH and the Measurement of Glucose-6-phosphate Dehydrogenase. *Electroanalysis* **1999**, *11*, 295–300. [[CrossRef](#)]
252. Musameh, M.; Wang, J.; Merkoci, A.; Lin, Y. Low-potential stable NADH detection at carbon-nanotube-modified glassy carbon electrodes. *ElectroChem. Commun.* **2002**, *4*, 743–746. [[CrossRef](#)]
253. Yang, H.H.; McCreery, L.M. Elucidation of the Mechanism of Dioxygen Reduction on Metal-Free Carbon Electrodes. *J. ElectroChem. Soc.* **2000**, *147*, 3420–3428. [[CrossRef](#)]
254. Lin, T.; Bajpai, V.; Ji, T.; Dai, L. Chemistry of carbon nanotubes. *Aust. J. Chem.* **2003**, *56*, 635–651. [[CrossRef](#)]
255. Mallakpour, S.; Soltaniana, M. Surface functionalization of carbon nanotubes: Fabrication and applications. *RSC Adv.* **2016**, *6*, 109916–109935. [[CrossRef](#)]
256. Balasubramanian, K.; Burghard, M. Chemically functionalized carbon nanotubes. *Small* **2005**, *1*, 180–192. [[CrossRef](#)]
257. Rana, A.; Baig, N.; Saleh, T.A. Electrochemically pretreated carbon electrodes and their electroanalytical applications—A review. *J. Electroanal. Chem.* **2019**, *833*, 313–332. [[CrossRef](#)]
258. González-Sánchez, M.I.; Gómez-Monedero, B.; Agrisuelas, J.; Iniesta, J.; Valero, E. Highly activated screen-printed carbon electrodes by electrochemical treatment with hydrogen peroxide. *ElectroChem. Commun.* **2018**, *91*, 36–40. [[CrossRef](#)]
259. Santiago-Rodríguez, L.; Sanchez-Pomales, G.; Cabrera, C.R. DNA-functionalized carbon nanotubes: Synthesis, self-assembly, and applications. *Isr. J. Chem.* **2010**, *50*, 277–290. [[CrossRef](#)]
260. Tasis, N.; Tagmatarchis, N.; Georgakilas, V.; Prato, M. Soluble carbon nanotubes. *Chemistry* **2003**, *9*, 4000–4008. [[CrossRef](#)]
261. Lu, F.; Gu, L.; Meziani, M.J.; Wang, X.; Luo, P.G.; Veca, L.M.; Cao, L.; Sun, Y.P. Advances in Bioapplications of Carbon Nanotubes. *Adv. Mater.* **2009**, *21*, 139–152. [[CrossRef](#)]
262. Zhou, Y.; Fang, Y.; Ramasamy, R.P. Non-Covalent Functionalization of Carbon Nanotubes for Electrochemical Biosensor Development. *Sensors* **2019**, *19*, 392. [[CrossRef](#)] [[PubMed](#)]
263. Georgakilas, V.; Gournis, D.; Tzitzios, V.; Pasquato, L.; Guldie, D.M.; Prato, M. Decorating carbon nanotubes with metal or semiconductor nanoparticles. *J. Mater. Chem.* **2007**, *17*, 2679–2694. [[CrossRef](#)]
264. Liu, Z.; Tabakman, S.; Welsher, K.; Dai, H. Carbon Nanotubes in Biology and Medicine: In vitro and in vivo Detection, Imaging and Drug Delivery. *Nano Res.* **2009**, *2*, 85–120. [[CrossRef](#)] [[PubMed](#)]
265. Zhu, Z. An Overview of Carbon Nanotubes and Graphene for Biosensing Applications. *Nano-Micro Lett.* **2017**, *9*, 25/1–25/24. [[CrossRef](#)] [[PubMed](#)]
266. Star, A.; Joshi, V.; Han, T.R.; Altoe, M.V.P.; Gruner, G.; Stoddart, J.F. Electronic Detection of the Enzymatic Degradation of Starch. *Org. Lett.* **2004**, *6*, 2089–2092. [[CrossRef](#)] [[PubMed](#)]

267. Cai, C.; Chen, J. Direct electron transfer of glucose oxidase promoted by carbon nanotubes. *Anal. BioChem.* **2004**, *332*, 75–83. [[CrossRef](#)]
268. Wang, S.G.; Zhang, Q.; Wang, R.; Yoon, S.F.; Ahn, J.; Yang, D.J.; Tian, J.Z.; Li, J.Q.; Zhou, Q. Multi-walled carbon nanotubes for the immobilization of enzyme in glucose biosensors. *ElectroChem. Commun.* **2003**, *5*, 800–803. [[CrossRef](#)]
269. Cai, H.; Cao, X.; Jiang, Y.; He, P.; Fang, Y. Carbon nanotube enhanced electrochemical DNA biosensor for DNA hybridization detection. *Anal. Bioanal. Chem.* **2003**, *375*, 287–293. [[CrossRef](#)]
270. Niu, S.; Zhao, M.; Ren, R.; Zhang, S. Carbon nanotube-enhanced DNA biosensor for DNA hybridization detection using manganese(II)-Schiff base complex as hybridization indicator. *J. Inorg. BioChem.* **2009**, *103*, 43–49. [[CrossRef](#)]
271. Weber, J.E.; Pillai, S.; Ram, M.K.; Kumar, A.; Singh, S.R. Electrochemical impedance-based DNA sensor using a modified single walled carbon nanotube electrode. *Mater. Sci. Eng. C* **2011**, *31*, 821–825. [[CrossRef](#)]
272. Liu, S.; Guo, X. Carbon nanomaterials field-effect-transistor based biosensors. *NPG Asia Mater.* **2012**, *4*, e23/1–e23/10. [[CrossRef](#)]
273. Martínez, M.T.; Tseng, Y.C.; Ormategui, N.; Loinaz, I.; Eritja, R.; Bokor, J. Label-free DNA biosensors based on functionalized carbon nanotube field effect transistors. *Nano Lett.* **2009**, *9*, 530–536. [[CrossRef](#)] [[PubMed](#)]
274. Sorgenfrei, S.; Chiu, C.; Gonzales, R.L.; Yu, Y.J.; Kim, P.; Nukolls, C.; Shepard, K.L. Label-free single-molecule detection of DNA-hybridization kinetics with a carbon nanotube field-effect transistor. *Nat. Nanotechnol.* **2011**, *6*, 126–132. [[CrossRef](#)] [[PubMed](#)]
275. Zheng, C.; Huang, L.; Zhang, H.; Sun, Z.; Zhang, Z.; Zhang, G.J. Fabrication of ultrasensitive field-effect transistor DNA biosensors by a directional transfer technique based on CVD-grown graphene. *ACS Appl. Mater. Interface* **2015**, *7*, 16953–16959. [[CrossRef](#)] [[PubMed](#)]
276. Cai, B.; Wang, S.; Huang, L.; Ning, Y.; Zhang, Z.; Zhang, G.J. Ultrasensitive label-free detection of PNA–DNA hybridization by reduced graphene oxide field-effect transistor biosensor. *ACS Nano* **2014**, *8*, 2632–2638. [[CrossRef](#)]
277. Yin, Z.; He, Q.; Huang, X.; Zhang, J.; Wu, S.; Chen, P.; Zhang, Q.; Yan, Q.; Zhang, H. Real-time DNA detection using Pt nanoparticle-decorated reduced graphene oxide field-effect transistors. *Nanoscale* **2012**, *4*, 293–297. [[CrossRef](#)]
278. Ramnani, P.; Gao, Y.; Ozsoz, M.; Mulchandani, A. Electronic detection of MicroRNA at attomolar level with high specificity. *Anal. Chem.* **2013**, *85*, 8061–8064. [[CrossRef](#)]
279. Park, M.; Celli, L.N.; Chen, W.; Myung, N.V.; Mulchandani, A. Carbon nanotubes based chemiresistive immunosensor for small molecules: Detection of nitroaromatic explosives. *Biosens. Bioelectron.* **2010**, *26*, 1297–1301. [[CrossRef](#)]
280. Tan, F.; Saucedo, M.N.; Ramnani, P.; Mulchandani, A. Label-free electrical immunosensor for highly sensitive and specific detection of microcystin-LR in water samples. *Environ. Sci. Technol.* **2015**, *49*, 9256–9263. [[CrossRef](#)]
281. Peña-Bahamond, J.; Nguyen, H.N.; Fanourakis, S.K.; Rodrigues, D.F. Recent advances in graphene-based biosensor technology with applications in life sciences. *J. NanobioTechnol.* **2018**, *16*, 75/1–75/17.
282. Kruss, S.; Hilmer, A.J.; Zhang, J.; Reuel, N.F.; Mu, B.; Strano, M.S. Carbon nanotubes as optical biomedical sensors. *Adv. Drug Deliv. Rev.* **2013**, *65*, 1933–1950. [[CrossRef](#)] [[PubMed](#)]
283. Heller, D.A.; Jeng, E.S.; Yeung, T.K.; Martinez, B.M.; Moll, A.E.; Gastala, J.B.; Strano, M.S. Optical detection of DNA conformational polymorphism on single-walled carbon nanotubes. *Science* **2006**, *311*, 508–511. [[CrossRef](#)] [[PubMed](#)]
284. Welsher, K.; Liu, Z.; Daranciang, D.; Dai, H. Selective probing and imaging of cells with single walled carbon nanotubes as near-infrared fluorescent molecules. *Nano Lett.* **2008**, *8*, 586–590. [[CrossRef](#)] [[PubMed](#)]
285. Erten-Ela, S.; Cogal, S.; Cogal, G.C.; Oksuz, A.U. Highly conductive polymer materials based multi-walled carbon nanotubes as counter electrodes for dye-sensitized solar cells. *J. Fuller. Nanotub. Carb Nanostruct* **2016**, *24*, 380–384. [[CrossRef](#)]
286. Yu, F.; Shi, Y.; Yao, W.; Han, S.; Ma, J. A new breakthrough for graphene/carbon nanotubes as counter electrodes of dye-sensitized solar cells with up to a 10.69% power conversion efficiency. *J. Power Sources* **2019**, *412*, 366–373. [[CrossRef](#)]
287. Han, J.W.; Kim, B.; Li, J.; Meyyappan, M. Carbon nanotube ink for writing on cellulose paper. *Mater. Res. Bull.* **2014**, *50*, 249–253. [[CrossRef](#)]

288. Jin, H.; Guo, C.; Liu, X.; Liu, J.; Vasileff, A.; Jiao, Y.; Zheng, Y.; Qiao, S.Z. Emerging Two-Dimensional Nanomaterials for Electrocatalysis. *Chem. Rev.* **2018**, *118*, 6337–6408. [[CrossRef](#)]
289. Matochova, D.; Medved, M.; Bakandritsos, A.; Stekly, T.; Zbiril, R.; Otyepka, M. 2D Chemistry: Chemical Control of Graphene Derivatization. *J. Phys. Chem. Lett.* **2018**, *9*, 3580–3585. [[CrossRef](#)]
290. Javed, M.S.; Shaheen, N.; Hussain, S.; Li, J.; Shah, S.S.A.; Abbas, Y.; Ahmad, M.A.; Raza, R.; Mai, W. An ultra-high energy density flexible asymmetric supercapacitor based on hierarchical fabric decorated with 2D bimetallic oxide nanosheets and MOF-derived porous carbon polyhedra. *J. Mater. Chem. A* **2019**, *7*, 946–957. [[CrossRef](#)]
291. Wang, X.; Wu, D.; Song, X.; Du, W.; Zhao, X.; Zhang, D. Review on Carbon/Polyaniline Hybrids: Design and Synthesis for Supercapacitor. *Molecules* **2019**, *24*, 2263. [[CrossRef](#)] [[PubMed](#)]
292. Fried, J.; Lebedeva, M.A.; Porfyrikas, K.; Stimming, U.; Chamberlain, T.W. All-Fullerene-Based Cells for Nonaqueous Redox Flow Batteries. *J. Am. Chem. Soc.* **2018**, *140*, 401–405. [[CrossRef](#)] [[PubMed](#)]
293. Imahori, H.; Sakata, Y. Fullerenes as Novel Acceptors in Photosynthetic Electron Transfer. *Eur. J. Org. Chem.* **1999**, *1999*, 2445–2457. [[CrossRef](#)]
294. Kim, Y.H.; Jin, X.; Hwang, S.J. Fullerene as an efficient hybridization matrix for exploring high performance layered-double-hydroxide-based electrodes. *J. Mater. Chem. A* **2019**, *7*, 10971–10979. [[CrossRef](#)]
295. Kamat, P. Carbon Nanomaterials: Building Blocks in Energy Conversion Devices. *ElectroChem. Soc. Interface* **2006**, *15*, 45–47.
296. Coro, J.; Suarez, M.; Silva, L.S.R.; Eguiluz, K.I.B.; Salazar-Banda, G.R. Fullerene applications in fuel cells: A review. *Int. J. Hydrog. Energy* **2016**, *41*, 17944–17959. [[CrossRef](#)]
297. Calamba, K.; Ringor, C.; Pascua, C.; Miyazawua, K. Pleated surface morphology of C60 fullerene nanowiskers incorporated by polyaniline in N-methyl-2-pyrrolidone. *Fuller. Nanotub. Carbon Nanostruct.* **2014**, *23*, 709–714. [[CrossRef](#)]
298. Guo, J.; Xu, Y.; Chen, X.; Yang, S. Single-crystalline C60 crossing microplates: Preparation, characterization, and applications as catalyst supports for methanol oxidation. *Fuller. Nanotub. Carbon Nanostruct.* **2014**, *23*, 424–430. [[CrossRef](#)]
299. Anafcheh, M.; Ghafouri, R.; Hadipour, N.L. A computational proof toward correlation between the theoretical chemical concept of electrophilicity index for the acceptors of C60 and C70 fullerene derivatives with the open-circuit voltage of polymer-fullerene solar cells. *Solar Energy Mater. Solar Cells* **2012**, *105*, 125–131. [[CrossRef](#)]
300. Collavini, S.; Delgado, J.L. Fullerenes: The Stars of Photovoltaics. *Sustain. Energy Fuels* **2018**, *2*, 2480–2493. [[CrossRef](#)]
301. Choi, J.H.; Son, K.; Kim, T.; Kim, K.; Ohkubo, K.; Fukuzumi, S. Thiienyl-substituted methanofullerene derivatives for organic photovoltaic cells. *J. Mater. Chem.* **2010**, *20*, 475–482. [[CrossRef](#)]
302. Chang, C.L.; Liang, C.W.; Syu, J.J.; Wang, L.; Leung, M.K. Triphenylamine-substituted methanofullerene derivatives for enhanced open-circuit voltages and efficiencies in polymer solar cells. *Solar Energy Mater. Solar Cells* **2011**, *95*, 2371–2379. [[CrossRef](#)]
303. Yu, D.; Yang, Y.; Durstock, M.; Baek, J.B.; Dai, L. Soluble P3HT-Grafted Graphene for Efficient Bilayer–Heterojunction Photovoltaic Devices. *ACS Nano* **2010**, *4*, 5633–5640. [[CrossRef](#)] [[PubMed](#)]
304. Caballero, R.; de la Cruz, P.; Langa, F. Basic principles of the chemical reactivity of fullerenes. In *In Fullerenes: Principles and Applications*; The Royal Society of Chemistry: London, UK, 2012; pp. 66–124.
305. Shiraishi, H.; Itoh, T.; Hayashi, H.; Takagi, K.; Sakane, M.; Mori, T.; Wang, J. Electrochemical detection of *E. coli* 16s rDNA sequence using air plasma activated fullerene impregnated screen printed electrodes. *Bioelectrochemistry* **2007**, *70*, 481–487. [[CrossRef](#)]
306. Pilehvar, S.; De Wael, K. Recent Advances in Electrochem. Biosens Based on C60 Nano-Structured Platforms. *Biosensors* **2015**, *5*, 712–735. [[CrossRef](#)]
307. Hu, X.; Jang, Z.; Jia, Z.; Huang, S.; Yang, X.; Li, Y.; Gan, L.; Zhang, S.; Zhu, D. Amination of [60] fullerene by ammonia and by primary and secondary aliphatic amines—preparation of amino [60] fullerene peroxides. *Chemistry* **2007**, *13*, 1129–11241. [[CrossRef](#)]
308. Zhou, D.; Cai, Z.; Lei, X.; Tian, W.; Bi, Y.; Jia, Y.; Han, N.; Gao, T.; Zhang, Q. NiCoFe-Layered Double Hydroxides/N-Doped Graphene Oxide Array Colloid Composite as an Efficient Bifunctional Catalyst for Oxygen Electrocatalytic Reactions. *Adv. Mater.* **2017**, *8*, 1701905/1–1701905/7. [[CrossRef](#)]

309. Zhao, J.; Chen, J.; Xu, S.; Shao, M.; Zhang, Q.; Wei, F.; Ma, J.; Wei, M.; Evans, D.G. Hierarchical NiMn Layered Double Hydroxide/Carbon Nanotubes Architecture with Superb Energy Density for Flexible Supercapacitors. *Adv. Mater.* **2014**, *24*, 2938–2946. [[CrossRef](#)]
310. Zhuo, Y.; Ma, N.; Chai, Q.; Zhao, M.; Yuan, R. Amplified electrochemiluminescent aptasensor using mimicking bi enzyme nanocomplexes as signal enhancement. *Anal. Chim. Acta* **2014**, *809*, 47–53. [[CrossRef](#)]
311. Wang, H.; Yuan, R.; Chai, Y.; Niu, H.; Cao, Y.; Liu, H. Bi enzyme synergistic catalysis to in situ generate coreactant of peroxydisulfate solution for ultrasensitive electrochemiluminescence immunoassay. *Biosens. Bioelectron.* **2012**, *37*, 6–10. [[CrossRef](#)]
312. Li, Y.; Fang, L.; Deng, J.; Jiang, L.; Huang, H.; Zengh, J. An electrochemical immunosensor for sensitive detection of Escherichia coli o157:H7 using C60 based biocompatible platform and enzyme functionalized pt nanochains tracing tag. *Biosens. Bioelectron.* **2013**, *49*, 485–491. [[CrossRef](#)] [[PubMed](#)]
313. Chuang, W.; Shih, S. Preparation and application of immobilized c60 glucose oxidase enzyme in fullerene C60 coated piezoelectric quartz crystal glucose sensor. *Sens. Actuators B* **2001**, *81*, 1–8. [[CrossRef](#)]
314. Cui, C.; Qian, W.; Yu, Y.; Kong, C.; Yu, B.; Xiang, L.; Wei, F. Highly electroconductive mesoporous graphene nanofibers and their capacitance performance at 4 V. *J. Am. Chem. Soc.* **2014**, *136*, 2256–2259. [[CrossRef](#)] [[PubMed](#)]
315. Chen, T.; Dai, L. Carbon nanomaterials for high-performance supercapacitors. *Mater. Today* **2013**, *16*, 272–280. [[CrossRef](#)]
316. Jayaramulu, K.; Dubal, D.P.; Nagar, B.; Ranc, V.; Tomanec, O.; Petr, M.; Datta, K.K.R.; Zboril, R.; Gómez-Romero, P.; Fisher, R.A. Ultrathin hierarchical porous carbon nanosheets for high-performance supercapacitors and redox electrolyte energy storage. *Adv. Mater.* **2018**, *30*, 1705789/1–1705789/9. [[CrossRef](#)]
317. Park, H.; Ambae, R.B.; Noh, S.H.; Eom, W.; Koh, K.H.; Ambade, S.B.; Lee, W.J.; Kim, S.H. Porous Graphene-Carbon Nanotube Scaffolds for Fiber Supercapacitors. *ACS Appl. Mater. Interface* **2019**, *11*, 9011–9022. [[CrossRef](#)]
318. Penza, M.; Martin, P.J.; Yeow, J.T.W. Carbon Nanotube Gas Sensors. In *Gas Sensing Fundamentals*; Springer Series on Chemical Sensors and Biosensors (Methods and Applications); Springer: Berlin/Heidelberg, Germany, 2014; Volume 15.
319. Hoa, N.D.; Van Quy, N.; Cho, Y. Porous single-wall carbon nanotube films formed by in situ arc-discharge deposition for gas sensors application. *Sens. Actuators B* **2009**, *135*, 656–663. [[CrossRef](#)]
320. Tian, W.; Liu, X.; Yu, W. Research Progress of Gas Sensor Based on Graphene and Its Derivatives: A Review. *Appl. Sci.* **2018**, *8*, 1118. [[CrossRef](#)]
321. Kong, J.; Chapline, M.G.; Dai, H. Functionalized carbon nanotubes for molecular hydrogen sensors. *Adv. Mater.* **2001**, *13*, 1384–1386. [[CrossRef](#)]
322. Mackin, C.; Schroeder, V.; Zurutuza, A.; Su, C.; Kong, J.; Swager, T.M.; Palacios, T. Chemiresistive Graphene Sensors for Ammonia Detection. *ACS Appl. Mater. Interface* **2018**, *10*, 16169–16176. [[CrossRef](#)]
323. Gutes, A.; Hsia, B.; Sussman, A.; Mickelson, W.; Zettl, A.; Carraro, C.; Maboudian, R. Graphene decoration with metal nanoparticles: Towards easy integration for sensing applications. *Nanoscale* **2012**, *4*, 438–440. [[CrossRef](#)] [[PubMed](#)]
324. Lange, U.; Hirsh, T.; Mirsky, V.M.; Wolfbeis, S. Hydrogen sensor based on a graphene–palladium nanocomposite. *Electrochim. Acta* **2011**, *56*, 3707–3712. [[CrossRef](#)]
325. Choi, K.Y.; Park, J.S.; Park, K.B.; Kim, H.J.; Park, H.D.; Kim, S.D. Low power micro gas sensors using mixed SnO₂ nanoparticles and MWCNTs to detect NO₂, NH₃, and xylene gases for ubiquitous sensor network applications. *Sens. Actuators B* **2010**, *150*, 65–72. [[CrossRef](#)]
326. Kerdcharoen, T.; Wongchoosuk, C. Carbon nanotube and metal oxide hybrid materials for gas sensing. In *Semiconductor Gas Sensors*; Woodhead Publishing Limited: Oxford, UK, 2013; pp. 386–407. ISBN 978-0-85709-236-6.
327. Cuong, T.V.; Pham, V.H.; Chung, J.S.; Shin, E.W.; Yoo, D.H.; Hahn, S.H.; Huh, J.S.; Rue, G.H.; Kim, E.J.; Hur, S.H.; et al. Solution-processed ZnO-chemically converted graphene gas sensor. *Mater. Lett.* **2011**, *2479*–2482. [[CrossRef](#)]
328. Zhang, X.; Hou, L.; Cnossen, A.; Coleman, A.C.; Rudolf, P.; van Wees, B.J.; Browne, W.R.; Feringa, B.L. One-pot functionalization of graphene with porphyrin through cycloaddition reaction. *Chem. Eur. J.* **2011**, *17*, 8957–8964. [[CrossRef](#)] [[PubMed](#)]

329. Jiang, Z.; Wang, J.; Meng, L.; Huang, Y.; Liu, L. A highly efficient chemical sensor material for ethanol: Al₂O₃/graphene nanocomposites fabricated from graphene oxide. *Chem. Commun.* **2011**, *47*, 6350–6352. [[CrossRef](#)]
330. Barkade, S.S.; Gajare, G.R.; Mishra, S.; Naik, J.B.; Gogate, P.R.; Pinjari, D.V.; Sonawane, S.H. Recent Trends in Carbon Nanotubes/Graphene Functionalization for Gas/Vapor Sensing: A Review. In *Chemical Functionalization of Carbon Nanomaterials, Chemistry and Applications*; CRC Press Taylor & Francis Group: Boca Raton, FL, USA, 2016; pp. 869–898.
331. Hasanzadeh, A.; Khataee, A.; Zarei, M.; Zhang, Y. Two-electron oxygen reduction on fullerene C₆₀-carbon nanotubes covalent hybrid as a metal-free electrocatalyst. *Sci. Rep.* **2019**, *9*, 13780/1–13780/12. [[CrossRef](#)]
332. Mazloum-Ardakani, M.; Hosseini-zadeh, L.; Khoshroo, A. Label-free electrochemical immunosensor for detection of tumor necrosis factor α based on fullerene-functionalized carbon nanotubes/ionic liquid. *J. Electroanal. Chem.* **2015**, *757*, 58–64. [[CrossRef](#)]
333. Qu, Y.; Piao, G.; Zhao, J.; Jiao, K. Reduced working electrode based on fullerene C₆₀ nanotubes@DNA: Characterization and application. *Mater. Sci. Eng. B* **2010**, *175*, 159–163.
334. Ma, J.; Guo, Q.; Gao, H.L.; Qin, X. Synthesis of C₆₀/Graphene Composite as Electrode in Supercapacitors. *Fuller Nanotub. Carbon Nanostruct.* **2015**, *23*, 477–482. [[CrossRef](#)]
335. Wan, Y.J.; Tang, L.C.; Yan, D.; Zhao, L.; Li, Y.B.; Wu, L.B.; Jiang, J.X.; Lai, G.Q. Improved dispersion and interface in the graphene/epoxy composites via a facile surfactant-assisted process. *Compos. Sci. Technol.* **2013**, *82*, 60–68. [[CrossRef](#)]
336. Morgan, P. *Carbon Fibers and Their Composites*, 1st ed.; Materials Engineering; CRC Press: Boca Raton, FL, USA, 2005; ISBN 978-0-8247-0983-9.
337. Xie, X.L.; Mai, Y.W.; Zhou, X.P. Dispersion and alignment of carbon nanotubes in polymer matrix: A review. *Mater. Sci. Eng. R* **2005**, *49*, 89–112. [[CrossRef](#)]
338. Chand, S. Review Carbon fibers for composites. *J. Mater. Sci.* **2000**, *35*, 1303–1313. [[CrossRef](#)]
339. Alam, P.; Mamalis, D.; Robert, C.; Floreani, C.; Brádaigh, C.M.O. The fatigue of carbon fibre reinforced plastics—A review. *Composites B* **2019**, *166*, 555–579. [[CrossRef](#)]
340. Tiwari, S.; Bijwe, J. Surface Treatment of Carbon Fibers—A Review. *Procedia Technol.* **2014**, *14*, 505–512. [[CrossRef](#)]
341. Li, J. The effect of surface modification with nitric acid on the mechanical and tribological properties of carbon. *Surf. Interface Anal.* **2009**, *41*, 759–763. [[CrossRef](#)]
342. Zhang, X.R.; Pei, X.Q.; Wang, Q.H. The effect of fiber oxidation on the friction and wear behaviors of short-cut CFs/polyimide composites. *Express Polym. Lett.* **2007**, *1*, 318–325. [[CrossRef](#)]
343. Mittal, G.; Dhand, V.; Rhee, K.Y.; Park, S.J.; Lee, W.R. A review on carbon nanotubes and graphene as fillers in reinforced polymer nanocomposites. *J. Ind. Eng. Chem.* **2015**, *21*, 11–25. [[CrossRef](#)]
344. Silva, L.L.G.; Santos, A.L.; Nascente, P.A.P.; Kostov, K.G. Atmospheric Plasma Treatment of Carbon Fibers for Enhancement of Their Adhesion Properties. *IEEE Trans. Plasma Sci.* **2013**, *41*, 319–324. [[CrossRef](#)]
345. Zaldivar, R.J.; Nokes, J.P.; Kim, H.I. The effect of surface treatment on graphite nanoplatelets used in fiber reinforced composites. *Appl. Polym.* **2014**, *131*, 39994/1–39994/10. [[CrossRef](#)]
346. Harris, P.J.F. *Carbon Nanotubes and Related Structures: New Materials for the Twenty-first Century*; Cambridge University Press: Cambridge, UK, 1999.
347. Wu, S.; Peng, S.; Wang, C.H. Multifunctional Polymer Nanocomposites Reinforced by Aligned Carbon Nanomaterials. *Polymers* **2018**, *10*, 542. [[CrossRef](#)] [[PubMed](#)]
348. Qian, D.; Dickey, E.C.; Andrews, R. Load transfer and deformation mechanisms in carbon nanotube-polystyrene composites. *Appl. Phys. Lett.* **2000**, *76*, 2868–2870. [[CrossRef](#)]
349. Biercuk, M.J.; Llaguno, M.C.; Radosavljevic, M.; Hyun, J.K.; Johnson, A.T. Carbon nanotube composites for thermal management. *Appl. Phys. Lett.* **2002**, *80*, 2767–2769. [[CrossRef](#)]
350. Lopez-Barroso, J.; Martinez-Hernandez, A.L.; Rivera-Armenta, J.L.; Velasco-Santos, C. Multidimensional Nanocomposites of Epoxy Reinforced with 1D and 2D Carbon Nanostructures for Improve Fracture Resistance. *Polymers* **2018**, *18*, 281. [[CrossRef](#)]
351. Fukushima, T.; Kosaka, A.; Yamamoto, Y.; Aimiya, T.; Notazawa, S.; Takigawa, T.; Inabe, T. Dramatic Effect of Dispersed Carbon Nanotubes on the Mechanical and Electroconductive Properties of Polymers Derived from Ionic Liquids. *Small* **2006**, *2*, 554–560. [[CrossRef](#)]

352. Papageorgiou, D.G.; Kinloch, I.A.; Young, R.J. Mechanical properties of graphene and graphene-based nanocomposites. *Prog. Mater. Sci.* **2017**, *90*, 75–127. [\[CrossRef\]](#)
353. Khanam, P.N.; Ponnamma, D.; AL-Madeed, M.A. Electrical Properties of Graphene Polymer Nanocomposites. In *Graphene-Based Polymer Nanocomposites in Electronics*; Series on Polymer and Composite Materials; Springer: Cham, Switzerland, 2015; ISBN 978-3-319-13874-9.
354. Cui, Y.; Kundalwal, S.I.; Kumar, S. Gas barrier performance of graphene/polymer nanocomposites. *Carbon* **2016**, *98*, 313–333. [\[CrossRef\]](#)
355. Dreyer, D.R.; Park, S.; Bielwaski, C.W.; Ruoff, R.S. The Chemistry of Graphene Oxide. *Chem. Soc. Rev.* **2010**, *39*, 228–240. [\[CrossRef\]](#)
356. Yang, Y.; Wang, J.; Zhang, J.; Liu, J.; Yang, X.; Zhao, H. Exfoliated Graphite Oxide Decorated by PDMAEMA Chains and Polymer Particles. *Langmuir* **2009**, *25*, 11808–11814. [\[CrossRef\]](#)
357. Matsuo, Y.; Tahara, K.; Sugie, Y. Structure and Thermal Properties of Poly (ethylene oxide)-intercalated Graphite Oxide. *Carbon* **1997**, *35*, 113–120. [\[CrossRef\]](#)
358. Salavagione, H.J.; Gomez, M.A.; Martmez, G. Polymeric Modification of Graphene through Esterification of Graphite Oxide and Poly(vinyl alcohol). *Macromolecules* **2009**, *42*, 6331–6334. [\[CrossRef\]](#)
359. Stankovich, S.; Dikin, D.A.; Dommet, G.H.B.; Kohlhaas, K.M.; Zimney, E.J.; Stach, E.A.; Piner, R.D.; Nguyen, S.T.; Ruoff, R.S. Graphene-based composite materials. *Nature* **2006**, *442*, 282–286. [\[CrossRef\]](#) [\[PubMed\]](#)
360. Yang, J.; Huang, L.; Li, L.; Zhang, Y.; Chen, F.; Zhong, M. Preparation of polystyrene/graphene oxide composites and their supercritical carbon dioxide foaming. *J. Polym. Res.* **2013**, *173/1–173/9*. [\[CrossRef\]](#)
361. Pham, V.H.; Dang, T.T.; Hur, S.H.; Kim, E.J.; Chung, J.S. Highly Conductive Poly (methyl methacrylate) (PMMA)-Reduced Graphene Oxide Composite Prepared by Self-Assembly of PMMA Latex and Graphene Oxide through Electrostatic Interaction. *ACS Appl. Mater. Interface* **2012**, *4*, 2630–2636. [\[CrossRef\]](#) [\[PubMed\]](#)
362. Wu, G.; Xu, X.; He, X.; Yan, Y. Preparation and Characterization of Graphene Oxide-Modified Sapium sebiferum Oil-Based Polyurethane Composites with Improved Thermal and Mechanical Properties. *Polymers* **2018**, *10*, 133. [\[CrossRef\]](#) [\[PubMed\]](#)
363. Gavgani, J.N.; Adelnia, H.; Zaarei, D.; Gudarzi, M.M. Lightweight flexible polyurethane/reduced ultralarge graphene oxide composite foams for electromagnetic interference shielding. *RSC Adv.* **2016**, *6*, 27517–27527. [\[CrossRef\]](#)
364. Li, Y.; Umer, R.; Samad, Y.A.; Zheng, L.; Liao, K. The effect of the ultrasonication pre-treatment of graphene oxide (GO) on the mechanical properties of GO/polyvinyl alcohol composites. *Carbon* **2013**, *55*, 321–327. [\[CrossRef\]](#)
365. Soheilmoghaddam, M.; Adelnia, H.; Bidsorkhi, H.C.; Sharifzadeh, G.; Wahit, M.U.; Akos, N.I. Development of Ethylene-Vinyl Acetate Composites Reinforced with Graphene Platelets. *Macromol. Mater. Eng.* **2017**, *302*, 1600260/1–1600260/9. [\[CrossRef\]](#)
366. Cheng, X.; Kumar, V.; Yokozeki, T.; Goto, T.; Takahashi, T.; Koyanagi, J.; Wu, L.; Wang, R. Highly conductive graphene oxide/polyaniline hybrid polymernanocomposites with simultaneously improved mechanical properties. *Composites A* **2016**, *82*, 100–107. [\[CrossRef\]](#)
367. Li, Y.; Liao, C.; Tjong, S.C. Synthetic Biodegradable Aliphatic Polyester Nanocomposites Reinforced with Nanohydroxyapatite and/or Graphene Oxide for Bone Tissue Engineering Applications. *Nanomaterials* **2019**, *9*, 590. [\[CrossRef\]](#)
368. Zhao, L.; Zhao, F.; Zeng, B. Preparation and application of sunset yellow imprinted ionic liquid polymer – ionic liquid functionalized graphene composite film coated glassy carbon electrodes. *Electrochim. Acta* **2014**, *115*, 247–254. [\[CrossRef\]](#)
369. Zhao, L.; Zhao, F.; Zeng, B. Electrochemical determination of methyl parathion using a molecularly imprinted polymer–ionic liquid–graphene composite film coated electrode. *Sens. Actuators B* **2013**, *176*, 818–824. [\[CrossRef\]](#)
370. Horn, M.; Gupta, B.; MacLeod, J.; Liu, J.; Motta, N. Graphene-based supercapacitor electrodes: Addressing challenges in mechanisms and materials. *Curr. Opin. Green Sustain. Chem.* **2019**, *17*, 42–48. [\[CrossRef\]](#)
371. Gupta, A.; Akhtar, A.J.; Saha, S.K. In-situ growth of P3HT/graphene composites for supercapacitor application. *Mater. Chem. Phys.* **2013**, *140*, 616–621. [\[CrossRef\]](#)
372. Luo, R.P.; Lyu, W.Q.; Wen, K.C.; He, W.D. Overview of Graphene as Anode in Lithium-Ion Batteries. *J. Electron. Sci. Technol.* **2018**, *16*, 57–68.

373. Cheng, Q.; Okamoto, Y.; Tamura, N.; Tsuji, M.; Maruyama, S.; Matsuo, Y. Graphene-Like-Graphite as Fast-Chargeable and High-Capacity Anode Materials for Lithium Ion Batteries. *Sci. Rep.* **2017**, *7*, 14782/1–14782/14. [[CrossRef](#)]
374. Adil, S.F.; Khan, M.; Kalpana, D. Graphene-based nanomaterials for solar cells. In *Multifunctional Photocatalytic Materials for Energy*; Woodhead Publishing in Materials: Oxford, UK, 2018; pp. 127–152.
375. Hsieh, Y.P.; Hong, B.J.; Ting, C.C.; Hofmann, M. Ultrathin graphene-based solar cells. *RSC Adv.* **2015**, *5*, 99627–99631. [[CrossRef](#)]
376. Huang, H.; Su, S.; Wu, N.; Wan, H.; Wan, S.; Bi, H.; Sun, L. Graphene-Based Sensors for Human Health Monitoring. *Front. Chem.* **2019**, *11*, 1–26. [[CrossRef](#)]
377. Nag, A.; Mitra, A.; Mukhopadhyaya, S.C. Graphene and its sensor-based applications: A review. *Sens. Actuators A* **2018**, *270*, 177–194. [[CrossRef](#)]
378. Shareena, T.P.D.; McShan, D.; Dasmahapatra, A.K.; Tchounwou, P.B. A Review on Graphene-Based Nanomaterials in Biomedical Applications and Risks in Environment and Health. *Nano-Micro Lett.* **2018**, *10*, 53. [[CrossRef](#)]
379. Tadyszak, K.; Wychowaniec, J.K.; Litowczenko, J. Biomedical Applications of Graphene-Based Structures. *Nanomaterials* **2018**, *8*, 944. [[CrossRef](#)] [[PubMed](#)]
380. Aghigha, A.; Alizadeha, V.; Wonga, H.Y.; Islamb, S.; Aminc, N.; Zaman, M. Recent advances in utilization of graphene for filtration and desalination of water: A review. *Desalination* **2015**, *365*, 389–397. [[CrossRef](#)]
381. Wei, Y.; Zhang, Y.; Gao, X.; Ma, Z.; Wang, X.; Gao, C. Multilayered graphene oxide membranes for water treatment: A review. *Carbon* **2018**, *139*, 964–981. [[CrossRef](#)]
382. Boretti, A.; Al-Zubaidy, S.; Vaclavikova, M.; Al-Abri, M.; Castelletto, S.; Mikhalovsky, S. Outlook for graphene-based desalination membranes. *NPJ Clean Water* **2018**, *1*, 5/1–5/11. [[CrossRef](#)]
383. Khalilnezhad, S.; Sajjadi, S.A.; Zebarjad, S.M. Effect of nanodiamond surface functionalization using oleylamine on the scratch behavior of polyacrylic/nanodiamond nanocomposite. *Diam. Relat. Mater.* **2014**, *45*, 7–11. [[CrossRef](#)]
384. Kharissova, O.V.; Oliva González, C.M.; Kharisov, B.I. Solubilization and Dispersion of Carbon Allotropes in Water and Non-aqueous Solvents. *Ind. Eng. Chem. Res.* **2018**, *57*, 12624–12645. [[CrossRef](#)]
385. Krueger, A.; Lang, D. Functionality is Key: Recent Progress in the Surface Modification of Nanodiamond. *Adv. Funct. Mater.* **2012**, *22*, 890–906. [[CrossRef](#)]
386. Karami, P.; Khasragli, S.S.; Hashemi, M.; Rabiei, S.; Shojaei, A. Polymer/nanodiamond composites—A comprehensive review from synthesis and fabrication to properties and applications. *Adv. Colloid Interface Sci.* **2019**, *269*, 122–151. [[CrossRef](#)]
387. Astuti, Y.; Saputra, F.D.; Wuning, S.; Bhaduri, G.; Arnelli. Enrichment of nanodiamond surfaces with carboxyl groups for doxorubicin loading and release. *IOP Conf. Ser. Mater. Sci. Eng.* **2017**, *172*, 012066/1–012066/8. [[CrossRef](#)]
388. Jee, A.Y.; Lee, M. Surface functionalization and physicochemical characterization of diamond nanoparticles. *Curr. Appl. Phys.* **2009**, *9*, e144–e147. [[CrossRef](#)]
389. Raymakers, J.; Haenen, K.; Maes, W. Diamond surface functionalization: From gemstone to photoelectrochemical applications. *J. Mater. Chem. C* **2019**, *7*, 10134–10165. [[CrossRef](#)]
390. Karami, P.; Shojaei, A. Morphological and mechanical properties of polyamide 6/nanodiamond composites prepared by melt mixing: Effect of surface functionality of nanodiamond. *Poly. Int.* **2017**, *66*, 557–565. [[CrossRef](#)]
391. Thakur, V.K.; Thakur, M.K.; Gupta, R.K. A Structure and chemistry of polymer/nanodiamond composites. In *Hybrid Polymer Composite Materials, Structure and Chemistry*; Woodhead Publishing: Oxford, UK, 2017.
392. Avazkonandeh-Gharavol, M.H.; Sajjadi, S.A.; Zebarjad, S.M.; Mohammadtaheri, M.; Abbasi, M.; Alimardani, M.; Mossadegh, K. Effect of heat treatment of nanodiamonds on the scratch behavior of polyacrylic/nanodiamond nanocomposite clear coats. *Prog. Org. Coat.* **2013**, *76*, 1258–1264. [[CrossRef](#)]
393. Haleem, Y.A.; Song, P.; Liu, D.; Wang, C.; Gan, W.; Saleem, M.F.; Song, L. The Effect of High Concentration and Small Size of Nanodiamonds on the Strength of Interface and Fracture Properties in Epoxy Nanocomposite. *Materials* **2016**, *9*, 507. [[CrossRef](#)] [[PubMed](#)]
394. Haleem, Y.A.; Liu, D.; Chen, W.; Wang, C.; Hong, C.; He, Z.; Liu, J.; Song, P.; Yu, S.; Song, L. Surface functionalization and structure characterizations of nanodiamond and its epoxy based nanocomposites. *Compos. Part. B* **2015**, *78*, 480–487. [[CrossRef](#)]

395. Choi, E.Y.; Kim, K.; Kim, C.K.; Kang, E. Reinforcement of nylon 6, 6/nylon 6, 6 grafted nanodiamond composites by in situ reactive extrusion. *Nat. Sci. Rep.* **2016**, *6*, 37010/1–37010/10. [[CrossRef](#)] [[PubMed](#)]
396. Mochalin, V.N.; Neitzel, I.; Etzold, B.J.M.; Paterson, A.; Palmese, G.; Gogotsi, Y. Covalent incorporation of aminated nanodiamond into an epoxy polymer network. *ACS Nano* **2011**, *5*, 7494–7502. [[CrossRef](#)]
397. Etemadi, H.; Yegani, R.; Seyfollahi, M. The effect of amino functionalized and polyethylene glycol grafted nanodiamond on anti-biofouling properties of cellulose acetate membrane in membrane bioreactor systems. *Sep. Purif. Technol.* **2017**, *177*, 350–362. [[CrossRef](#)]
398. Loktev, V.F.; Makal'skii, V.I.; Stoyanova, I.V.; Kalinkin, A.V.; Likhолобов, В.А.; Мит'кин, В.Н. Surface modification of ultradispersed diamonds. *Carbon* **1991**, *29*, 817–819. [[CrossRef](#)]
399. Tasaki, T.; Guo, Y.; Machida, H.; Akasaka, S.; Fujimori, A. Nano-dispersion of fluorinated phosphonate-modified nanodiamond in crystalline fluoropolymer matrix to achieve a transparent polymer/nanofiller hybrid. *Polym. Compos.* **2019**, *40*(S1), E842–E855. [[CrossRef](#)]
400. Li, C.C.; Huang, C.L. Preparation of clear colloidal solutions of detonation nanodiamond in organic solvents. *Colloids Surf. A* **2010**, *353*, 52–56. [[CrossRef](#)]
401. Aris, A.; Shojaei, A.; Bagheri, R. Cure kinetics of nanodiamond-filled epoxy resin: Influence of nanodiamond surface functionality. *Ind. Eng. Chem. Res.* **2015**, *54*, 8954–8962. [[CrossRef](#)]



© 2019 by the author. Licensee MDPI, Basel, Switzerland. This article is an open access article distributed under the terms and conditions of the Creative Commons Attribution (CC BY) license (<http://creativecommons.org/licenses/by/4.0/>).